Thermodynamic properties of selected ionic liquids with carboxylic acids at several temperatures

Submitted in fulfilment of the academic requirements for the degree of Master of Applied Sciences in Chemistry, Faculty of Applied Sciences, Durban University of Technology

Oriyomi Pelumi Ogundele

2019

DECLARATION

I, Oriyomi Pelumi Ogundele, declare that this dissertation is my own work. This work has not been previously submitted for another degree. I also declare that all sources used in this work have been duly acknowledged and referenced in the text.

Signed

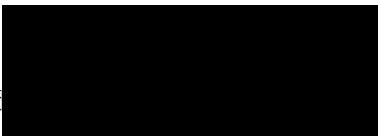Oriyomi P. Ogundele   Date: 19/08/2019

Signed

Prof. G. G. Redhi (Supervisor)   Date: 19/08/2019

Signed

Prof. K. G. Moodley (Co-Supervisor)   Date: 19/08/2019

ABSTRACT

Over the years, ionic liquids (ILs) have become an essential tool in chemistry owing to their various applications such as catalysis, electrochemistry, pharmaceuticals, nanotechnology, biotechnology, separation and extraction processes, amongst many others. With respect to the above applications, ionic liquids have desired properties like low flammability, low vapour pressure, high thermal and chemical stability, good electrical conductivity and low volatility. Ionic liquids possess the ability of being "tailored" to meet specific needs for different applications due to the flexibility in their physicochemical properties. This is done by replacing or substituting the side chain length of cation or anion structure.

This project focused on the thermodynamic as well as thermo-physical parameters of two-component combinations of ionic liquids (ILs) and carboxylic acids (ethanoic or propanoic or butanoic or pentanoic or 2-methylpropanoic acids) which were investigated at several temperatures. The ionic liquids utilized for this research investigation includes:

- 1-ethyl-3-methylimidazolium ethylsulphate ([EMIM]$^+$[EtSO$_4$]$^-$)
- 1-butyl-3-methylimidazolium methylsulphate ([BMIM]$^+$[MeSO$_4$]$^-$)
- N-2′, 3′-epoxypropyl-N-methyl-2-oxopyrrolidinium salicylate ([EPMpyr]$^+$[SAL]$^-$)
- N-2′, 3′-epoxypropyl-N-methyl-2-oxopyrrolidinium acetate ([EPMpyr]$^+$[OAC]$^-$)
- N-2′, 3′-dihydroxypropyl-N-methyl-2-oxopyrrolidinium chloride ([PYR-PDO]$^+$[Cl]$^-$)

Density and speed of sound measurements were examined obtained for the following two component systems: {([EMIM]$^+$[EtSO$_4$]$^-$) + pentanoic or 2-methylpropanoic acid, ([BMIM]$^+$[MeSO$_4$]$^-$) + ethanoic or propanoic acid, ([EPMpyr]$^+$[SAL]$^-$) + ethanoic or propanoic acid, [EPMpyr]$^+$[OAC]$^-$ + propanoic or butanoic acid, [PYR-PDO]$^+$[Cl]$^-$ + ethanoic or propanoic or butanoic acid) throughout the concentration of the ionic liquid at T = (288.15, 293.15, 298.15, 303.15, 308.15 and 313.15) K).

Parameters such as excess molar volumes (V_m^E), isentropic compressibilities (k_s) isentropic compressibilities deviation (Δk_s) and intermolecular free length (L_f) were computed from the measured values of densities and speeds of sound.

The experimental data revealed that densities and speeds of sound value decrease with rise in temperature. Furthermore, excess molar volumes and isentropic compressibility deviation for

all systems studied were found to be negative and increased with a rise in temperature. The negative outcomes obtained for excess molar volumes of all the two-component systems studied suggest chemical interactions occur between unlike molecules in the component mixtures. These interactions are ascribed to formation of weak bonds and electron donor and acceptor complexes. Furthermore, the interaction interstices of IL gave some space for the acids to achieve structural arrangement.

The Redlich-Kister equation was used to correlate the derived parameters; V_m^E, Δk_s and L_f whereas a least squares method was utilized in determining the fitting parameters and standard errors. These was done to check the precision of the measured data and the standard deviations which show moderately lower values for V_m^E, Δk_s and L_f with the examined temperatures for all the binary systems.

ACKNOWLEDGEMENTS

TABLE OF CONTENTS

LIST OF TABLES

LIST OF FIGURES

LIST OF SYMBOLS

ρ = density (g·cm^{-3})

V_m^E = excess molar volume (cm^3·mol^{-1})

T = temperature (K)

x_1 = mole fraction of 1st component

x_2 = mole fraction of 2nd component

σ = standard deviation

M_1 = molar mass of ionic liquid (g·mol^{-1})

M_2 = molar mass of carboxylic acid (g·mol^{-1})

A_i = polynomial coefficient

N = polynomial degree

n = number of experimental points

N_A = Avogadro's number (mol^{-1})

k = number of coefficients used in Redlich-Kister equation

u = speed of sound (m·s^{-1})

k_s = isentropic compressibility (Pa^{-1})

Δk_s = deviation in isentropic compressibility (Pa^{-1})

L_f = intermolecular free length (m)

LIST OF PUBLICATIONS

1. **Ogundele Oriyomi**, Vasanthakumar Arumugam, Kandasamy G. Moodley, Gan G. Redhi. 2019. Thermophysical and thermodynamic properties of 1-ethyl-3-methylimidazolium ethylsulphate ionic liquid and its binary mixtures with pentanoic or 2-methylpropanoic acid at various temperatures. *Physics and Chemistry of Liquids*, https://doi.org/10.1080/00319104.2019.1566461

2. **Oriyomi Ogundele**, Vasanthakumar Arumugam, Kandasamy G. Moodley, Gan G. Redhi. Interaction studies of 2′, 3′-N-epoxypropyl-N-methyl-2-oxopyrrolidinium salicylate ionic liquid and its binary mixtures with carboxylic acids at different temperatures. (Under Review)

3. **Oriyomi Ogundele**, Vasanthakumar Arumugam, Kandasamy G. Moodley, Gan G. Redhi. Effects of temperature and composition on pyrrolidinium based ionic liquids with carboxylic acids binary mixtures at various temperatures. (In preparation for submission to a suitable journal)

INTRODUCTION

For many industrial applications and processes, it is essential to study thermodynamic properties which have become increasingly important for many process industries. The acquisition of thermophysical data for binary liquid combinations of ionic liquids (ILs) and other organic solvents is important for advancement in definite chemical processes (Cann and Connelly, 2000; Dupont *et al.,* 2002; Anastas and Warner, 2000). Moreover, thermophysical and thermodynamic parameters are important means used to investigate intermolecular interactions which occur between different component molecules in liquid mixtures. Thus, there is a need for the measurement of these thermophysical properties.

1.1   Background of ionic liquids

Since organic solvents in general are volatile and easily enter into the atmosphere and become hazards to human health, they should be replaced wherever possible with eco-friendly solvents. This is particularly important for industries which use large volumes of volatile organic compounds in their processes. To achieve a safer environment, ILs have been considered as a perfect alternative which are known to possess low volatility and toxicity, high chemical and physical stability and negligible vapour pressure. Ionic liquids can be regarded as an organic salt that possess melting point which is less than 100°C. ILs are comprised of organic cations and organic or inorganic anions and are responsible for high conductivities in ions (Plechkova and Seddon, 2008; González *et al.* 2007; Flieger *et al.* 2014).

Although the discovery of 'first' ionic liquid, the identity of its discoverer and the date of discovery are not known, ethanol ammonium nitrate having a melting point of $325.15 - 328.15$ K was described in 1888 by S. Gabriel and J. Weiner (Gabriel and Weiner, 1888). Ethyl ammonium nitrate having melting point of 285.15 K was regarded as a room temperature ionic liquid and was synthesized first by Paul Walden (Walden, 1914). In the seventies and eighties of the 20th century, ionic liquids with alkyl group substituted pyridinium and imidazolium based cations, and tetrahalogenoaluminate or halide anions were synthesised and utilized as electrolytes in batteries (Chum *et al.*, 1975; Wilkes *et al.*, 1982). The importance of these imidazolium/pyridinium based salts is that their acidity and viscosity can be modified by

altering the alkyl group substituent on their cations and the ratios of its anions (Gale and Osteryoung, 1979).

However, the major limitations of ILs were their acidity and basicity as well as their affinity for moisture. Fortunately, Wilkes and Zaworotko in 1992 produced ionic liquids which have weak anions, for example, tetrafluoroborate and hexafluorophosphate. These anions allow for a much wider range of applications (Wilkes and Zaworotko, 1992).

1.2 Chemical composition and structures of common ionic liquids

As already mentioned, ionic liquids are typically composed of a cation and an anion. The name "designer solvent" for ionic liquids was given due to their unique properties of being extremely tunable and because they allow several anion and cation combinations (Chiappe and Pieraccini, 2003). Figure 1.1 shows some of the common cations and anions that have been studied over the years.
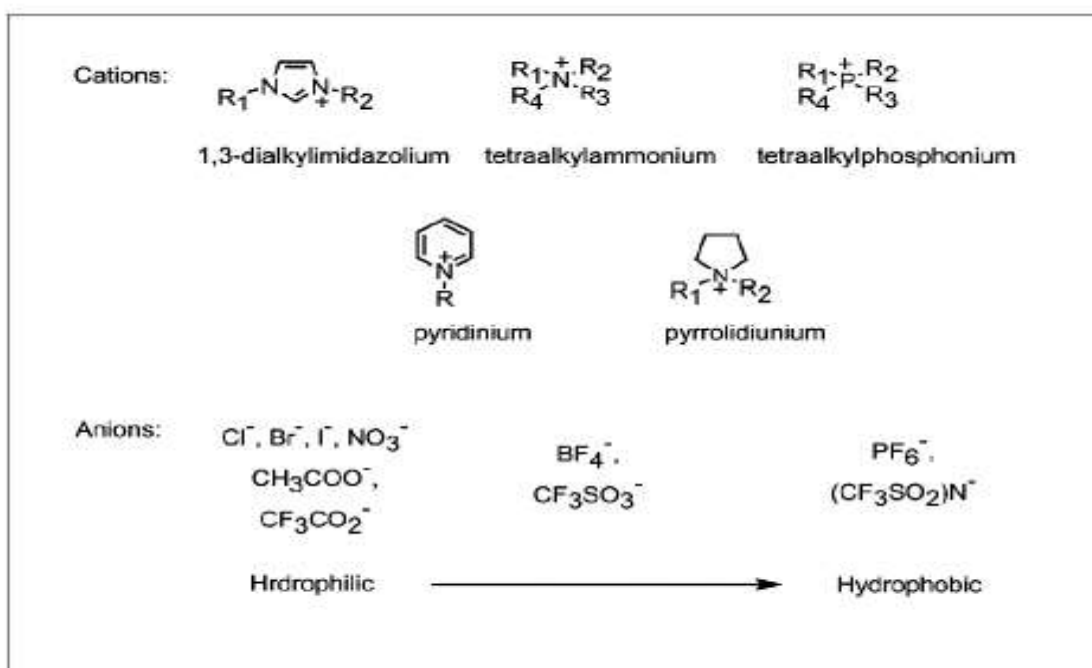
Figure 1.1   Common cations and anions of ionic liquids

1.3   Importance of ionic liquids

Ionic liquids have been recognised as excellent alternatives for traditional organic solvents in many industrial processes such as separation science (Shao *et al*., 2012) and chemical manufacturing. Their successes arise mostly from their properties as solvents and as storage and heat transfer agents. Also, ILs can be 'tailor-made' for specific applications. This is achieved through multiple options of anion and cation combinations; thus, making it possible for ionic liquids to be used in a wide range of applications (Nieto de Castro and Santos, 2007; Earle and Seddon, 2000; Ribeiro *et al*., 2011).

Ionic liquids are attractive solvents which exists as liquids below temperature of 100° C. Further benefits of ionic liquids comprise high ionic conductivity, high thermal and chemical stability, non-volatility, non-flammability, negligible vapour pressure, relatively inexpensive to manufacture and capacity to solubilize an extensive variety of inorganic and organic compounds. As a result, these interesting properties were studied broadly as replacements to molecular solvents utilized in liquid-phase reactions (Wasserscheid and Welton, 2008; Pârvulescu and Hardacre, 2007).

Furthermore, many more researchers in academia and industry have used their knowledge and resources to explore new applications for these compounds; such as their use in separation technology, as lubricants, synthesis of nano-materials, as heat transfer fluids, solvents in catalysis, chemical processing, biomass processing, as electrolytes in Li-ion batteries, adsorption media in gas separations, amongst many others (González *et al*., 2012; Alvarez *et al*., 2011; Domańska *et al*., 2009; Zafarani-Moattar and Shekaari, 2005; Zhong *et al*., 2007).

With respect to the importance and also their applications, ionic liquids are presently involved several investigations in the fields of chemical and materials processing, and as environment friendly solvents and reaction fluids (Wasserscheid and Welton, 2008; Earle and Seddon, 2000; Nunes *et al*., 2010). The majority of these ionic liquids have low-flammability and non-volatility at room temperature.

1.4   General properties of ionic liquids

ILs have been regarded as significant solvent due to the collection of their unique properties which makes them fit for several task specific applications for which the traditional solvents are either unsuitable or inadequately effective. Below are a list of physical and chemical properties of ILs.

- Density: ionic liquids generally possess a density of 1.10 to 1.69 $g \cdot cm^{-3}$ at room temperature.

- Viscosity: viscosity of ionic liquids is usually attributed to presence of hydrogen bonds as well as Van der Waals forces at room temperature.

- Non-corrosive: in order to replace strong corrosive chemicals, ILs which are absolutely free of moisture can be used as anti-corrosive coatings on metal exposed to the environment. Such ILs may also be used as solvents in industrial processes to eliminate possibilities of corrosion of reaction vessels.

- Recyclable: a desirable property of ionic liquids is in their recyclability and reusability. Successful retrieval and substantial manufacture of ILs would minimize costs when compared with other organic solvents.

- Electrochemical and conductivity properties: density and conductivity of ionic liquids are usually influenced by viscosity, molecular weight and mass of the ions. Solar panel materials and electrochemical cells are prepared from room temperature ionic liquids.

Table 1.1   Properties of ionic liquids

Property	Property value
Freezing point	< 373.15 K
Liquid range	$298.15 - 473.15$ K
Thermal stability	High
Viscosity	< 100 Cp
Dielectric constant	< 30 ($F \cdot m^{-1}$)
Polarity	47 - 49
Specific conductivity	< 10 mS$\cdot$cm^{-1}
Molar conductivity	< 10 Scm$^2 \cdot$mol^{-1}
Electrochemical window	2V - 4.5V
Solvent and / or catalyst	Excellent for many organic reactions
Vapour pressure	Usually negligible

* Singh 2013; Mbali 2016

The above listed properties make ionic liquids a prospective substitute to extremely volatile organic materials; thus, reducing the total volume of air pollution caused by loss of solvent (Brennecke *et al.,* 2011). ILs are also regarded as inflammable in nature (Singh *et al.,* 2010). However, there were few reports which have reported on the combustibility of several ionic liquids. Hence, care should be taken while at work with or near a heat or ignition source (FitzPatrick, 2011).

1.5   Limitations of ionic liquids

Presently, there are major limitations according to some reports to fully exploring the use of ionic liquids. They are listed below:

- Part of the biggest problem of implementing the utilization of ionic liquids is its high cost of production (Shamsuri and Abdullah, 2011). Most of the available ILs are produced in relatively small quantities and are not adequate for commercial purposes.
- Impurities (specifically moisture) also have an effect on its physical properties. It is also not easy to synthesize and because of its low volatility, it is difficult to purify (Rogers *et al.,* 2003).
- A larger percentage of the research done on ionic liquids have focused more on, *n*-alkylimidazolium, *n*-alkylpyridinium, *n*-alkylthiazolium, tetraalkylammonium and *n, n*-dialkylpyrazolium cations (Shamsuri and Abdullah, 2011).
- ILs can only be termed as designer solvents when they are flexible to different combinations and known to suit the exact design they are created for (Crowhurst et al., 2003).
- Safety and toxicology: Information on toxicology of ILs is very limited. Many of the ILs that have been investigated are water soluble and can pollute marine environments. Many halogens containing anions (e.g. $[Tf_2N]^-$, $[PF_6]^-$, $[CF_3SO_3]^-$, $[BF_4]^-$ or $[AlCl_4]^-$) have a weak hydrolysis stability (Swapnil, 2012) and have the ability to release toxic hydrogen halides (HF or HCl) into aquatic systems.

1.6   Industrial applications of ionic liquids

Several research studies have been done over the years on the application of ILs in many fields. Due to the characteristic of ionic liquids having low vapour pressure, they are used as sealants (Zhong *et al*., 2007); they are also used in recycling homogenous catalysts as immobilizers; as electrolytes in electro-chemistry. They are useful as propellants for electrospray thrusters owing to their conductivity and low vapour pressure characteristics (Chiu *et al*., 2006). In view of these numerous potential industrial applications, a few are detailed below:

1.6.1 Batteries

Many researchers have found ILs to be suitable for water replacement as electrolyte in batteries. These occur since ILs evaporate at a much lower rate as compared to water, thereby increasing battery life. In addition, ionic liquids hold an electrochemical window of about six volts (Armand *et al*., 2009) in comparison with that of water (1.23 volts), supporting more energy-dense metals.

Usually, a metal air battery derives oxygen with the aid of an "air" electrode which represent the cathode to produce hydrogen peroxide, water and hydroxide anions which are liable to the behaviour of the electrolyte and catalyst that reduces oxygen.

1.6.2 Solar thermal energy

Ionic liquids are used as fluids to transfer and store heat in solar power systems. Solar energy amenities, for example, a parabolic trough, which is a solar thermal collector, and solar power towers concentrate on energy from the sun into a receiver; generating a temperature at about 873.15 K (1,112°F). The heat in return generates electricity into a steam cycle.

From the early 1980s, nitrate salts have been the main choice of researchers. However, they freeze at 493.15 K (428°F) and require heat to avoid solidification. Ionic liquids such as $[BMIM]^+[BF_4]^-$ possess a favourable temperature range of about (198.15 to 732.15 K) in the liquid phase. On account of this, they can be used as an excellent means of heat transfer and as a medium for storing thermal liquids (Wu *et al*., 2001).

1.6.3 Nuclear fuel processing

Ionic liquids are broadly utilized for several novel applications in nuclear-powered plants. The IL: 1-butyl-3-methylimidazolium chloride has been studied as a non-aqueous solution medium for recovering of uranium and other metals from consumed nuclear fuel and other sources (Giridhar *et al*., 2007; Rao *et al*., 2008). Likewise, protonated betaine bis(trifluoromethanesulfonyl)imide was also explored as a solvent for uranium oxides (Rao *et al*., 2008). Ionic liquids N-methyl-N-propyl piperidinium bis(trifluoromethanesulfonyl)imide and N-butyl-N-methyl pyrrolidinium bis(trifluoromethyl sulfonyl)imide were also employed

for the electrodeposition of uranium and europium metals respectively (Rao *et al*., 2009; Rao *et al*., 2011).

1.6.4 Cellulose processing

Cellulose is a naturally abundant organic compound found on earth. They are extremely vital as a bio-renewable material. 5% is used as feedstock in further processing out of the nature's abundant 40 billion tons output.

ILs have been demonstrated to be efficient solvents which have been used in dissolution of cellulose to technically useful concentrations (Swatloski *et al*., 2002). An in-depth utilization of cellulose as a bio-renewable material is aided through developing an appropriate solvent that can be used for chemical processes.

1.6.5 Pharmaceuticals

A combination of a pharmaceutically active cation with a pharmaceutically active anion results in a dual active ionic liquid in which the actions of two drugs are combined. These has led to an appreciable rate of 50% of commercial pharmaceuticals, which are organic salts, to be designed from a good number of ILs and have in turn been studied (Stoimenovski *et al*., 2010).

1.6.6 Gas handling

Owing to many unique properties of ILs which include, thermal stability at high temperatures, low vapour pressure, solvation of different compounds and gases effecting their usefulness in gas storage and management applications. They possess weak coordinating anions and cations that can give stability to polar transition states. Also, various ionic liquids could be recycled with minute loss in activities.

ILs are been used in place of pressurized gas cylinders to transport reactive gases like phosphine, arsine and borane by a company known as "Air Products". The gases are liquified below atmospheric pressure so they can be withdrawn easily from the vessels when vacuum is applied.

Ionic liquid 1-butyl-3-methylimidazolium chloride is explored in separating hydrogen from borazane (Karkamkar *et al.,* 2007). Similarly, the company called "Linde" have used hydrogen

solubility in ILs in compressing gas to about 450 bars in gas stations using ionic liquid piston compressor.

1.6.7 Paint additives

ILs are marketed by a company known as Degussa with a trade appellation of "TEGO® Dispers". Their products are part of 'pliolite' paint range. ILs have the ability to improve on the finish, appearance as well as drying properties of paints (Plechkova and Seddon 2008).

1.6.8 BASIL process

BASIL (Biphasic Acid Scavenging utilizing Ionic Liquids) process is one of the initial main application for industry where its development is achieved by BASF. The IL precursor: 1-methylimidazole was used in place of triethylamine as an acid scavenger leading to an ionic liquid being formed which can be separated effortlessly from the reaction components (Plechkova and Seddon, 2008). In addition, this BASIL process has also been used successfully in scavenging acids in esterification, acylation, elimination and deprotonation processes.

1.6.9 Separation or extraction processes

Due to the properties of ILs having high thermal stability, ILs have been used for azeotropic and extractive distillations.

Ionic liquids have been utilized in diverse micro extraction procedures. An example is the extraction of fatty acid methyl-esters and esters in white and red wines. This is achieved using a porous coating that is made with polymeric ILs for solid phase micro extraction. Similarly, ionic liquids, which are hydrophobic in nature, are utilized for liquid micro extraction so that they can detect organic pollutants such as polymathic hydrocarbons which has a very low concentration in sediments.

A detailed schematic diagram of some of the applications of ILs are shown in Figure 1.2
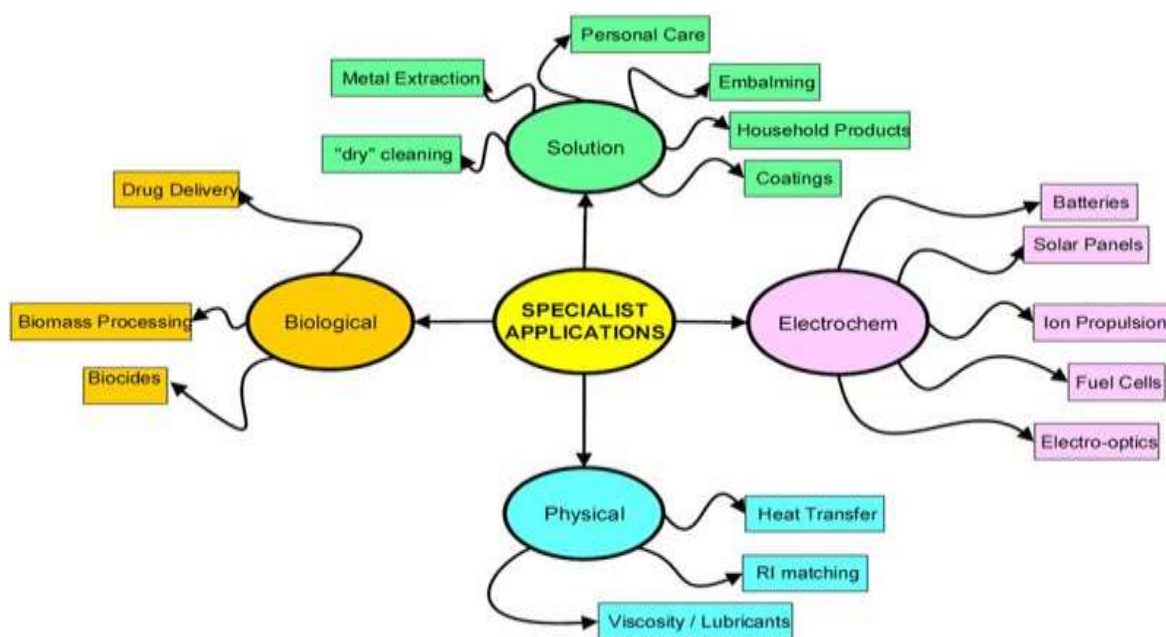
Figure 1.2 Schematic diagram of applications of ionic liquids (taken from Bahadur 2010 Thesis)

1.7 Carboxylic acids

Carboxylic acids are organic compounds which contain a carboxyl group (-COOH) and have a general formula of RCOOH. The choice of carboxylic acids as solvent used in this work was based on its significant role in various industries. Carboxylic acids are an essential class of compounds which occur widely in nature and have many industrial uses and applications.

1.7.1 General properties of carboxylic acids

- Solubility in water: They do not dimerise in the presence of water but forms weak H-bonds between water molecules and individual molecules of the acids.
- Acidity: Carboxylic acids are generally weak acids that partially dissociates in water to give H+ cations and RCOO− anions in neutral aqueous solvents such as water at room temperature.
- Boiling point: Carboxylic acids have higher boiling points than alkanes and alcohols. Their boiling points increase as the molecules get bigger.
- Odour: Generally, carboxylic acids possess unpleasant odours especially the ones that are volatile. They have foul and disagreeable odours. Example of such are in vinegar which comprise ethanoic acid as well as in a rancid butter where butanoic acid can be

found. Carboxylic acids esters have pleasing odours and are generally used in production of perfumes.

A summary of nomenclature, source and properties of carboxylic acids are presented in Table 1.2 below:

Table 1.2   Nomenclature, Source and Properties of Carboxylic acids

Chemical Formula	Common Name	IUPAC Name	Source	Melting Point (°C)	Boiling Point (°C)
HCOOH	Formic acid	Methanoic acid	Ants	8.4	101
CH_3COOH	Acetic acid	Ethanoic acid	Vinegar	16.6	118
CH_3CH_2COOH	Propionic acid	Propanoic acid	Milk	-20.8	141
$CH_3(CH_2)_2COOH$	Butyric acid	Butanoic acid	Butter	-5.5	164
$CH_3(CH_2)_3COOH$	Valeric acid	Pentanoic acid	Valerian root	-34.5	186
$CH_3(CH_2)_4COOH$	Caproic acid	Hexanoic acid	Goats	-4.0	205
$CH_3(CH_2)_5COOH$	Enanthic acid	Heptanoic acid	Vines	-7.5	223
$CH_3(CH_2)_6COOH$	Caprylic acid	Octanoic acid	Goats	16.3	239
$CH_3(CH_2)_7COOH$	Pelargonic acid	Nonanoic acid	Pelargonium	12.0	253
$CH_3(CH_2)_8COOH$	Capric acid	Decanoic acid	Goats	31.0	268

1.7.2   Applications of carboxylic acids

Carboxylic acids are important chemicals which are widely used in many industrial processes. They occur widely in nature. An example is in the production of plastics, cellulose and esters where acetic acid is broadly utilized. Also, derivatives of carboxylic acid can be used in various applications; for example, methanoic acid is the simplest carboxylic acid. It is used as disinfectant and also used in the treatment of textile materials, methanoic acid can also act as an acid reducing agent. An ester of salicylic acid is marketed as Aspirin. Palmitic acid has a

wide range of uses such as in the production of soaps and cosmetics, pharmaceuticals and protective coatings. Stearic acid is employed in the production of rubber. Fatty acids are components of glycerides and also a component of fat. Hydroxy carboxylic acids for example lactic acid can be found in sour milk products.

Proteins comprise of amino acids which also contain carboxy groups. Acrylic acid is utilised as an ester in manufacturing polymers identified as acrylates. Methacrylic is broken down to form Lucite. Oleic acid is employed in producing soaps and detergents. Carboxylic acids such as acetic acid are useful in solvents and coating, while propionic acid can be utilized as food preservatives. Citric acid is essentially important in beverages while maleic and adipic acids are used in the production of polymers.

1.8   Thermodynamic properties investigated in this work

In this research work, the chosen ionic liquids were:$[EMIM]^+[EtSO_4]^-$, $[BMIM]^+[MeSO_4]^-$, $[EPMpyr]^+[SAL]^-$, $[EPMpyr]^+[OAC]^-$ and $[PYR-PDO]^+[Cl]^-$. Carboxylic acids used in this work (ethanoic, propanoic, butanoic, pentanoic and 2-methylpropanoic acids) were chosen on the basis of their miscibility with the ionic liquids and because of their versatility as solvents in chemical and technological procedures. They are also relatively cheap and obtainable at high purity. In addition, carboxylic acids have hydrogen bonds which could interact with ionic liquids. The thermodynamics of these interactions may prove to be useful for the development of specific chemical processes.

 ILs are regarded as important solvents because of their characteristics such as very low vapor pressure, low melting point, ability to dissolve organic, inorganic, and polymeric materials, good thermal stability, and varied fluid range. ILs can also be used as replacement solvents for traditional volatile organic compounds (VOCs). They are readily recycled and generally non-flammable.

 Densities and speeds of sound were measured for the two component combinations of: $\{[EMIM]^+[EtSO_4]^- (x_1)$ + pentanoic or 2-methylpropanoic acid $(x_2)\}$ at T = (288.15, 293.15, 298.15, 303.15, 308.15 and 313.15) K and the binary mixtures of $\{[BMIM]^+[MeSO_4]^- (x_1)$ + ethanoic or propanoic acid $(x_2)\}$, $\{[EPMpyr]^+[SAL]^- (x_1)$ + ethanoic or propanoic acid $(x_2)\}$, $\{[EPMpyr]^+[OAC]^- (x_1)$ + propanoic or butanoic acid $(x_2)\}$, $\{[PYR-PDO]^+[Cl]^- (x_1)$ + ethanoic or propanoic or butanoic acid $(x_2)\}$ all at T = (293.15, 298.15, 303.15, 308.15 and 313.15) K at a range of different mole compositions. From the above measurements the values,

V_m^E, k_s, Δk_s and L_f were computed. The Redlich-Kister polynomial equation was used as a smoothing functions for the values of V_m^E, Δk_s and L_f. The derived thermodynamic parameters were analyzed with respect to inter-molecular connections that occur in the molecules of the binary combinations. The chemical structures of two IL used in this work are presented in Figure 1.3 – 1.4.
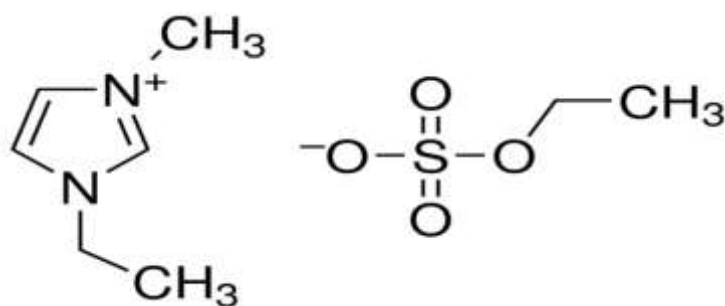
Figure 1.3 Chemical structure of 1-ethyl-3-methylimidazolium ethylsulphate ([EMIM]$^+$[EtSO$_4$]$^-$).
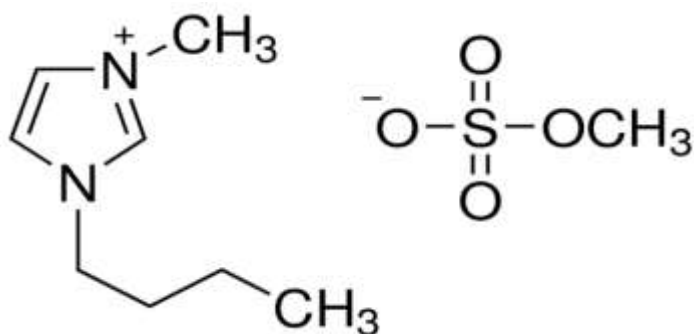
Figure 1.4 Chemical structure of 1-butyl-3-methylimidazolium methylsulphate ([BMIM]$^+$[MeSO$_4$]$^-$).

1.9 Importance of studying thermophysical and thermodynamic properties

A considerable number of investigations have been done on thermophysical and thermodynamic properties of binary systems but they have not been exhausted (Tokuda *et al.*, 2004; Domanska 2006; Fredlake e*t al.*, 2004; Tokuda *et al.,* 2005). Likewise, studies on

thermophysical and thermodynamic characteristics of ionic liquids (ILs) are increasing in number on account of the need for thermodynamic properties such as excess molar volumes, deviation in isentropic compressibilities and intermolecular free length in designing industrial and chemical methods and for theoretical purposes (Cann and Connelly 2000; Iglesias et a*l.,* 1999; Anastas and Warner 1998; Dupont *et al.,* 2002).

The thermodynamic data of mixtures gives information on their intermolecular connections (Lomba e*t al.*, 2011). Thermodynamic parameters are generally utilized as tools in studying the thermophysical parameters of liquid components as well as the behaviour of molecules in the liquid combinations (Yang e*t al.,* 2004).

Excess molar volume is an important parameter utilized in the development of various technological processes in a reaction (Gómez *et al.*, 2006) while speed of sound, *u*, in liquids sheds light on the effects of changes in minimal concentrations on the thermophysical parameters of liquid components and combinations (Azevedo *et al.*, 2004).

1.10   Aim and objectives of the research

The aim of this study is:

Determination of the thermophysical properties of mixtures of ILs and carboxylic acids in order to make contributions to the existing results of derived thermodynamic properties of IL carboxylic mixtures and to deduce the types of interactions that occur in these mixtures for the purpose of establishing ideologies for the design of appropriate ILs for chemical separation procedures (Azevedo *et al.*, 2004).

The objectives of the study are:

- To determine the densities and speeds of sound for two-component combinations of the five selected ionic liquids with carboxylic acids at different temperatures.
- To calculate the derivative parameters such as excess molar volumes, isentropic compressibility, deviation in isentropic compressibility and intermolecular free length at different temperatures.
- To acquire knowledge regarding the types of interactions between the selected ILs and carboxylic acids.

1.11   Outline of the dissertation

- Chapter 1: Introduction
- Chapter 2: Literature review
- Chapter 3: Explains the theoretical framework
- Chapter 4: Outlines the experimental design and procedures
- Chapter 5: The results (tables and graphs) are presented and discussed
- Chapter 6: The results are summarized and conclusion were given.

LITERATURE REVIEW

Thermophysical parameters of binary combinations of ionic liquids with organic compounds are of importance in designing various technological processes and industrial equipment (Maia *et al*., 2013). The need to study thermophysical and thermodynamic parameters of ionic liquids and their two-component combinations with molecular organic solvents has greatly increased in the last 20 years (Freemantle, 2010). These thermodynamic parameters are utilized to comprehend the behaviour of molecular relations that occur in the binary liquid mixtures. Very few researchers have studied the two-component combinations of ionic liquids with carboxylic acids. This literature review will consider some of the studied binary systems of ionic liquids and other solvents as well as other imidazolium based ionic liquids with other organic solvents.

Vasantha *et al*. (2016) measured thermophysical parameters such as density, speed of sound, refractive index and viscosity. They studied the interactions between ionic liquid N-(2',3'-epoxypropyl)-N-methyl-2-oxopyrrolidinium chloride [EPMpyr]$^+$[Cl]$^-$ and carboxylic acids (ethanoic acid or propanoic acid). From the measured thermophysical parameters, excess molar volumes, isentropic compressibilities deviation, refractive index deviation, viscosities deviation and intermolecular free length were derived. Their results showed that V_m^E and Δk_s values were negative throughout the concentration of IL in both component systems. The results were described based on the molecular contacts that occurs between the IL and the carboxylic acids. Redlich-Kister polynomials were used in correlating the derived thermodynamic properties.

Reddy *et al.* (2017) reported density, refractive index and speed of sound measurements of two components combination of 1-ethyl-3-methylimidazolium trifluoromethanesulphonate with 1-butanol) throughout the concentration of IL at temperature range of $T = (298.15$ and $328.15)$ K. The resultant values were used in obtaining excess parameters like excess molar volumes, isentropic compressibilities, partial molar volumes, partial molar volume at infinite dilution, free length and isobaric thermal expansion coefficients. The thermodynamic properties results were used in explaining molecular connections between the system: 1-ethyl-3-methylimidazolium trifluoromethanesulphonate with 1-butanol, that was studied. These

thermodynamic properties data were linked into the Redlich–Kister type model equation in order to get the factors and standard errors.

Hoffman *et al.* (2008) investigated the densities of $[EMIM]^+[EtSO_4]^-$ with methanol at $T =$ (283.15 to 333.15) K and pressure of (0.1 − 3.5) MPa. They found the calculated excess molar volume to be negative over the examined temperatures throughout the mole fraction concentration.

Sibiya and Deenadayalu (2009) reported the densities of IL: $[BMIM]^+[MeSO_4]^-$ with different alcohols such as: 1-propanol or ethanol or methanol, all at $T =$ (298.15 − 313.15) K. They calculated the thermodynamic parameters such as excess and partial molar volumes. Their results gave a negative value for excess molar volumes. They correlated their results using Redlich-Kister equation to acquire the two-components variables for the systems studied . Their results were explained with respect to the alcohol chain-length and inter-molecular connections.

Rao *et al*. (2016) conducted measurements on refractive indices, speeds of sound and densities for two-component combinations of 1-butyl-3-methylimidazolium tetrafluoroborate and 2-pyrrolidone at temperature $T =$ (298.15 to 323.15) K under atmospheric pressure. Excess molar volume results were obtained from measured density results. This demonstrated an inversion from negative to positive deviation. They used FT-IR to deduce the connections between the molecules which may occur in the two-component mixtures. This in turn showed an ion-dipole contacts between IL and the solvent-2-pyrrolidone.

Chaudhary *et al.* (2012) measured speed of sound, density and specific conductivity of the imidazolium based ionic liquid: $[BMIM]^+[BF_4]^-$ and its two-component mixtures with Triton (X-45 or X-100) throughout the mole concentration at temperature of $T =$ 293.15 to 323.15 K. The obtained thermodynamic properties such as change in molar volume, partial change in molar volume, isentropic compressibilities deviation, partial molar isentropic compressibilities deviation and specific conductivities deviation were calculated from the measured results. So as to further explain and comprehend the structural and interactional activities of the binary mixtures, they conducted spectroscopic measurements using FT-IR, hydrogen ^{1}H and carbon [13] NMR.

Deenadayalu *et al.* (2009) investigated the density measurements for two-component combinations of [EMIM]$^+$[EtSO$_4$]$^-$ + 2-propanol or 1-propanol or methanol. They derived excess molar volumes from densities and the results of V_m^E showed negative values throughout the whole composition at all temperatures. They discussed the results in terms of alcohol chain length and inter-molecular connections. Their findings revealed that V_m^E values increase as alcohol chain length increases and decreases slightly with temperature. The derived parameter was fitted to Redlich Kister model to get binary quantities. The pentic four virial parameter (PVF) and equation of state (EoS) model was also used in fitting the excess molar volume results.

Andreatta *et al.* (2009) determined excess molar volumes for two-component systems of 1-octyl-3-methylimidazolium bis(trifluoromethylsulfonyl)imide) with methyl acetate and methanol. They reported that the V_m^E have negative deviation throughout the concentration range of IL and their findings was that the excess molar volume results can be attributed to a more efficient packing and attractive interactions in the liquid combinations than in their pure liquid component states.

Alvarez *et al.* (2011) examined the densities and speeds of sound data for the two-component mixtures of IL: 2-hydroxy ethylammonium acetate (2-HEAA) with methanol or water or ethanol. They derived thermodynamic parameters: excess molar volumes, variations in isentropic compressibilities, apparent molar volumes and thermal expansion coefficient. The excess molar volume gave a negative result throughout the mole concentrations studied. The Peng-Robinson equation of state, Wong-Sandler mixing rule and COSMO-SAC model were utilized for predicting density. They found that the calculated deviations were lower than 3%, for all the two-component combinations studied.

Singh *et al.* (2014) determined the density and speed of sound for pure and two-component mixtures of [EMIM]$^+$[EtSO$_4$]$^-$ with acetic and propionic acids at several temperatures. They calculated the excess molar volumes and deviation in isentropic compressibility of these two-component combinations from density and speed of sound values obtained. They found that excess molar volumes and deviation in isentropic compressibility values were negative throughout the concentration range of the mixtures. The results were interpreted based on

formed spaces, formation of the weak bonds, ion–dipole interactions and structure arrangement occurring in the mixtures.

Patel *et al*. (2016) investigated densities, speeds of sound and refractive indices of pure 1-alkyl-3-methylimidazolium bromide [$C_n$mim][Br] where (n = 4, 6 and 8) with poly ethylene glycol 400 (PEG 400) two-component combinations at a pressure of 0.1 MPa, over throughout the concentration and temperature ranging from (293.15 − 323.15) K. Excess molar volumes, excess molar isentropic compressibilities and deviation in refractive indices were derived from investigated results and then correlated via Redlich–Kister equation to generate the binary coefficients. Excess molar volumes and excess molar isentropic compressibilities were found to be largely negative and it decreases with a rise in temperature. Also, the deviations of refractive index were found to be negative.

Arce *et al*. (2006) investigated the densities, viscosities, refractive indices, and speeds of sound for binary mixtures of the IL: 1-ethyl-3-methylimidazolium ethyl sulphate [EMIM]$^+$[EtSO4]$^-$ with ethanol or 2-ethoxy-2-methylpropane and ternary mixture of [EMIM]$^+$[EtSO4]$^-$ with ethanol and 2-ethoxy-2-methylpropane at T = 298.15 K. Based on their obtained values, the excess molar volume of both two and three-component combinations were found to be negative as well as viscosities deviations were negative throughout the evaluated systems. Density and speed of sound values were utilized in determining isentropic compressibility values and was found to be negative. Redlich-Kister equation was successfully utilized in correlating the derivative parameters.

Gómez *et al*. (2006) conducted measurements on the density, refractive index and sound velocity for pure ionic liquid: 1-ethyl-3-methylimidazolium ethylsulphate [EMIM]$^+$[EtSO$_4$]$^-$ and its two-component combinations with water or ethanol at temperature T = 298.15 to 313.15 K. Calculated data on refractive index deviation were positive for both systems while the data on excess molar volumes and viscosity deviations were negative. The obtained resulting data were observed to decrease with rise in temperature.

Vaid *et al.* (2016) determined the thermophysical parameters such as densities, speeds of sound and refractive indices of the two-component solutions of 1-octyl-3-methylimidazolium tetrafluoroborate [C_8mim][BF$_4$] with different molecular structures of alcohol (1-butanol, 2-methyl-1-propanol, and 2-methyl-2-propanol). Derived thermodynamic properties are estimated from determined data of the binary solutions which were linked into Redlich Kister model. The acquired values were discussed based on accommodation spaces, hydrogen bonds

formation, ion–dipole contacts and structural influences that occurred in the ionic liquid and molecular organic solvent mixture. Additionally, Prigogine–Flory–Patterson (PFP) model and the extended real associated solution (ERAS) model were used in analyzing the excess molar volume data.

Rao *et al.* (2015) investigated thermophysical parameters such as densities, speeds of sound and refractive indices as well as FT-IR spectra of the ionic liquid: $[BMIM]^+[BF_4]^-$ and its two-component combinations with N-methyl-2-pyrrolidinone [NMP] at different concentrations from $T = (298.15$ to $323.15)$ K. The results for excess isentropic compressibility were found to be negative. These values showed strong attractive contacts, molecular re-adjustments and effective packing when the liquid components are mixed. Furthermore, the FT-IR spectrum indicated ion-dipole connections between $[BMIM]^+[BF_4]^-$ and [NMP].

Rao *et al.* (2015) investigated densities, refractive indexes and speed of sound of $[BMIM]^+[BF_4]^-$ with two-component combinations of vinyl-2-pyrrolidinone [NVP] at temperatures ranging from $T = (298.15$ to $323.15)$ K under atmospheric pressure. The excess parameters such as excess isentropic compressibility, excess intermolecular free length, and excess molar volume values were all negative throughout the concentrations at temperature examined. The FT-IR spectrum for the binary mixtures was run to give information about molecular interactions and its results showed ion-dipole interactions between these mixtures.

González *et al.* (2007) studied density, sound velocity and viscosity of 1-ethyl-3-methyl imidazolium ethylsulphate $[EMIM]^+[EtSO_4]^-$, with binary combinations with methanol, 1-propanol and 2-propanol at temperature ranging from $T = (298.15$ to $328.15)$ K. Furthermore, the refractive index measurements of the binary mixtures were conducted at $T = 298.15$ K, and excess molar volumes of the studied systems were negative as well as excess molar isentropic compressions due to ion-dipole interactions. The deviation in viscosities were found to be negative but decreased in negativity with rise in temperature. However, deviation of refractive index were found to be positive.

Zhang *et al.* (2004) investigated the densities as well as viscosities of binary mixtures of IL: 1-ethyl-3-methylimidazolium tetrafluoroborate $[EMIM]^+[BF_4]^-$ with water at $T = (293.15$ to $323.15)$ K. Their values exhibited that the density and viscosity largely depend on water mole fraction but weakly on temperature. Also, they observed that deviations in viscosities are more sensitive to temperature in comparison to excess molar volume, this shows that physical and derived properties of $[EMIM]^+[BF_4]^-$ depend solely on the amount of water content. The

acquired results of excess molar volume and viscosity deviation were interrelated utilizing Redlich Kister equation.

Domanska and Laskowska (2008) evaluated the densities of 1-ethyl-3-methylimidazolium ethyl sulphate $[EMIM]^+[EtSO_4]^-$ with several alcohols (propanol or 1-butanol or 1-pentanol or 1-hexanol or 1-heptanol or 1-octanol or 1-nonanol or 1-decanol) at $T = 298.15$ K under ambient pressure. They found that excess molar volume values were both negative and positive. However, the binary mixtures for 1-propanol and 1-butanol were negative, this is due to weaker bonds that occurs between the short chain alcohols and IL and as well high packing effects between the component mixtures.

Bhattacharjee *et al.* (2012) examined densities and viscosities of 1-alkyl-3-methylimidazolium alkyl sulphates with its binary mixtures of water at $T = (278 - 343)$ K at atmospheric pressure. The alkyl group substituents were: butyl and ethyl while the sulphates types were: hydrogensulphate ($[HSO_4]^-$), methylsulphate ($[MeSO_4]^-$) and ethylsulphate ($[EtSO_4]^-$). The densities and viscosities of the pure IL had higher values, but the values of the mixtures strongly depended on the mole fraction composition of water. As concentration of water increased, the density and viscosity of the IL decreased. In addition, the thermophysical parameters of the two-component combinations also decreased with an increment in alkyl side chain of the cation. The calculated thermodynamic properties showed negative results. This was taken to imply that there is denser molecular packing in IL than in the pure liquids. Both excess molar volume and deviation in viscosities decreased with increasing temperature. In addition, the deviation in viscosity increased with increment in cation alkyl chain whereas changes in anion structure had minimal effect.

Zafarani-Moattar and Shekaari (2005) measured the densities and speed of sound for $[BMIM]^+[PF_6]^-$ and their two component combinations with methanol or acetonitrile throughout the concentration at $T = (298.15$ to $318.15)$ K. Density results were utilized in obtaining excess molar volume, speed of sound was utilized in obtaining isentropic compressibility deviations for the systems and their results were negative with the binary system containing methanol more negative than the one containing acetonitrile.

Vercher *et al.* (2015) conducted measurements on thermophysical parameter such as densities, sound velocity, viscosities and refractive indices of pure compounds and two-component combinations of $[BMIM]^+[BF_4]^-$ or $[EMIM]^+[BF_4]^-$ with methanol at temperature ranging from $T = (278.15$ to $318.15)$ K. Results of excess isentropic compressibility and excess molar

21

volume obtained were negative. Moreover, they became more negative as temperature increased due to changes in free volume. Deviation in refractive index showed positive results at all temperatures and across the whole composition of ILs while deviation in viscosity gave negative results at all temperatures.

Papovic *et al.* (2016) measured densities and viscosities of γ-butyrolactone (GBL) with 1-alkyl-3-methylimidazolium bis(trifluoromethylsulfonyl)imide ionic liquids (where alkyl = ethyl, hexyl, octyl) two-component combinations throughout the concentration at pressure of 0.1MPa. The calculated excess molar volume as well as deviation of viscosities were interrelated via the Redlich Kister equation. The derived resulting data were utilized to acquire data about connections of GBL and ionic liquids studied.

Vatašcin and Dohnal (2015) studied density, viscosity, and refractive index of the two-component combinations of water and 1-ethyl-3-methylimidazolium tricyanomethanide [EMIM]$^+$[TCM]$^-$, the IL were investigated at temperature from T = (288.15 to 318.15) K. Thermophysical properties were estimated to obtain excess thermodynamic parameters: Gibbs free energy, enthalpy, heat capacity, and volume and property deviations. Results for excess molar volume were found to be positive while deviations in viscosity and deviation in refractive index were found to be negative.

Rao *et al*. (2015) investigated densities, refractive indexes and sound velocity of [BMIM]$^+$[BF$_4$]$^-$ with its binary mixtures of N-octyl-2-pyrrolidinone at temperatures ranging from T = (298.15 to 323.15) K under atmospheric pressure. The excess isentropic compressibility, excess intermolecular free length, and excess molar volume data were negative throughout the concentration at the evaluated temperatures. The FT-IR spectrum for the binary mixtures was run to give information about molecular interactions and its results showed ion-dipole interactions between these mixtures.

Reddy *et al*. (2016) determined density, sound velocity and refractive index of pure component of [EMIM]$^+$[EtSO$_4$]$^-$ and its binary mixture with 2-ethoxyethanol at T = (298.15 to 328.15) K. Derived properties determined were excess molar volume, excess values of partial molar volumes, partial molar volume at infinite dilution, deviation in isentropic compressibility, free length, isothermal compressibility and isobaric thermal expansion coefficient. The results showed a negative results whereas speed of sound, refractive index, internal pressure gave a positive results which showed dominance of stronger intermolecular contacts in the

compositions studied. Redlich-Kister equation were utilized in linking the excess parameters to obtain coefficients and standard deviations.

Reddy *et al.* (2016) studied density, sound velocity and refractive index of $[EMIM]^+[BF_4]^-$ and 2-methoxyethanol. The thermophysical characteristics of pure and binary mixtures were evaluated at atmospheric pressure and temperature from $T = (298.15$ to $328.15)$ K. The results exhibited stronger inter-molecule contacts in the two component combinations which were also confirmed using Infrared spectroscopy.

Rafiee and Frouzesh (2015) obtained density and speed of sound measurements on two-component and three-component combinations of $[EMIM]^+[EtSO_4]^-$ with alkyl alcohol and 1,3-dichloro-2-propanol at temperature $T = (298.15$ to $318.15)$ K and under pressure of 0.087 MPa. Negative results were obtained for excess molar volume of the two component combinations of IL with an alkyl alcohol while positive results of the excess molar volume of the two-component mixtures of IL with 1,3-dichloro-2-propanol were obtained. Furthermore, excess molar volume decreased with an increase in temperature and this was ascribed due to intermolecular interaction and steric effects. Thermal expansion coefficients were also calculated, and the results were negative for all two-component combinations studied.

Pereiro and Rodríguez (2007) studied the speed of sound, refractive index and density of two-component combinations of ethanol with five ILs: $[MMIM]^+[MeSO_4]^-$, $[BMIM]^+[MeSO_4]^-$, $[BMIM]^+[PF_6]^-$, $[HMIM]^+[PF_6]^-$ and $[OMIM]^+[PF_6]^-$ at $T = (293.15$ to $303.15)$ K. The derivative thermodynamic parameters such as excess molar volumes, deviations in isentropic compressibilities and deviations in refractive indices were calculated. It was observed that the ionic liquid $[MMIM]^+[MeSO_4]^-$ gave the most negative value with the ethanol system studied. They used Redlich-Kister equation to correlate the thermodynamic properties to obtain binary coefficients and standard deviations.

In the light of the above and based on the knowledge of the literature, the systems selected for this work have not been investigated.

THEORETICAL FRAMEWORK

3.1   Density

Density (ρ) can be expressed as mass per unit volume and it can be calculated by ratio of mass to its volume.

$$\rho = \frac{m}{v} \tag{3.1}$$

where m stands for mass of a substance; v represents its volume.

Density (ρ) as well as its derived volumetric properties are useful in several industrial applications and also for theoretical calculations. Density of pure component and its liquid mixtures are also essential in distillation, heat transfer and in liquid-liquid extraction processes (Wang *et al*., 2015; Lazaro *et al*., 2015). Density is also expressed as a temperature dependant of pure liquids by the following equation:

$$\rho = kT + m' \tag{3.2}$$

where k and m' are constants, T represents temperature and ρ is the density.

3.2   Excess molar volume (V_m^E)

The excess molar volume V_m^E by definition is the difference in volume between the molar volume of the mixture and the ideal molar volume of a liquid combination under same pressure, temperature and concentration conditions (Walas, 1985; Letcher, 1975). Excess molar volume is an important thermodynamic parameter of liquid mixtures. It can be given by equation (3.3) as:

$$V_m^E = V_{mixture} - \sum_{i=1}^{N} x_i V_i^0 \tag{3.3}$$

where V_m^E denotes excess molar volume, x_i represents molar concentration of the components, V_i^0 represents molar volume of the real liquid i. Also, a binary liquid mixture of an excess molar volume is given by equation (3.4)

$$V_m^E = V_{mixture} - (x_1 V_1^0 + x_2 V_2^0) \tag{3.4}$$

24

The excess molar volume V_m^E of a two-component liquid mixture can arise from a combination of some or all of the following factors:

(a) Formation of new chemical products in solution

(b) Variations in size or shape of the constituent molecules due to packing effects causing positive or negative effect on the molecules involved

(c) Change in inter-molecular relationship between like and unlike molecules causing a decreasing volume mixture

(d) Changes in molecular orientations which makes positive effect on the volume of the mixture

From these factors stated above, it can be deduced that V_m^E is a complex property (Mercer-Chalmers, 1992).

Formation of an ideal binary liquid solution at constant temperature and pressure does not accompany any volume change, but a volume change either increase or decrease tends to occur when there is molecular interaction between components of two real mixtures. This volume change has been expressed in equation 3.3 (Patill *et al.*, 2011).

3.3   Speed of Sound

Speed of sound is also an important parameter of liquids as well as their mixtures in determining molecular interactions of the liquids. The advancement and applicability of speed of sound measurements have greatly increased and has thus reached a level which has driven extensive research regarding theoretical aspects of thermodynamic and kinetic properties of solutions and binary combinations. The determination of sound velocity in liquids gives information for getting value of thermodynamic parameters which cannot be acquired via other experiment procedures. Several researchers have shown that a relationship exists between sound velocity and deviation in thermodynamic parameters of liquid mixtures (Aziz *et al.*, 1972; Auslander and Onitiu, 1971; Poole and Aziz, 1972). The speed of sound of liquids u_{liq} could be derived from free volume (V). However, free volume depends upon the nature of liquid where the calculated free volume (V) provides other results. Kittel (1946) gave a simple relationship in respect of u_{liq} via Tonks model and is expressed below as:

$$u_{liq} = \left(\frac{V}{V_a}\right) \left(\frac{3\gamma liq}{\gamma_{gas}}\right)^{1/2} u_{gas} \qquad (3.5)$$

This relationship gave an acceptable estimation of speed of sound in some liquids. The speed of sound of liquid combinations can also be calculated by using the Free Length Theory (FLT). The key importance of free length (L_f) is the distance in surfaces of two components. Jacobson (1951) presented free length theory in order to describe the speed of sound in pure liquids and their liquid combinations. Jacobson gave an equation expressed as:

$$u_{liq} = \frac{K}{L_f \rho^{1/2}} \tag{3.6}$$

where ρ represents density, K represents temperature dependent variable and L_f is the free length in the liquid. Various researchers have used this Jacobson's theory of free length (Mahajan et al., 2012 and Altuwaim et al., 2012). They evaluated the speed of sound in the liquid combinations of binary or ternary mixtures as:

$$u_{mix} L_{mix} \rho_{mix}^{1/2} = K \tag{3.7}$$

where u_{mix} and ρ_{mix} are speed of sound and density of liquid mixtures respectively. L_{mix} represents the free-length of the constituents. Free length (L_f) of pure component can be estimated using the expression:

$$L_f = \frac{K}{u_{exp} \rho_{exp}^{1/2}} \tag{3.8}$$

where u_{exp} and ρ_{exp} are measured values of speed of sound and density of liquid mixtures respectively.

3.4   Isentropic compressibility and deviation in isentropic compressibility

The thermodynamic parameter which determines the associations between the constituents of the liquid mixtures is known as isentropic compressibilities and can be expressed as:

$$k_s = \frac{-1}{V} \left(\frac{\delta V}{\delta P} \right) \tag{3.9}$$

The isentropic compressibility (k_s) for liquid mixtures can also be calculated by using an indirect method from the Newton-Laplace formula expressed as:

$$k_s = \frac{1}{\rho u^2} \tag{3.10}$$

ρ denotes density and u represents the speed of sound of the two-component combinations.

The deviation in isentropic compressibility for the two-component combinations is the change in the compressibility of an actual solution from an ideal one. It can be calculated by equation (3.11); Rao and Naidu (1974) defined a quantity Δk_s for liquid mixtures as:

$$\Delta k_s = k_s - k_s^{id} \tag{3.11}$$

where Δk_s represents isentropic compressibilities deviation, k_s and k_s^{id} represents isentropic compressibility for the actual and ideal combinations. The ideal isentropic-compressibility can be estimated as:

$$k_s^{id} = \sum_{i=1}^{n} \Phi_i k_{si} \tag{3.12}$$

where Φ_i and k_{si} are portions of the volume and isentropic compressibility of liquid constituent i, respectively. Isentropic compressibility deviations of liquid mixtures are determined so as to know the behaviour and strength of contacts amongst the constituents in liquid combinations.

3.5   Intermolecular free length

Intermolecular free length otherwise known as free length can be defined as the distance between surfaces of two molecules. Free length theory was introduced by Jacobson (1951) in order to explain speed of sound in pure constituents and their liquid combinations. Intermolecular free length is expressed as:

$$u_{liq} = \frac{K}{L_f \, \rho^{1/2}} \tag{3.13}$$

Where K represents temperature dependent constant, ρ is the density while L_f refers to the free length in the liquid.

Several investigators (Altwaim et al., 2012, Mahajan et al., 2012, Vasanthakumar et al., 2016) have used Jacobson free length theory in determining the speed of sound in liquid mixtures both in binary and ternary mixtures which is given by:

$$u_{mix} L_{mix} \rho_{mix}^{1/2} = K \tag{3.14}$$

where ρ_{mix} and u_{mix} are the density and speed of sound of liquid combinations respectively. L_{mix} refers to the free length in the composition. Free length (L_f) of pure liquids can be estimated using the following formula:

$$L_f = \frac{K}{u_{exp}\rho_{exp}^{1/2}} \tag{3.15}$$

where u_{exp} and ρ_{exp} are measured data of speed of sound and density of liquid combinations.

The surface area Y, per mole for the pure liquid is estimated using equation:

$$Y = \frac{2V_a}{L_f} \tag{3.16}$$

L_{mix} is expressed by the equation:

$$L_{mix} = \frac{2\left[V - \sum_{i=1}^{3} x_i V_0^i\right]}{\sum_{i=1}^{3} x_i y_i} \tag{3.17}$$

Where x_i and V_0^i denotes concentration and molar volume at absolute zero component of i and V denotes the molar volume of the mixture.

EXPERIMENTAL DESIGN

4.1   Experimental methods for determining excess molar volumes

The change in volume of binary mixtures V_m^E can be determined either by direct or indirect measurements. Direct measurements involve measuring the resultant change in volume when the two components are mixed while indirect deals with determining the densities of liquid component and their combinations.

4.1.1   Direct measurements

The direct determination of the volume change occurs when the liquid components are mixed. The instrument used in measuring this type of method includes batch dilatometer which is categorized by determining just one data point per loading on the device at a single temperature and the continuous dilution dilatometer which determines many data points at each loading on the device at each desired temperature (Mercer-Chalmers 1992; Redhi 2003).

(i) Batch dilatometer

A diagrammatic representation of a batch dilatometer is shown in Figure 4.1. where a certain mass of the liquid constituent, separated by mercury is filled into the instrument where the mercury height is noted in the marked column. The constituents are combined when the instrument is rotated. The variations in volume when the mixing occurs is shown by the change in height of the mercury in the marked capillary column. A major limitation of this method is the difficulty encountered during filling since it is generally done using a narrow needle. An error that can occur in this type of technique is in the volume of the components since it is necessary to weigh the dilatometer while containing mercury thereby resulting in huge error in mass measurements; thereby affecting the excess molar volume results. (Nevines 1997; Redhi 2003).

Pure liquid 1 ⎯
Pure liquid 2 ⎯

Hg level after mixing
Calibarted capillary
Hg level before mixing
mixture 1 and 2
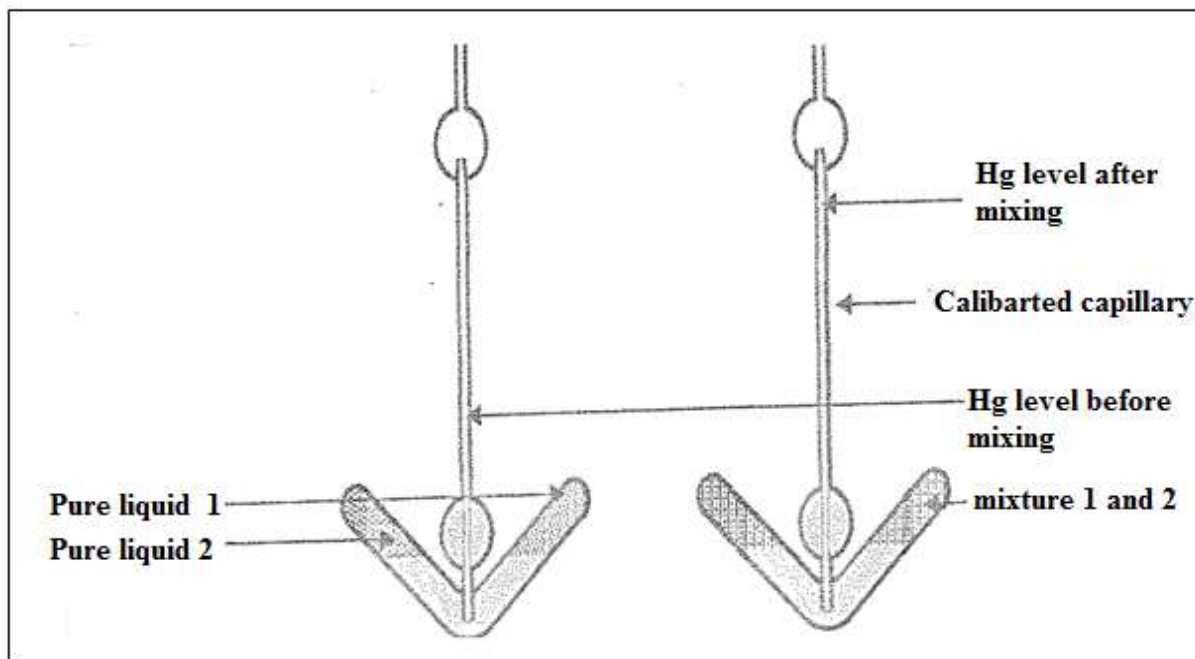
Figure 4.1   Typical diagram of a batch dilatometer

(ii) Continuous dilatometer

This method is more frequently utilized due to the fact that it is not time consuming and many values can be produced on each loading when compared with the batch dilatometer technique. The mode of operation of this instrument entails the sequential adding of a liquid into the basin containing another liquid to be used; it thereafter detects the volume change which occurs after the addition.

Diagrammatic representation of Kumaran and McGlashan (1977) and Bottomly and Scott (1974) are given in Figure 4.2. There was an improvement on the continuous dilatometer of Kumaran and McGlashan (1977) when compared to Bottomly and Scott (1974) instrument due to the fact that it is simpler to load and a precision of 0.0003 cm^3·mol^{-1} in V_m^E was reported.
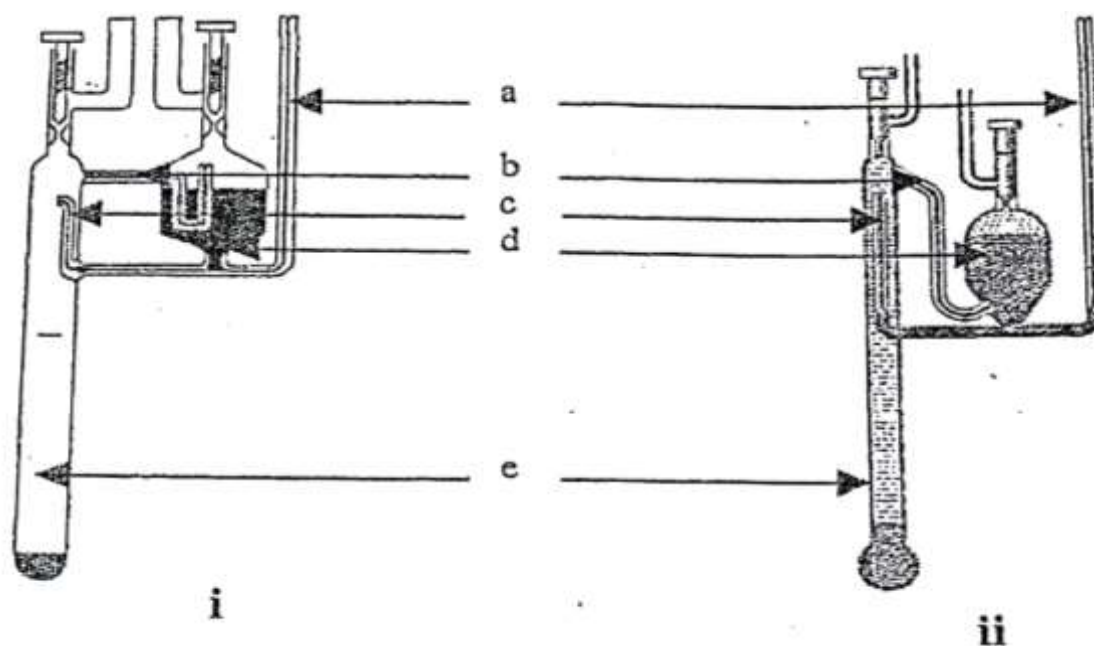
Figure 4.2   Typical diagram of a continuous dilatometer (i) design of Bottomly and Scott (1974); (ii) Kumaran and McGlashan (1977)

From the diagram in Figure 4.2 above, (e) is the burette that measures the filled pure liquid (d) contains the second pure liquid. Upon rotating the equipment, part of the mercury in the burette changes position and this can be observed through the capillary (c). This process begins mixing of the liquids by allowing pure liquids in the burette to go to the bulb by the higher capillary (b). (a) is the calibrated capillary which contains the mercury, the change in level after mixing is considered as a change in volume of the liquids which implies the excess molar volume.

4.2   Speed of sound and isentropic compressibility

Speed of sound is a significant property in chemistry as well as in physics. They are used in developing equation of state which describes the fluid. They are also used in deriving several thermophysical and thermodynamic properties such as isothermal and isentropic compressibilities, bulk modulus, reduced isobaric thermal expansion coefficient, thermal pressure coefficient, heat capacities amongst many others (Sattarib *et al.*, 2014). Speed of sound u, measurements, in liquids proves to be good means of information by detecting slight variations in gas composition or in minute variation in concentration of components and their combinations (Azev*edo et al.*, 2004). Speeds of sound and densities measurement can be utilized in calculation of isentropic compressibilities by using the Newton-Laplace equation:

31

$$k_s = \frac{1}{\rho u^2} \tag{4.1}$$

4.3 Correlation of derived properties

4.3.1 Redlich-Kister equation

The excess properties V_m^E, Δk_s and L_f data were correlated using the Redlich-Kister equation (Redlich and Kister, 1948) at temperatures T = (288.15, 293.15, 298.15, 303.15, 308.15 and 313.15) K. The Redlich-Kister equation for the two-component liquid combinations are given below:

$$X = x_1 x_2 \sum_{i=1}^{k} A_i (1 - 2x_i)^{i-1} \tag{4.2}$$

where X represent V_m^E, Δk_s, L_f and x_1 represents the mole fraction of IL used: [EMIM]$^+$[EtSO$_4$]$^-$, [BMIM]$^+$[MeSO$_4$]$^-$, [EPMpyr]$^+$[SAL]$^-$, [EPMpyr]$^+$[OAC]$^-$, [PYR-PDO]$^+$[Cl]$^-$, x_2 represents the mole fraction of carboxylic acids, k is the amount of coefficients used, and A_i is the Redlich-Kister result obtained using least-square method. The standard error σ, was estimated by:

$$\sigma(X) = \sum_{i=1}^{n} \left[\frac{X_{exp} - X_{calc}}{N - k} \right]^{1/2} \tag{4.3}$$

where k is the factor utilized in the Redlich-Kister equation, N is the number of measured data points while X_{exp} and X_{calc} are measured and derived results of excess parameters.

4.4 Experimental instrumentation and design of this work

4.4.1 Density and speed of sound measurements

In this research work, the density ρ, and speed of sound u, of pure constituents and their two-component combinations have been determined by utilizing Anton Paar oscillating U-tube DSA 5000 M instrument. The device is a two-in-one instrument which simultaneously regulates two different physical parameters using one sample. This device is equipped with a density and speed of sound cell which combines the instrumental process with a vast accuracy in measuring speed of sound. The cells have a built-in thermostat which regulates the temperature to an accuracy of ± 0.02 K. The rate and period of vibration of the analyzed sample

is measured to acquire precise measurements on density. This technique is based on the law of harmonic oscillation.

Speed of sound measurements are achieved by introducing the sample into the speed of sound measuring cell; this equipment uses the ultrasonic transmitter to travel through the sample where the speed of sound is obtained at a rate of 3MHz (Fortin *et al.*, 2013). The transmitter sends a signal through the sample such that when the samples encounters an obstacle, part of the pulse is reflected, and the other part is transmitted. On the other hand, this implies that the instrument stores the time between the pulse emission and reception of the echo, thereby changing it into distance (Cunha 2013).

The density ρ can also be estimated with proportion of the time of oscillation of the tube and the reference oscillator which is given by the equation:

$$\rho = (KA \times Q^2 \times f_1) - (KB \times f_2) \tag{4.4}$$

where KA, KB denotes apparatus coefficients; Q represents the proportion of the time of oscillation of the U-tube divided by the period of oscillation of the reference oscillator; f_1, f_2 are the modification terms for temperature, viscosity and non-linearity.

The speed of sound u, is estimated using the period of the sound waves and the distance between the transmitter and receiver with the equation (4.5) expressed below:

$$u = \frac{l \times \left(1 + 1.6 \times 10^{-5} \times \Delta T\right)}{\frac{P_S}{512} - A \times f_3} \tag{4.5}$$

where l represents the original path length of the sound waves, Ps refers to oscillation period of the sound waves received, A is the apparatus factor for speed of sound, ΔT represents the change in temperature to 278.15 K, while f_3 is the modification term for temperature.

4.5   Features of DSA 5000 M

The DSA 5000 M instrument is equipped with a computer that is embedded with program which automatically saves experimental density and speed of sound values which are also displayed on the LCD screen as the experiment progresses. The photograph of the Density and Speed of sound meter (DSA 5000 M) is presented in Figure 4.3 and Figure 4.4. The main features of the DSA 5000 M are as follows:

4.5.1 Accuracy

This instrument is equipped with an advanced digital density and speed of sound measurement technological procedure in which the period of oscillation of the U-tube is analyzed by optical pickups which also has thermometers alongside Peltier elements which gives accurate sample measurements.

4.5.2 User Interface

This device also supports an easier operating procedure. The user interface permits density and speed of sound data to be converted to sample values for large number of programmed compounds. DSA 5000 M can be used and operated under harsh industrial conditions with the traditional soft keys instead of the touch screen where it can be connected to an external keyboard, and bar-code reader.

Figure 4.3   Anton Paar DSA 5000 M Density and Speed of sound analyzer

Figure 4.4   Anton Paar DSA 5000 M Density and speed of sound analyzer coupled with Lovis 2000 ME viscometer and X sampler 452 (taken from the manual)

4.5.3   Detection of error

When utilizing density and speed of sound meter, there tends to be gas bubbles in the measuring cells. This happens to be a major source of error. In order to diminish gas bubble being formed in the cell, an innovative concept was produced by Anton Paar on the DSA 5000 M in order to combat the above-mentioned setbacks which are:

- Ability to check the filling in the sample tube whereby the device can routinely notice air or bubble in the tube through an advanced breakdown of its vibrational pattern thereby giving a caution message.
- The U-tube can be checked to inspect the presence of air or bubble in the cell through a part using a real-time camera which also have the ability to zoom the camera.

4.5.4   Data management and safety

This instrument possesses latest data management and protection features that have the ability of storing about a thousand data in the archives with or without pictures. The instrument also has the ability of printing reports and exporting results in any preferred format (Excel, text or

PDF). It can also select between the boundaries: $4 \times$ USB, Ethernet, RS-232, $2 \times$ S-BUS and CAN BUS and as well use the inspection track task with tamper-proof value export.

4.5.5 Design

The previously manufactured DSA instrument was replaced with M-series having a compact design, a closed housing with strong materials in the housing compartment with coated aluminum.

The specifications of the DSA 5000 M instrument is shown in Table 4.1 given below:

Table 4.1   Specifications of the DSA 5000 M

Measuring range density	0 to 3 g/cm^3
Measuring range sound velocity	1000 to 2000 m/s
Measuring range temperature	273.15 to 343.15 K (32 to 158 ^{o}F)
Pressure range	0 to 3 bars (0 to 44 psi)
Repeatability density	0.000001 g/cm^3
Repeatability sound velocity	0.1 m/s
Repeatability temperatures	273.151 K (0.002 ^{o}F)
Measuring time per sample	1 to 4 minutes
Sample volume	approx. 3 ml
Ambient air pressure sensor	yes
Reference oscillator	yes
Automatic bubble detection	yes
Visual check of the density measuring cell	camera

4.6   Chemicals

The carboxylic acids utilized in this research study were obtained from Fluka Chemicals with mass purity of $\geq$ 98.0 % for both pentanoic acid and 2-methylpropanoic acid. Ethanoic, propanoic and butanoic acids were purchased from Sigma Aldrich with mass purity of $\geq$ 99.0 %. The ILs ([EMIM]$^+$[EtSO$_4$]$^-$) and ([BMIM]$^+$[MeSO$_4$]$^-$) were obtained from Sigma Aldrich chemicals having a purity of $\geq$ 95.0 % by mass. Other ILs such as ([EPMpyr]$^+$[SAL]$^-$), ([EPMpyr]$^+$[OAC]$^-$) and ([PYR-PDO]$^+$[Cl]$^-$) were synthesized and collected from our research group. These samples were evaluated using the Karl Fischer titration (831 Metrohm). The percentage moisture in all the ILs were found to be less than 0.08 %. Table 4.2 present the details of the chemicals utilized for this work as well as the manufacturers. Table 4.3 and 4.4 shows the assessment of density and speed of sound data on liquid components at T = 298.15 K with those reported in this study and literature. The chemicals were utilized as obtained without any additional purification.

Table 4.2   Chemicals, suppliers, mass % purity and CAS number

Chemical	Supplier	Mass % purity	CAS number
Ethanoic acid	Sigma Aldrich	$\geq$ 99.0 %	79 - 09 - 4
Propanoic acid	Sigma Aldrich	$\geq$ 99.0 %	64 - 19 - 7
Butanoic acid	Sigma Aldrich	$\geq$ 99.0 %	107 - 92 - 6
Pentanoic acid	Fluka	$\geq$ 98.0 %	109 - 52 - 4
2-methylpropanoic acid	Fluka	$\geq$ 98.0 %	79 - 31 - 2
[EMIM]$^+$[EtSO$_4$]$^-$	Sigma Aldrich	$\geq$ 95.0 %	342573 - 75 - 5
[BMIM]$^+$[MeSO$_4$]$^-$	Sigma Aldrich	$\geq$ 95.0 %	401788 - 98 - 5
[EPMpyr]$^+$[SAL]$^-$	Synthesized	$\geq$ 98.0 %	
[EPMpyr]$^+$[OAC]$^-$	Synthesized	$\geq$ 98.0 %	
[PYR-PDO]$^+$[Cl]$^-$	Synthesized	$\geq$ 98.0 %	

Table 4. 3   Experimental and literature values for density (ρ) of pure components at T = 298.15 K.

Chemicals	Experimental	Literature
Ethanoic acid	1.04401	1.04413[d], 1.04365[e]
Propanoic acid	0.98841	0.98794[d], 0.98848[c]
Butanoic acid	0.95265	0.95240[c,a]
Pentanoic acid	0.93479	0.93485[a], 0.9346[b]
2-methylpropanoic acid	0.94270	0.94319[c], 0.9431[b]
[EMIM]$^+$[EtSO$_4$]$^-$	1.22633	1.2296[f], 1.23689[d]
[BMIM]$^+$[MeSO$_4$]$^-$	1.21214	1.21206[g], 1.21222[h]
[EPMpyr]$^+$[SAL]$^-$	1.20554	1.2055[j]
[EPMpyr]$^+$[OAC]$^-$	1.05911	1.0590[i]
[PYR-PDO]$^+$[Cl]$^-$	1.15516	

[Bahadur *et al.*, 2014][a], [Letcher and Redhi, 2002][b], [Bahadur *et al.*, 2013][c], [Singh *et al.*, 2014][d], [Gonzalez *et al.*, 2004][e], [Yang *et al.*, 2013][f], [Singh *et al.*, 2013][g], [Pereiro *et al.*, 2007][h], [Arumugam *et al.*, 2017a][i], [Arumugam *et al.*, 2017b][j]

Table 4.4   Experimental and literature values for speed of sound (u) of pure components at $T = 298.15$ K.

Chemicals	Experimental	Literature
Ethanoic acid	1142.78	1149.00[d],
Propanoic acid	1148.13	1146.00[c], 1146.70[b]
Butanoic acid	1178.07	1172[a,c]
Pentanoic acid	1217.57	1216.00[a]
2-methylpropanoic acid	1121.25	1125.36[k]
[EMIM]+[EtSO4]−	1671.38	1680.80[c], 1679.00[e]
[BMIM]+[MeSO4]−	1656.23	1654.61[f], 1658.40[g]
[EPMpyr]+[SAL]−	1614.45	1613.45[j]
[EPMpyr]+[OAC]−	1550.61	1546.70[i]
[PYR-PDO]+[Cl]−	1537.84	

[a][Bahadur *et al.* 2014], [b][Bahadur *et al.* 2013], [c][Singh *et al.* 2014], [d][Anouti *et al.* 2009] [e][Gomez *et al.* 2006], [f][Singh *et al.* 2013], [g][Pereiro *et al.* 2007], [Arumugam *et al.*2017][i], [Arumugam *et al.*2017][j], [k][Wong *et al.* 1991]

4.7   Preparation of binary liquid mixtures

The binary liquid combinations were weighed with OHAUS (Pine Brook, USA) analytical weighing device having an accuracy of ± 0.0001 g. The two-component solutions were prepared by transferring the pure liquids components via a syringe into air-tight bottles to avoid any loss in the solution. The liquid component mixture, before stacking on the instrument was ensured to have a proper mix since the ionic liquid are a bit viscous. The binary composition was calculated using excel spreadsheet to give an accurate mole fraction range of the samples. The uncertainty of the mole concentrations was assessed to be ± 0.0002.

4.8   Experimental procedure for using the instrument

The instrument had an accuracy and repeatability of $\pm$ 0.02 K for temperature, $\pm$ 0.000005 g·cm^{-3} for density and $\pm$ 0.01 m·s^{-1} for speed of sound simultaneously measures densities and speeds of sound of pure liquids and the two-component combinations. This two-in-one instrument is equipped with a density cell and a speed of sound cell in which both cells are temperature-controlled by a built-in Peltier thermostat. The experimental error limits of density and speed of sound were found to be $\pm$ 0.0002 g·cm^{-3} and $\pm$ 0.6 m·s^{-1} respectively.

Before each analysis, ethanol was used in cleaning the cell and thereafter dried with acetone with the aid of an automatic Xsampler 452 which does the cleaning after each sample analysis thereby dissolving any sample residues in the measuring cell. The objective of calibrating the instrument is to ensure that the values of the density and speed of sound parameters measured are correct.

The instrument recognizes the coupled Xsampler 452 where a portion of the machine fill in the liquid components from each sample bottle into the measuring cell of the DSA 5000 M at a single time. Both densities along with the speed of sound results are displayed on the LED through the computerized pre-installed program. The error in excess molar volumes, isentropic compressibilities and deviation in isentropic compressibilities were found to be $\pm$ 0.005 cm^3·mol^{-1}, $\pm$ 0.2 $\times 10^8$ Pa^{-1} and $\pm$ 0.7 $\times 10^8$ Pa^{-1} correspondingly.

4.9   Systems studied in this work

The excess molar volume V_m^E, isentropic compressibilities k_s, deviation in isentropic compressibilities Δk_s and free length L_f were determined for different binary liquid mixtures of {[EMIM]$^+$[EtSO$_4$]$^-$ or [BMIM]$^+$[MeSO$_4$]$^-$ or [EPMpyr]$^+$[SAL]$^-$ or [EPMpyr]$^+$[OAC]$^-$ or [PYR-PDO]$^+$[Cl]$^-$ (x_1) + ethanoic or propanoic or butanoic or pentanoic or 2-methylpropanoic acids (x_2)} at T = (288.15, 293.15, 298.15, 303.15, 308.15 and 313.15) K at a pressure of 0.1 MPa using experimental density and speed of sound measurements. A total of 11 systems were studied:

1. {[EMIM]$^+$[EtSO$_4$]$^-$} + pentanoic acid at T = (288.15, 293.15, 298.15, 303.15, 308.15 and 313.15) K.

2. {[EMIM]$^+$[EtSO$_4$]$^-$} + 2-methylpropanoic acid at T = (288.15, 293.15, 298.15, 303.15, 308.15 and 313.15) K.

3. {[BMIM]$^+$[MeSO$_4$]$^-$} + ethanoic acid at T = (293.15, 298.15, 303.15, 308.15 and 313.15) K.

4. {[BMIM]$^+$[MeSO$_4$]$^-$} + propanoic acid at T = (293.15, 298.15, 303.15, 308.15 and 313.15)K.

5. {[EPMpyr]$^+$[SAL]$^-$} + ethanoic acid at T = (293.15, 298.15, 303.15, 308.15 and 313.15)K.

6. {[EPMpyr]$^+$[SAL]$^-$} + propanoic acid at T = (293.15, 298.15, 303.15, 308.15 and 313.15)K.

7. {[EPMpyr]$^+$[OAC]$^-$} + propanoic acid at T = (293.15, 298.15, 303.15, 308.15 and 313.15)K.

8. {[EPMpyr]$^+$[OAC]$^-$} + butanoic acid at T = (293.15, 298.15, 303.15, 308.15 and 313.15)K.

9. {[PYR-PDO]$^+$[Cl]$^-$} + ethanoic acid at T = (293.15, 298.15, 303.15, 308.15 and 313.15)K.

10. {[PYR-PDO]$^+$[Cl]$^-$} + propanoic acid at T = (293.15, 298.15, 303.15, 308.15 and 313.15)K.

11. {[PYR-PDO]$^+$[Cl]$^-$} + butanoic acid at T = (293.15, 298.15, 303.15, 308.15 and 313.15)K.

RESULTS AND DISCUSSION

5.1   Measured thermophysical and thermodynamic properties

This chapter presents the values of density (ρ) and speed of sound (u) investigated for {[EMIM]$^+$[EtSO$_4$]$^-$}, {[BMIM]$^+$[MeSO$_4$]$^-$}, {[EPMpyr]$^+$[SAL]$^-$}, {[EPMpyr]$^+$[OAC]$^-$}, {[PYR-PDO]$^+$[Cl]$^-$}, as well as carboxylic acids such as ethanoic or propanoic or butanoic or pentanoic or 2-methylpropanoic acids and their two-component combinations: {[EMIM]$^+$[EtSO$_4$]$^-$} with pentanoic or 2-methylpropanoic acid, {[BMIM]$^+$[MeSO$_4$]$^-$} with ethanoic or propanoic acid, {[EPMpyr]$^+$[SAL]$^-$} with ethanoic or propanoic acid, {[EPMpyr]$^+$[OAC]$^-$} with propanoic or butanoic acid, {[PYR−PDO]$^+$[Cl]$^-$} with ethanoic or propanoic or butanoic acid.

All these binary mixtures were investigated at various temperatures under atmospheric pressure. The derived properties such as excess molar volume V_m^E, isentropic compressibility k_s, deviation in isentropic compressibility Δk_s and intermolecular free length L_f were determined using investigated values of density and speed of sound. These derived parameters were interrelated with Redlich-Kister type equation. The findings have been explained based on inter-molecular relations, structure and property relationships, molecular arrangements and structural effects existing between constituent in the component combinations.

5.1.1   Ionic liquid {[EMIM]$^+$[EtSO$_4$]$^-$ with pentanoic or 2-methylpropanoic acid}

The experimental density results of pure IL, carboxylic acid as well as their two-component combinations were examined throughout the mole concentration of {[EMIM]$^+$[EtSO$_4$]$^-$ (x_1) + pentanoic acid or 2-methylpropanoic acid (x_2)} at T = (288.15, 293.15, 298.15, 303.15, 308.15 and 313.15) K. The results were presented in Tables 5.1 and 5.2. Also, the plots of density against concentration of [EMIM]$^+$[EtSO$_4$]$^-$ at examined temperatures were presented in Figures 5.1 and 5.2. It was observed that density (ρ) data for binary systems of IL with pentanoic or 2-methylpropanoic acid increases with increasing concentration but decreases with rise in temperature.
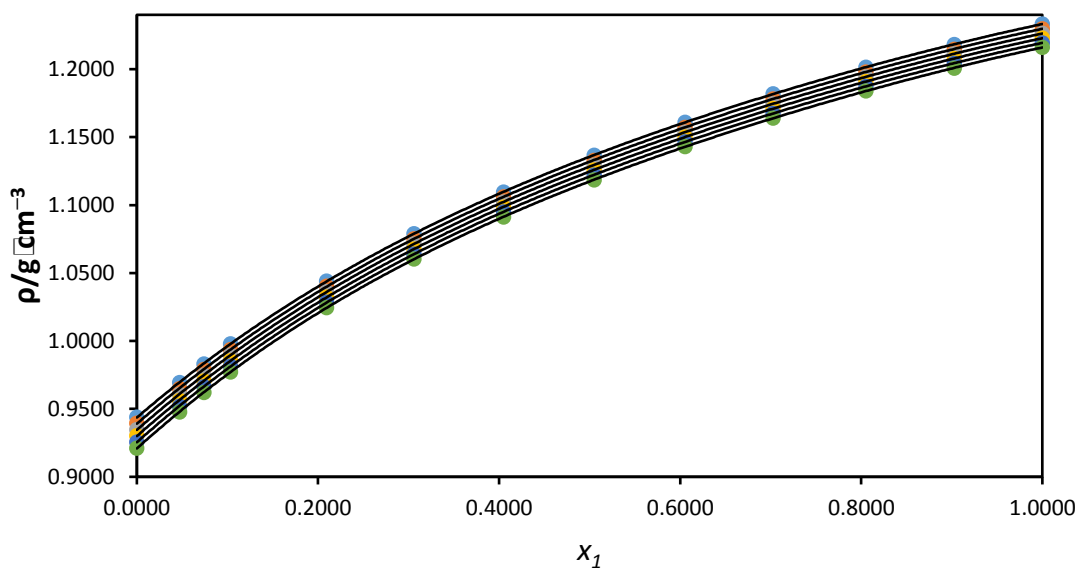
Figure 5.1 Density (ρ) for the binary mixture of $\{[EMIM]^+[EtSO_4]^-$ (x_1) + pentanoic acid (x_2)\} plotted against mole fraction of $[EMIM]^+[EtSO_4]^-$ at T = 288.15 K (●), 293.15 K (●), 298.15 K (●), 303.15 K (●), 308.15 K (●), 313.15 K (●). The line represents the smoothness of the data.
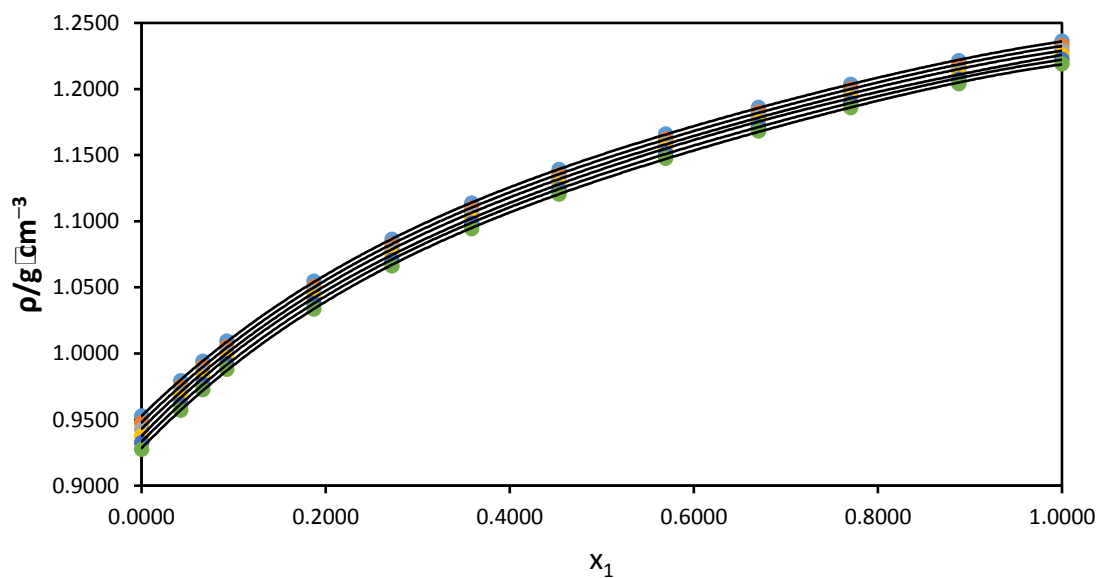
Figure 5.2 Density (ρ) for the binary mixture of $\{[EMIM]^+[EtSO_4]^-$ (x_1) + 2-methylpropanoic acid (x_2)\} plotted against mole fraction of $[EMIM]^+[EtSO_4]^-$ at T = 288.15 K (●), 293.15 K (●), 298.15 K (●), 303.15 K (●), 308.15 K (●), 313.15 K (●). The line represents the smoothness of the data.

Speed of sound (u), were investigated at the entire composition range of {[EMIM]$^+$[EtSO$_4$]$^-$ (x_1) + pentanoic acid or 2-methylpropanoic acid (x_2)} at T = (288.15, 293.15, 298.15, 303.15, 308.15 and 313.15) K which were given in Tables 5.1 and 5.2. The plots of speed of sound against concentration of [EMIM]$^+$[EtSO$_4$]$^-$ at examined temperatures are presented in Figures 5.3 and 5.4. Speed of sound is a significant parameter used in describing the interactions of solvent and solvent, solute and solute and solute and solvent that happens in the liquid component combinations. From the experimental results, it was discovered that there was a rise in speed of sound values with increasing concentration of [EMIM]$^+$[EtSO$_4$]$^-$ at the studied temperatures. In addition, it was also found that u results reduced with a rise in temperature for the studied systems.
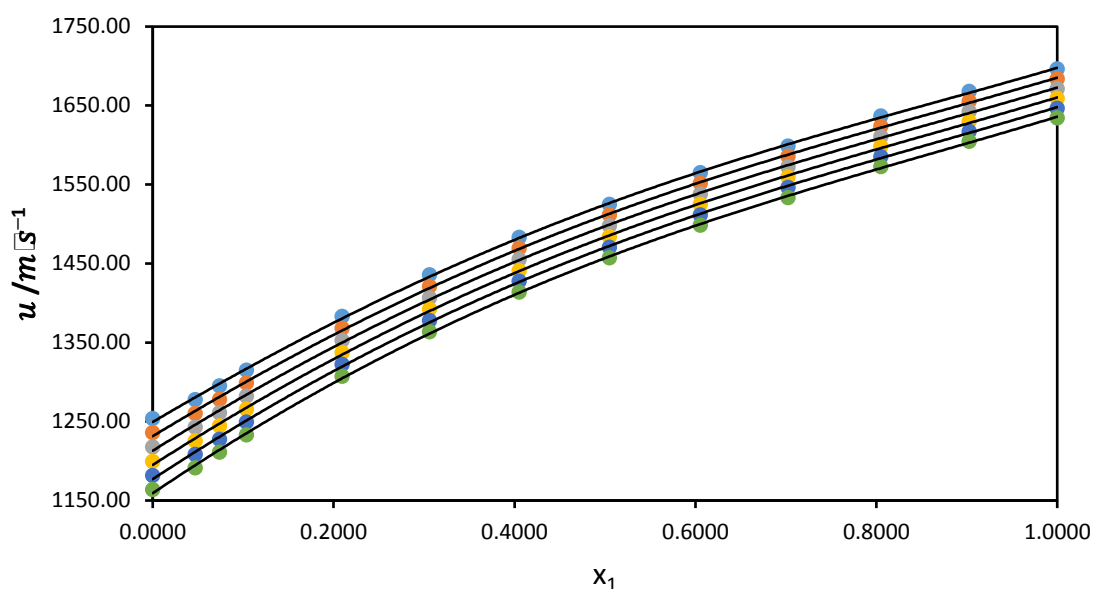
Figure 5.3   Speed of sound (u) for the binary mixture of {[EMIM]$^+$[EtSO$_4$]$^-$ (x_1) + pentanoic acid (x_2)} plotted against mole fraction of [EMIM]$^+$[EtSO$_4$]$^-$ at T = 288.15 K (●), 293.15 K (●), 298.15 K (●), 303.15 K (●), 308.15 K (●), 313.15 K (●). The line represents the smoothness of the data.
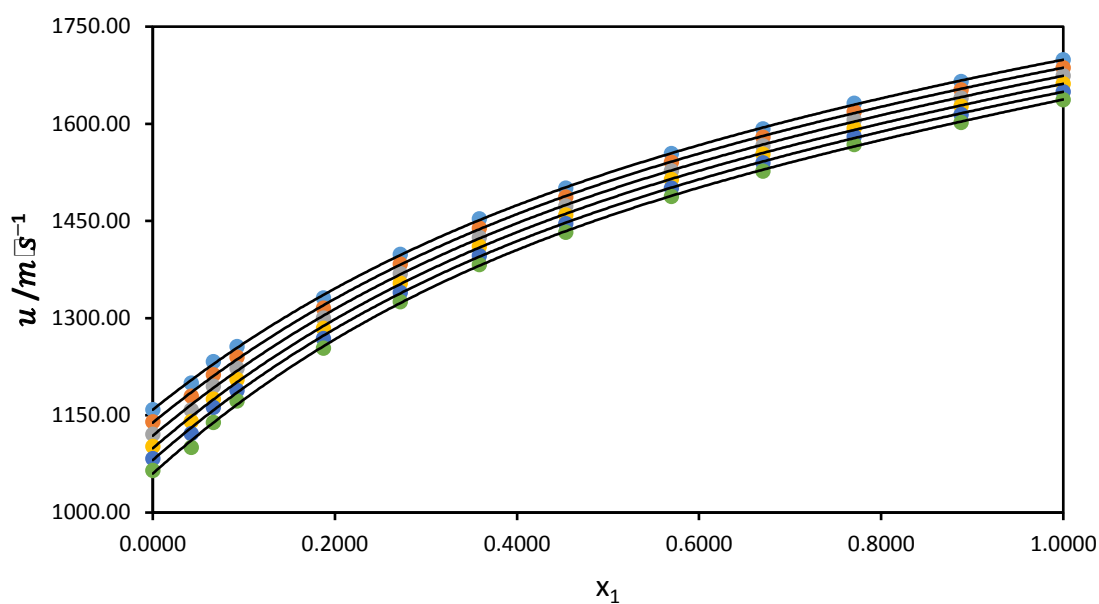
Figure 5.4   Speed of sound (u) for the binary mixture of {[EMIM]$^+$[EtSO$_4$]$^-$ (x_1) + 2-methylpropanoic acid (x_2)} plotted against mole fraction of [EMIM]$^+$[EtSO$_4$]$^-$ at T = 288.15 K (●), 293.15 K (●), 298.15 K (●), 303.15 K (●), 308.15 K (●), 313.15 K (●). The line represents the smoothness of the data.

Table 5.1 and 5.2 below shows the results of excess molar volume V_m^E for the binary mixtures of {[EMIM]$^+$[EtSO$_4$]$^-$ (x_1) + pentanoic or 2-methylpropanoic acid (x_2)} at all investigated temperatures.

Table 5.1 Density (ρ), excess molar volume (V_m^E), speed of sound (u), isentropic compressibility (k_s), deviation in isentropic compressibility (Δk_s) for the binary system {[EMIM]$^+$[EtSO$_4$]$^-$ (x_1) + pentanoic acid (x_2)} from $T = (288.15 - 313.15)$ K.

x_1	ρ/g·cm^{-3}	V_m^E/cm^3·mol^{-1}	u/m□s^{-1}	k_s/10$^8 \times$ Pa^{-1}	Δk_s/10$^8 \times$ Pa^{-1}
			$T = 288.15$ K		
0.0000	0.94393	0.0000	1253.71	67.4007	0.0000
0.0471	0.96938	-0.2499	1277.53	63.2069	-2.3464
0.0740	0.98303	-0.3759	1295.14	60.6457	-3.8524
0.1035	0.99790	-0.5692	1314.96	57.9544	-5.3866
0.2095	1.04410	-0.9340	1383.00	50.0740	-9.1091
0.3059	1.07899	-1.0213	1435.67	44.9648	-10.4371
0.4050	1.10965	-0.9716	1483.26	40.9617	-10.5530
0.5050	1.13666	-0.8593	1525.03	37.8279	-9.7643
0.6053	1.16082	-0.7430	1564.93	35.1760	-8.4820
0.7025	1.18180	-0.6193	1598.77	33.1044	-6.7410
0.8051	1.20153	-0.4494	1636.90	31.0614	-4.7595
0.9026	1.21825	-0.2447	1667.96	29.5048	-2.4917
1.0000	1.23324	0.0000	1696.43	28.1760	0.0000
			$T = 293.15$ K		
0.0000	0.93937	0.0000	1235.79	69.7067	0.0000
0.0471	0.96501	-0.2694	1260.29	65.2423	-2.5318
0.0740	0.97896	-0.4292	1278.32	62.5107	-4.1596
0.1035	0.99374	-0.6091	1298.61	59.6721	-5.7878
0.2095	1.04018	-0.9926	1367.94	51.3757	-9.7349
0.3059	1.07520	-1.0836	1421.31	46.0399	-11.1153
0.4050	1.10594	-1.0301	1469.36	41.8806	-11.2084
0.5050	1.13300	-0.9097	1511.47	38.6343	-10.3516
0.6053	1.15724	-0.7902	1551.61	35.8931	-8.9773
0.7025	1.17820	-0.6492	1585.67	33.7563	-7.1259
0.8051	1.19797	-0.4685	1623.99	31.6510	-5.0214

0.9026	1.21473	-0.2536	1655.25	30.0465	-2.6253
1.0000	1.22977	0.0000	1683.97	28.6754	0.0000

$T = 298.15$ K

0.0000	0.93480	0.0000	1217.57	72.1596	0.0000
0.0471	0.96064	-0.2906	1242.78	67.3987	-2.7371
0.0740	0.97470	-0.4614	1261.30	64.4897	-4.4902
0.1035	0.98958	-0.6517	1282.04	61.4816	-6.2308
0.2095	1.03626	-1.0535	1352.61	52.7454	-10.4123
0.3059	1.07146	-1.1547	1406.72	47.1636	-11.8519
0.4050	1.10223	-1.0905	1455.27	42.8391	-11.9183
0.5050	1.12934	-0.9619	1497.71	39.4747	-10.9858
0.6053	1.15368	-0.8390	1538.10	36.6393	-9.5115
0.7025	1.17462	-0.6806	1572.40	34.4331	-7.5412
0.8051	1.19443	-0.4886	1610.97	32.2601	-5.3057
0.9026	1.21122	-0.2635	1642.42	30.6061	-2.7703
1.0000	1.22630	0.0000	1671.38	29.1912	0.0000

$T = 303.15$ K

0.0000	0.93023	0.0000	1199.51	74.7141	0.0000
0.0471	0.95628	-0.3127	1225.45	69.6346	-2.9600
0.0740	0.97046	-0.4956	1244.41	66.5421	-4.8421
0.1035	0.98544	-0.6958	1265.63	63.3517	-6.7049
0.2095	1.03236	-1.1164	1337.46	54.1510	-11.1355
0.3059	1.06769	-1.2212	1392.26	48.3185	-12.6300
0.4050	1.09854	-1.1525	1441.23	43.8246	-12.6644
0.5050	1.12570	-1.0154	1484.13	40.3303	-11.6586
0.6053	1.15008	-0.8822	1524.78	37.3989	-10.0765
0.7025	1.17106	-0.7133	1559.33	35.1192	-7.9822
0.8051	1.19090	-0.5095	1598.13	32.8775	-5.6068
0.9026	1.20773	-0.2731	1629.76	31.1732	-2.9236
1.0000	1.22286	0.0000	1658.95	29.7137	0.0000

T = 308.15 K

0.0000	0.92565	0.0000	1181.56	77.3820	0.0000
0.0471	0.95202	-0.3481	1208.26	71.9505	-3.2113
0.0740	0.96622	-0.5313	1227.66	68.6704	-5.2234
0.1035	0.98130	-0.7418	1249.36	65.2867	-7.2165
0.2095	1.02847	-1.1818	1322.42	55.5993	-11.9073
0.3059	1.06395	-1.2919	1377.92	49.5031	-13.4594
0.4050	1.09486	-1.2166	1427.50	44.8218	-13.4693
0.5050	1.12208	-1.0708	1470.65	41.2058	-12.3716
0.6053	1.14650	-0.9273	1511.60	38.1727	-10.6767
0.7025	1.16751	-0.7465	1546.37	35.8189	-8.4488
0.8051	1.18739	-0.5311	1585.43	33.5051	-5.9261
0.9026	1.20426	-0.2838	1617.24	31.7489	-3.0864
1.0000	1.21943	0.0000	1646.65	30.2441	0.0000

T = 313.15 K

0.0000	0.92108	0.0000	1163.87	80.1481	0.0000
0.0471	0.94776	-0.3842	1191.28	74.3485	-3.4745
0.0740	0.96198	-0.5677	1211.13	70.8686	-5.6264
0.1035	0.97716	-0.7889	1233.16	67.2969	-7.7418
0.2095	1.02459	-1.2487	1307.51	57.0902	-12.7156
0.3059	1.06025	-1.3695	1363.72	50.7155	-14.3314
0.4050	1.09119	-1.2822	1413.81	45.8477	-14.3069
0.5050	1.11847	-1.1274	1457.33	42.0980	-13.1200
0.6053	1.14293	-0.9731	1498.57	38.9608	-11.3057
0.7025	1.16400	-0.7835	1533.53	36.5312	-8.9369
0.8051	1.18390	-0.5533	1572.86	34.1433	-6.2598
0.9026	1.20081	-0.2942	1604.87	32.3331	-3.2568
1.0000	1.21602	0.0000	1634.50	30.7816	0.0000

Table 5.2 Density (ρ), excess molar volume (V_m^E), speed of sound (u), isentropic compressibility (k_s), deviation in isentropic compressibility (Δk_s) for the binary system {[EMIM]$^+$[EtSO$_4$]$^-$ (x_1) + 2-methylpropanoic acid (x_2)} from $T = (288.15 - 313.15)$ K.

x_1	$\rho/\text{g·cm}^{-3}$	$V_m^E/\text{cm}^3\text{·mol}^{-1}$	$u/\text{m·s}^{-1}$	$k_s/10^8 \times \text{Pa}^{-1}$	$\Delta k_s/10^8 \times \text{Pa}^{-1}$
			$T = 288.15$ K		
0.0000	0.95279	0.0000	1159.03	78.1295	0.0000
0.0424	0.97946	-0.2871	1200.18	70.8793	-5.1254
0.0664	0.99408	-0.4943	1233.10	66.1581	-8.6439
0.0927	1.00949	-0.7330	1256.71	62.7230	-10.7610
0.1873	1.05460	-1.0886	1331.45	53.4890	-15.2542
0.2720	1.08639	-1.1077	1398.53	47.0619	-17.4366
0.3588	1.11370	-1.0199	1453.45	42.5043	-17.6442
0.4536	1.13913	-0.8733	1501.07	38.9605	-16.4372
0.5695	1.16597	-0.7169	1554.51	35.4915	-14.0979
0.6703	1.18618	-0.5902	1592.53	33.2409	-11.2970
0.7705	1.20371	-0.4411	1632.19	31.1844	-8.3321
0.8878	1.22147	-0.2273	1665.46	29.5154	-4.1227
1.0000	1.23626	0.0000	1699.21	28.0153	0.0000
			$T = 293.15$ K		
0.0000	0.94776	0.0000	1140.35	81.1384	0.0000
0.0424	0.97495	-0.3334	1179.67	73.7052	-5.2017
0.0664	0.98978	-0.5607	1213.22	68.6405	-9.0033
0.0927	1.00516	-0.7928	1240.04	64.6987	-11.5609
0.1873	1.05058	-1.1685	1315.99	54.9623	-16.3185
0.2720	1.08232	-1.1666	1383.94	48.2402	-18.5828
0.3588	1.10988	-1.0910	1439.39	43.4880	-18.7668
0.4536	1.13539	-0.9365	1487.43	39.8090	-17.4565
0.5695	1.16231	-0.7682	1541.21	36.2206	-14.9450
0.6703	1.18246	-0.6158	1579.49	33.8984	-11.9622
0.7705	1.20014	-0.4685	1619.31	31.7768	-8.8103

0.8878	1.21794	-0.2390	1652.80	30.0562	-4.3573
1.0000	1.23279	0.0000	1686.82	28.5084	0.0000

T = 298.15 K

0.0000	0.94271	0.0000	1121.25	84.3761	0.0000
0.0424	0.97062	-0.4017	1158.86	76.7166	-5.3123
0.0664	0.98560	-0.6414	1195.05	71.0440	-9.6563
0.0927	1.00082	-0.8555	1222.84	66.8200	-12.4244
0.1873	1.04638	-1.2313	1300.29	56.5237	-17.4839
0.2720	1.07835	-1.2389	1369.12	49.4718	-19.8471
0.3588	1.10606	-1.1652	1425.11	44.5167	-19.9972
0.4536	1.13167	-1.0028	1473.52	40.6977	-18.5683
0.5695	1.15856	-0.8092	1527.70	36.9834	-15.8667
0.6703	1.17886	-0.6574	1566.25	34.5791	-12.6910
0.7705	1.19658	-0.4974	1606.31	32.3891	-9.3342
0.8878	1.21433	-0.2371	1640.02	30.6172	-4.6127
1.0000	1.22933	0.0000	1674.27	29.0188	0.0000

T = 303.15 K

0.0000	0.93764	0.0000	1102.35	87.7655	0.0000
0.0424	0.96625	-0.4683	1140.96	79.5003	-5.7963
0.0664	0.98125	-0.7082	1175.43	73.7608	-10.1383
0.0927	0.99650	-0.9228	1205.61	69.0412	-13.3264
0.1873	1.04218	-1.2967	1284.76	58.1315	-18.7275
0.2720	1.07438	-1.3126	1354.41	50.7391	-21.1878
0.3588	1.10227	-1.2422	1410.95	45.5711	-21.3014
0.4536	1.12796	-1.0715	1459.78	41.6038	-19.7485
0.5695	1.15502	-0.8778	1514.36	37.7530	-16.8504
0.6703	1.17538	-0.7138	1553.18	35.2678	-13.4661
0.7705	1.19305	-0.5273	1593.47	33.0108	-9.8884
0.8878	1.21093	-0.2650	1627.40	31.1811	-4.8877
1.0000	1.22590	0.0000	1661.89	29.5353	0.0000

T = 308.15 K

0.0000	0.93257	0.0000	1083.60	91.3229	0.0000
0.0424	0.96172	-0.5196	1122.21	82.5667	-6.1586
0.0664	0.97683	-0.7693	1162.51	75.7506	-11.5044
0.0927	0.99214	-0.9866	1188.87	71.3115	-14.3323
0.1873	1.03800	-1.3649	1269.03	59.8216	-20.0267
0.2720	1.07051	-1.3990	1339.90	52.0314	-22.6279
0.3588	1.09848	-1.3213	1396.94	46.6500	-22.6916
0.4536	1.12427	-1.1432	1446.17	42.5297	-21.0042
0.5695	1.15140	-0.9349	1501.13	38.5423	-17.8913
0.6703	1.17181	-0.7579	1540.22	35.9730	-14.2853
0.7705	1.18952	-0.5578	1580.77	33.6426	-10.4770
0.8878	1.20746	-0.2783	1614.91	31.7565	-5.1770
1.0000	1.22248	0.0000	1649.63	30.0598	0.0000

T = 313.15 K

0.0000	0.92749	0.0000	1065.12	95.0372	0.0000
0.0424	0.95711	-0.5654	1100.73	86.2341	-6.0707
0.0664	0.97251	-0.8422	1139.51	79.1903	-11.5678
0.0927	0.98804	-1.0808	1172.45	73.6269	-15.4363
0.1873	1.03373	-1.4251	1253.80	61.5372	-21.4294
0.2720	1.06634	-1.4535	1325.51	53.3753	-24.1328
0.3588	1.09451	-1.3801	1383.08	47.7625	-24.1518
0.4536	1.12047	-1.2032	1432.71	43.4793	-22.3256
0.5695	1.14770	-0.9817	1488.06	39.3489	-18.9868
0.6703	1.16826	-0.8039	1527.42	36.6897	-15.1499
0.7705	1.18602	-0.5901	1568.18	34.2860	-11.0961
0.8878	1.20408	-0.3062	1602.57	32.3378	-5.4850
1.0000	1.21907	0.0000	1637.50	30.5920	0.0000

The plots of excess molar volume V_m^E against mole fraction of {[EMIM]$^+$[EtSO$_4$]$^-$ for the binary systems of {[EMIM]$^+$[EtSO$_4$]$^-$ + pentanoic or 2-methylpropanoic acid} at T = (288.15, 293.15, 298.15, 303.15, 308.15 and 313.15) K have been presented in Figures 5.5 and 5.6 below:
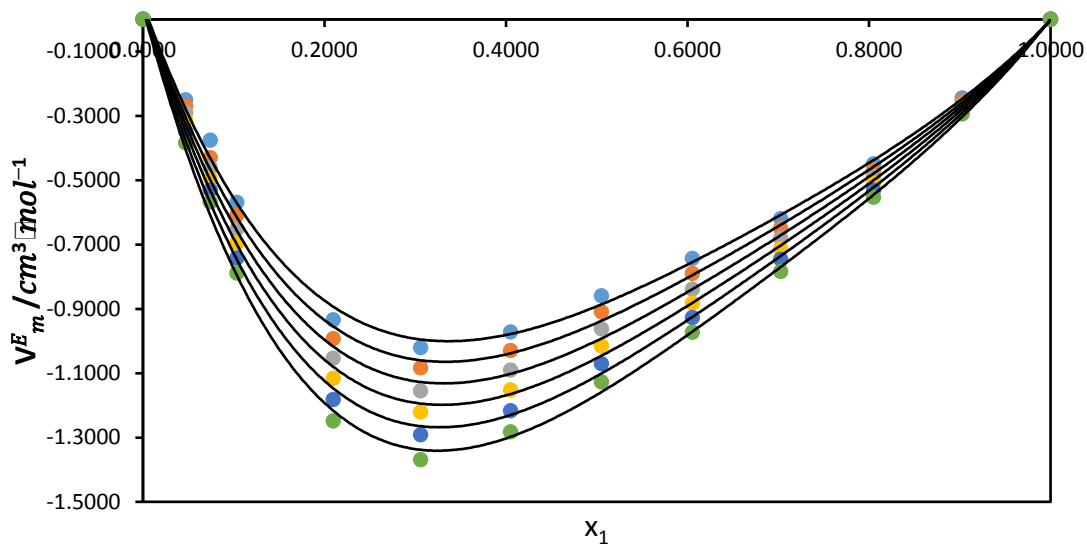
Figure 5.5 Excess molar volumes (V_m^E) for the binary mixture of ({[EMIM]$^+$[EtSO$_4$]$^-$ (x_1) + pentanoic acid (x_2)} as a function of the composition expressed in mole fraction of [EMIM]$^+$[EtSO$_4$]$^-$ at T = 288.15 K (●), 293.15 K (●), 298.15 K (●), 303.15 K (●), 308.15 K (●), 313.15 K (●). The lines were generated using Redlich-Kister curve-fitting.
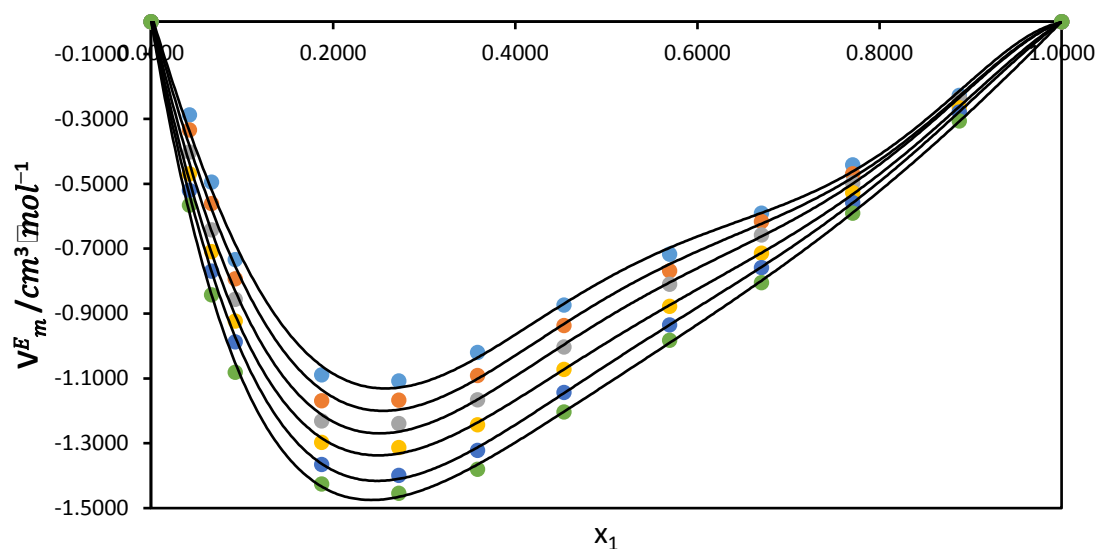
Figure 5.6 Excess molar volumes (V_m^E) for the binary mixture of {[EMIM]⁺[EtSO₄]⁻ (x_1)+ 2-methylpropanoic acid (x_2)} as a function of the composition expressed in mole fraction of [EMIM]⁺[EtSO₄]⁻ at T = 288.15 K (•), 293.15 K (•), 298.15 K (•), 303.15 K (•), 308.15 K (•), 313.15 K (•). The lines were generated using Redlich-Kister curve-fitting.

As seen from the results obtained for the excess molar volume for two-component combinations of {[EMIM]⁺[EtSO₄]⁻ (x_1) + pentanoic acid or 2-methylpropanoic acid (x_2)} which are given in tables 5.1 and 5.2 and are as well plotted in figures 5.5 and 5.6. An observation of V_m^E for both systems studied in this work were negative. Excess molar volume V_m^E depends solely on two factors (i) disparities in intermolecular forces between two components mixtures and (ii) differences in association of molecules, this is as a result of different sizes and shape of the molecules (Anouti, 2010).

According to (Kurnia *et al*., 2011; Jacquemin *et al*., 2011; Govinda *et al*., 2011; Chen, 2014), the excess molar volumes are the outcome of different contrasting occurrence, it was discovered that association between same molecules show an increment in V_m^E results whereas negative results occur as a result of contacts between unlike molecules such as ion-dipole and hydrogen bonding, or structural effects. Therefore, when contact or filling effectiveness between unlike molecules in the two-component liquid mixtures is greater than those between like molecules, V_m^E values become negative, which implies there is stronger attraction/ intermolecular contact between the unlike molecules. It is also noted that ion-dipole contact

that occurs between organic molecular liquid and the ionic liquid also contributes to the negative value of the excess molar volume (Sibiya and Deenadayalu, 2008).

Figure 5.5 and 5.6 shows that V_m^E for the two-component mixture {IL (x_1) + pentanoic or 2-methylpropanoic acid (x_2)} are negative throughout the temperature and concentration, this shows that a more effective contact arose when ionic liquid and carboxylic acids were combined. Ion dipole contacts between the organic molecular liquid and the ionic liquid contributes to the negative value of excess molar volume (Sibiya and Deenadayalu, 2008). The minimum $V_{m,min}^E$ values were found to be -1.3695 cm^3□mol^{-1} and -1.4535 cm^3□mol^{-1} which occurred at $x_1 = 0.3059$ and 0.2720 respectively, for both studied systems. The incidence can be ascribed to large contacts occurring in the molecules of the carboxylic acid in the ionic liquid spaces. This same incidence was noticed for {[EMIM]$^+$[EtSO$_4$]$^-$ + acetic or propionic acid} two-component systems (Singh *et al*., 2014).

However, the values of isentropic compressibility k_s and deviation in isentropic compressibility Δk_s for {[EMIM]$^+$[EtSO$_4$]$^-$ (x_1) + pentanoic or 2-methylpropanoic acid (x_2)} binary systems at different $T = (288.15 - 313.15)$ K are also given in Table 5.1 and 5.2. Figures 5.7 and 5.8 presents the plots of deviation in isentropic compressibility of the binary systems.
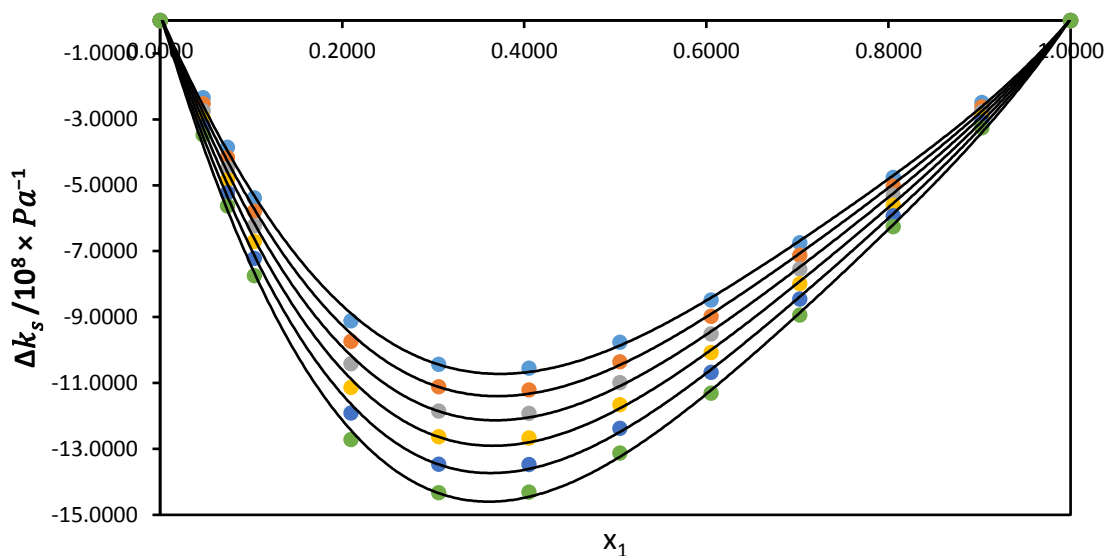
Figure 5.7   Deviation in isentropic compressibility (Δk_s) for the binary mixture of {[EMIM]$^+$[EtSO$_4$]$^-$ (x_1) + pentanoic acid (x_2)} as a function of the composition expressed in mole fraction of [EMIM]$^+$[EtSO$_4$]$^-$ at T = 288.15 K (●), 293.15 K (●), 298.15 K (●), 303.15 K (●), 308.15 K (●), 313.15 K (●). The lines were generated using Redlich-Kister curve-fitting.
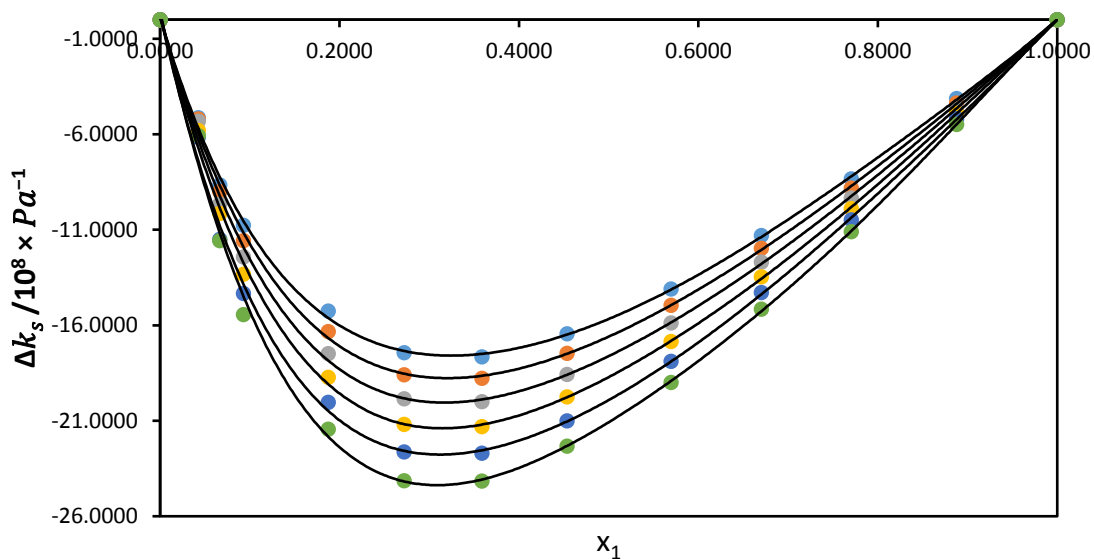
Figure 5.8   Deviation in isentropic compressibility (Δk_s) for the binary mixture of {[EMIM]$^+$[EtSO$_4$]$^-$ (x_1) + 2-methylpropanoic acid (x_2)} as a function of the composition expressed in mole fraction of [EMIM]$^+$[EtSO$_4$]$^-$ at T = 288.15 K (●), 293.15 K (●), 298.15 K (●), 303.15 K (●), 308.15 K (●), 313.15 K (●). The lines were generated using Redlich-Kister curve-fitting.

Furthermore, isentropic compressibility, k_s of the two-component systems studied were given in Tables 5.1 and 5.2 shows that there was an increase with rise in temperature and a decrease with rise in concentration of the IL. The increase in isentropic compressibility explains that there is a rise in random arrangements related to heat and this make the combinations of the mixture to be further compressible (Zafarani-Moattar and Shekaari, 2005). The positive results observed for isentropic compressibility show that the binary mixture is compressible.

For the binary systems studied, the deviation in isentropic compressibility values shows negative results throughout the concentration and at the temperatures examined. This behaviour implies that the binary combinations are less compressible, this probably occurs because there is nearer approach of different molecules as well as strong interface between carboxylic acids and IL mixtures, leading to a reduction in compressibility of binary mixtures (Zafarani-Moattar and Shekaari, 2005). The minimum $\Delta k_{s,min}$ values for the two-component systems of {[EMIM]$^+$[EtSO$_4$]$^-$ (x_1) + pentanoic or 2-methylpropanoic acid (x_2)} were found to be -14.3314 (10^8 Pa^{-1}) and -24.1518(10^8 Pa^{-1}) which occurred at $x_1 = 0.3059$ and 0.3588 respectively.

The Redlich-Kister fitting parameters were calculated from equation (4.2) given as:

$$X = x_1 x_2 \sum_{i=1}^{k} A_i (1 - 2x_i)^{i-1} \tag{4.2}$$

where X symbolizes V_m^E, Δk_s and x_1 represents the concentration of ([EMIM]$^+$[EtSO$_4$]$^-$), x_2 represents the concentration of carboxylic acids, k is the number of coefficients of the polynomial equation, and A_i is for the Redlich-Kister values obtained using least-square method. The standard error σ, have been derived using the equation given below:

$$\sigma(X) = \sum_{i=1}^{n} \left[\frac{X_{exp} - X_{calc}}{N - k} \right]^{1/2} \tag{4.3}$$

N is the number of measured data points, k is the number of coefficients utilized in the equation, X_{exp} and X_{calc} represent the data of the experimental and calculated excess parameters.

The Redlich-Kister values and the standard errors for the two-component systems studied are given in Table 5.3 below:

Table 5.3 Redlich- Kister fitting coefficients and standard deviation, σ, for binary systems of $\{[EMIM]^+[EtSO_4]^- (x_1) +$ pentanoic or 2-methylpropanoic acid $(x_2)\}$ studied at $T = (288.15, 293.15, 298.15, 303.15, 308.15$ and $313.15)$ K.

	T/(K)	A_0	A_1	A_2	A_3	σ
		\{[EMIM]$^+$[EtSO$_4$]$^-$ (x_1) + pentanoic acid (x_2)\}				
V_m^E /cm$^3 \cdot$mol^{-1}	288.15	-3.572	-2.682	-1.523	1.368	0.023
	293.15	-3.779	-2.815	-1.656	1.156	0.021
	298.15	-4.001	-3.012	-1.752	1.127	0.022
	303.15	-4.218	-3.205	-1.870	1.079	0.022
	308.15	-4.441	-3.396	-2.022	0.974	0.021
	313.15	-4.673	-3.603	-2.177	0.886	0.021
Δk_s /10$^8 \times$ Pa^{-1}	288.15	-39.741	-23.372	-6.046	9.736	0.124
	293.15	-42.127	-25.137	-6.93	9.831	0.132
	298.15	-44.704	-27.060	-7.932	9.921	0.139
	303.15	-47.425	-29.068	-9.044	9.909	0.148
	308.15	-50.322	-31.226	-10.281	9.823	0.154
	313.15	-53.355	-33.490	-11.556	9.760	0.160
		\{[EMIM]$^+$[EtSO$_4$]$^-$ (x_1) + 2-methylpropanoic acid (x_2)\}				
V_m^E /cm$^3 \cdot$mol^{-1}	288.15	-3.323	-3.359	-3.226	-0.186	0.036
	293.15	-3.528	-3.494	-3.540	-0.666	0.031
	298.15	-3.746	-3.537	-3.816	-1.496	0.022
	303.15	-4.003	-3.538	-4.146	-2.165	0.013
	308.15	-4.258	-3.692	-4.406	-2.590	0.008
	313.15	-4.441	-3.626	-4.904	-3.393	0.013
Δk_s/10$^8 \times$ Pa^{-1}	288.15	-62.259	-38.671	-30.001	-20.174	0.232
	293.15	-66.149	-42.366	-31.733	-18.809	0.266

298.15	-70.344	-46.018	-34.240	-19.049	0.338
303.15	-74.788	-49.679	-36.980	-19.946	0.326
308.15	-79.342	-52.449	-41.589	-25.872	0.426
313.15	-84.495	-58.215	-42.967	-20.543	0.510

Standard uncertainties u is $u(T) = \pm 0.01$ K and the combined expanded uncertainty Uc in density and speed of sound measurements were less than $Uc\,(\rho) = \pm\,2 \times 10^{-4}$ g·cm^{-3} and $Uc(u)=$ 0.6 m·s^{-1} respectively (0.95 level of confidence).

5.1.2   Ionic liquid {[BMIM]$^{+}$[MeSO$_4$]$^{-}$ with ethanoic or propanoic acid}

Density (ρ) was examined at T = (293.15, 298.15, 303.15, 308.15 and 313.15) K under atmospheric pressure of 0.1 MPa for [BMIM]$^{+}$[MeSO$_4$]$^{-}$, ethanoic acid, propanoic acid, and their two-component combinations of {[BMIM]$^{+}$[MeSO$_4$]$^{-}$ (x_1) + ethanoic or propanoic acid (x_2)}. The resulting data values were presented in Table 5.4 and 5.5. The plots of density (ρ) against mole concentration of [BMIM]$^{+}$[MeSO$_4$]$^{-}$ at studied T = (293.15 – 313.15) K are given in Fig. 5.9 and 5.10 for both binary systems. The results obtained are presented in Tables 5.4 and 5.5 showed that ρ values decrease with rise in temperature and ρ values also rise with increment in concentration of IL. The reason for an increment in ρ values with increasing concentration of ionic liquid may be due to strong interactions of the IL ([BMIM]$^{+}$[MeSO$_4$]$^{-}$) and acetic or propionic acid connections when [BMIM]$^{+}$[MeSO$_4$]$^{-}$ and acids were mixed (Deosarkar, 2013).
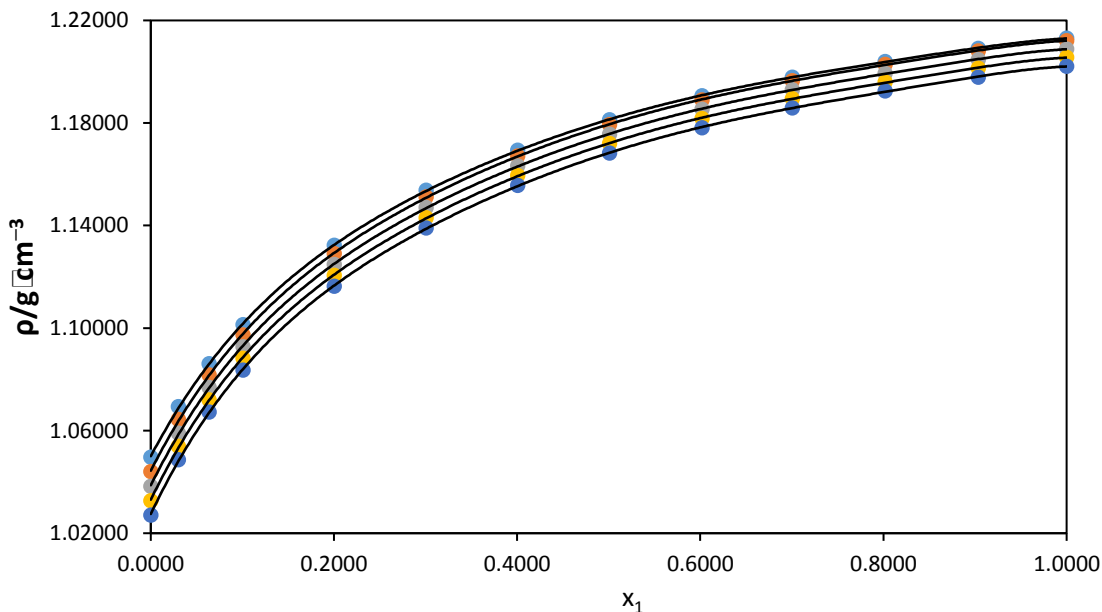
Figure 5.9   Density (ρ) for the binary mixture of {[BMIM]$^+$[MeSO$_4$]$^-$ (x_1) + ethanoic acid (x_2)} plotted against mole fraction of [BMIM]$^+$[MeSO$_4$]$^-$ at T = 293.15 K (●), 298.15 K (●), 303.15 K (●), 308.15 K (●), 313.15 K (●). The line represents the smoothness of the data.
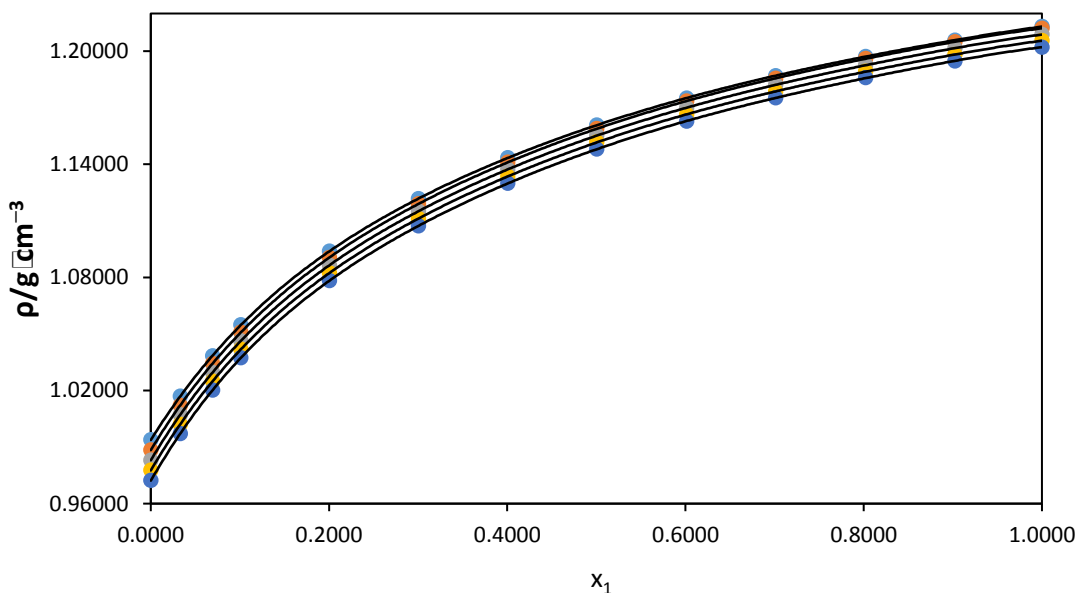
Figure 5.10   Density (ρ) for the binary mixture of {[BMIM]$^+$[MeSO$_4$]$^-$ (x_1) + propanoic acid (x_2)} plotted against mole fraction of [BMIM]$^+$[MeSO$_4$]$^-$ at T = 293.15 K (●), 298.15 K (●), 303.15 K (●), 308.15 K (●), 313.15 K (●). The line represents the smoothness of the data.

Another significant property of liquids which can be used to describe interactions of solvent and solvent, solute and solute, solute and solvent of liquid combinations is speed of sound. Hence, speed of sound (u) of IL $\{[BMIM]^+[MeSO_4]^-\ (x_1)$ + ethanoic acid or propanoic acid $(x_2)\}$ at T = (293.15, 298.15, 303.15, 308.15 and 313.15) K were determined throughout the total range of concentrations of 0.1 to 1.0, the resulting data were given in Tables 5.4 and 5.5. The plots of speeds of sound against mole fraction of $[BMIM]^+[MeSO_4]^-$ at investigated temperatures were presented in Figures 5.11 and 5.12. From the experimental results, it was deduced that there was an increment as concentration of $[BMIM]^+[MeSO_4]^-$ increases at the studied temperatures for u values. In addition, it was also found that there was a decrease in u values whenever there is a rise in temperature for both studied systems.
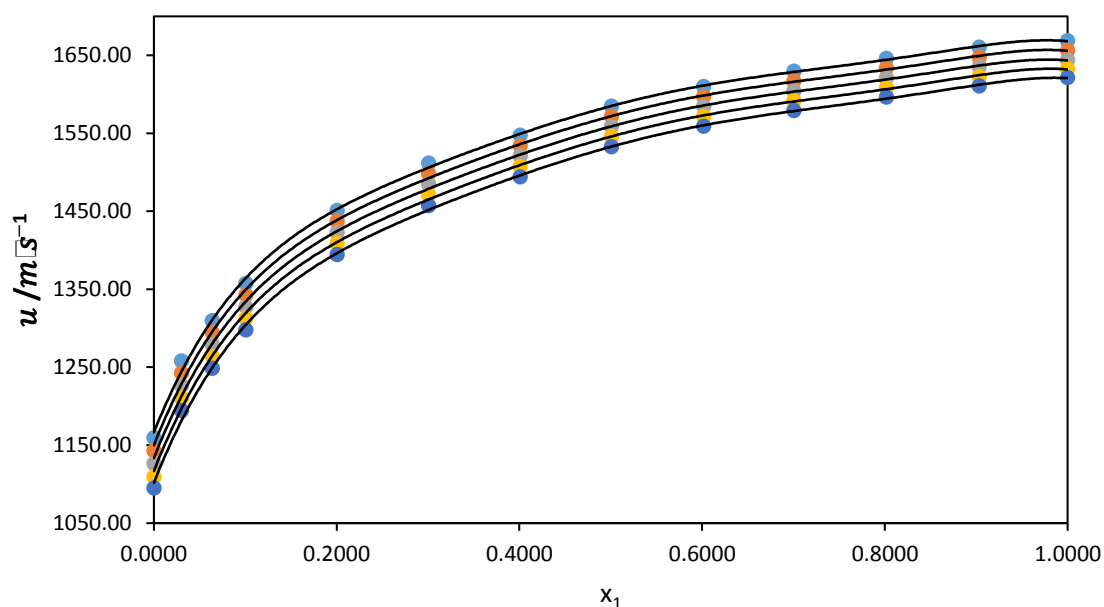
Figure 5.11 Speed of sound (u) for the binary mixture of $\{[BMIM]^+[MeSO_4]^-\ (x_1)$ + ethanoic acid $(x_2)\}$ plotted against mole fraction of $[BMIM]^+[MeSO_4]^-$ at T = 293.15 K (●), 298.15 K (●), 303.15 K (●), 308.15 K (●), 313.15 K (●). The line represents the smoothness of the data.
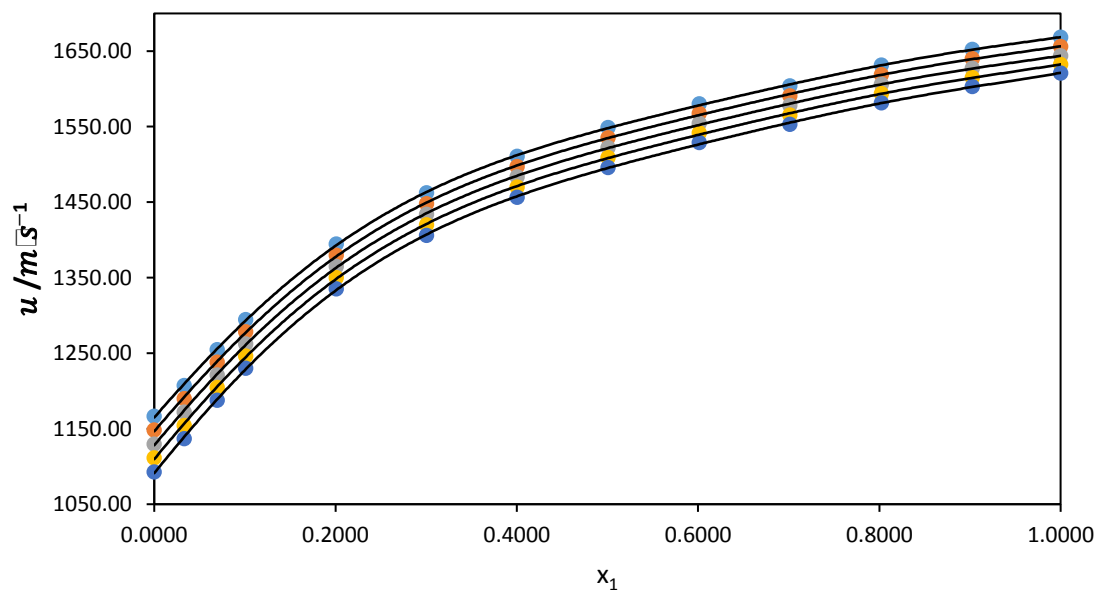
Figure 5.12 Speed of sound (u) for the binary mixture of $\{[BMIM]^+[MeSO_4]^-$ (x_1) + propanoic acid (x_2)$\}$ plotted against mole fraction of $[BMIM]^+[MeSO_4]^-$ at $T = 293.15$ K (●), 298.15 K (●), 303.15 K (●), 308.15 K (●), 313.15 K (●). The line represents the smoothness of the data.

Tables 5.4 and 5.5 show the results of excess molar volumes V_m^E for the binary mixtures of $\{[BMIM]^+[MeSO_4]^-$ (x_1) + ethanoic or propanoic acid (x_2)$\}$ at all investigated temperatures.

Table 5.4   Density (ρ), excess molar volume (V_m^E), speed of sound (u), isentropic compressibility (k_s), deviation in isentropic compressibility (Δk_s) and intermolecular free length (L_f) for the binary system {[BMIM]$^+$[MeSO$_4$]$^-$ (x_1) + ethanoic acid (x_2)} from $T =$ (293.15 – 313.15) K.

x_1	ρ/g·cm^{-3}	V_m^E /cm^3·mol^{-1}	u/m·s^{-1}	k_s/10$^8 \times$ Pa^{-1}	Δk_s/10$^8 \times$ Pa^{-1}	L_f/10^{-5} m
			T = 293.15 K			
0.0000	1.04965	0.0000	1159.31	70.8853	0.0000	1.7159
0.0302	1.06943	-0.1885	1258.02	59.0843	-10.5534	1.5666
0.0637	1.08613	-0.2627	1309.73	53.6729	-14.5826	1.4931
0.1006	1.10139	-0.3131	1357.33	49.2818	-17.4515	1.4307
0.2004	1.13226	-0.3865	1450.86	41.9570	-20.6559	1.3201
0.3008	1.15379	-0.4234	1511.68	37.9275	-20.5435	1.2551
0.4008	1.16934	-0.4194	1547.28	35.7207	-18.6244	1.2181
0.5008	1.18126	-0.4024	1584.60	33.7145	-16.5033	1.1834
0.6018	1.19063	-0.3613	1609.94	32.4044	-13.6446	1.1602
0.7006	1.19792	-0.2968	1629.40	31.4425	-10.5294	1.1428
0.8017	1.20403	-0.2170	1646.09	30.6519	-7.1442	1.1284
0.9034	1.20912	-0.1259	1660.23	30.0050	-3.5940	1.1164
1.0000	1.21303	0.0000	1668.47	29.6136	0.0000	1.1091
			T = 298.15 K			
0.0000	1.04401	0.0000	1142.78	73.3449	0.0000	1.7615
0.0302	1.06437	-0.2003	1242.27	60.8800	-11.1568	1.6048
0.0637	1.08170	-0.2897	1294.52	55.1665	-15.4213	1.5277
0.1006	1.09741	-0.3450	1342.57	50.5544	-18.4375	1.4624
0.2004	1.12906	-0.4185	1436.86	42.8997	-21.7723	1.3472
0.3008	1.15113	-0.4499	1498.17	38.7039	-21.6256	1.2796
0.4008	1.16713	-0.4440	1534.01	36.4104	-19.5935	1.2411
0.5008	1.17937	-0.4222	1571.62	34.3285	-17.3482	1.2051
0.6018	1.18898	-0.3726	1597.19	32.9694	-14.3367	1.1810
0.7006	1.19651	-0.3056	1616.76	31.9736	-11.0580	1.1630

0.8017	1.20285	-0.2270	1633.53	31.1555	-7.4982	1.1481
0.9034	1.20809	-0.1284	1647.68	30.4899	-3.7634	1.1357
1.0000	1.21214	0.0000	1656.23	30.0750	0.0000	1.1280

T = 303.15 K

0.0000	1.03833	0.0000	1126.27	75.9241	0.0000	1.8085
0.0302	1.05909	-0.2142	1226.29	62.7888	-11.7656	1.6447
0.0637	1.07686	-0.3207	1279.10	56.7585	-16.2786	1.5637
0.1006	1.09275	-0.3776	1327.58	51.9229	-19.4432	1.4956
0.2004	1.12481	-0.4555	1422.68	43.9244	-22.9185	1.3756
0.3008	1.14707	-0.4802	1484.47	39.5612	-22.7348	1.3055
0.4008	1.16325	-0.4709	1520.62	37.1780	-20.5888	1.2655
0.5008	1.17565	-0.4469	1558.55	35.0172	-18.2188	1.2282
0.6018	1.18531	-0.3855	1584.33	33.6105	-15.0491	1.2033
0.7006	1.19297	-0.3179	1603.99	32.5813	-11.6027	1.1847
0.8017	1.19940	-0.2374	1620.95	31.7319	-7.8681	1.1692
0.9034	1.20468	-0.1290	1635.14	31.0470	-3.9455	1.1565
1.0000	1.20881	0.0000	1643.75	30.6175	0.0000	1.1485

T = 308.15 K

0.0000	1.03270	0.0000	1109.56	78.6545	0.0000	1.8574
0.0302	1.05388	-0.2300	1210.35	64.7718	-12.4460	1.6855
0.0637	1.07205	-0.3508	1263.72	58.4094	-17.2167	1.6006
0.1006	1.08824	-0.4172	1312.63	53.3324	-20.5407	1.5295
0.2004	1.12056	-0.4890	1408.55	44.9801	-24.1482	1.4046
0.3008	1.14310	-0.5152	1470.81	40.4391	-23.9194	1.3318
0.4008	1.15949	-0.5046	1507.25	37.9633	-21.6440	1.2904
0.5008	1.17201	-0.4755	1545.60	35.7170	-19.1375	1.2516
0.6018	1.18177	-0.4078	1571.59	34.2600	-15.7938	1.2258
0.7006	1.18951	-0.3345	1591.39	33.1955	-12.1633	1.2066
0.8017	1.19597	-0.2411	1608.50	32.3175	-8.2326	1.1906
0.9034	1.20135	-0.1330	1622.77	31.6095	-4.1073	1.1775
1.0000	1.20554	0.0000	1632.44	31.1274	0.0000	1.1685

_T_ = 313.15 K

0.0000	1.02711	0.0000	1094.85	81.2218	0.0000	1.9044
0.0302	1.04872	-0.2471	1194.44	66.8365	-12.8868	1.7275
0.0637	1.06727	-0.3831	1248.36	60.1237	-17.9394	1.6385
0.1006	1.08363	-0.4517	1297.72	54.7971	-21.4378	1.5642
0.2004	1.11628	-0.5245	1394.47	46.0689	-25.2171	1.4342
0.3008	1.13905	-0.5493	1457.23	41.3428	-24.9685	1.3587
0.4008	1.15562	-0.5381	1493.96	38.7709	-22.5850	1.3157
0.5008	1.16827	-0.5055	1532.70	36.4369	-19.9619	1.2755
0.6018	1.17811	-0.4302	1558.97	34.9252	-16.4666	1.2488
0.7006	1.18590	-0.3493	1579.01	33.8206	-12.6744	1.2289
0.8017	1.19246	-0.2551	1596.28	32.9107	-8.5689	1.2122
0.9034	1.19787	-0.1372	1610.57	32.1834	-4.2552	1.1987
1.0000	1.20212	0.0000	1621.16	31.6519	0.0000	1.1888

Table 5.5   Density (ρ), excess molar volume (V_m^E), speed of sound (u), isentropic compressibility (k_s), deviation in isentropic compressibility (Δk_s) and intermolecular free length (L_f) for the binary system {[BMIM]$^+$[MeSO$_4$]$^-$ (x_1) + propanoic acid (x_2)} from T = (293.15 – 313.15) K.

x_1	ρ/g·cm^{-3}	V_m^E /cm^3·mol^{-1}	u/m·s^{-1}	k_s/10^8 × Pa^{-1}	Δk_s/10^8 × Pa^{-1}	L_f/10^{-5} m
			T = 293.15 K			
0.0000	0.99378	0.0000	1166.35	73.9692	0.0000	1.7528
0.0332	1.01692	-0.3178	1207.36	67.4592	-5.0369	1.6739
0.0693	1.03840	-0.5761	1254.69	61.1736	-9.7222	1.5940
0.1009	1.05483	-0.7554	1294.60	56.5646	-12.9280	1.5328
0.2007	1.09389	-0.9420	1394.45	47.0133	-18.0540	1.3974
0.3004	1.12176	-0.9053	1462.27	41.6914	-18.9530	1.3160
0.4005	1.14340	-0.8147	1510.96	38.3086	-17.8965	1.2614
0.5005	1.16078	-0.7073	1548.72	35.9174	-15.8513	1.2214
0.6014	1.17510	-0.5796	1580.51	34.0667	-13.2284	1.1895
0.7012	1.18700	-0.4534	1603.84	32.7511	-10.1172	1.1664
0.8022	1.19717	-0.3108	1631.41	31.3848	-7.0014	1.1418
0.9024	1.20583	-0.1664	1652.53	30.3680	-3.5728	1.1231
1.0000	1.21303	0.0000	1668.47	29.6136	0.0000	1.1091
			T = 298.15 K			
0.0000	0.98841	0.0000	1148.13	76.7503	0.0000	1.8019
0.0332	1.01210	-0.3406	1189.79	69.7967	-5.4035	1.7184
0.0693	1.03428	-0.6327	1238.08	63.0762	-10.4400	1.6335
0.1009	1.05091	-0.8099	1278.63	58.2029	-13.8367	1.5692
0.2007	1.09055	-0.9901	1379.73	48.1687	-19.2142	1.4275
0.3004	1.11895	-0.9502	1448.21	42.6115	-20.1172	1.3426
0.4005	1.14105	-0.8575	1497.39	39.0865	-18.9707	1.2859
0.5005	1.15894	-0.7636	1535.52	36.5956	-16.7933	1.2443
0.6014	1.17345	-0.6159	1567.56	34.6808	-14.0005	1.2113
0.7012	1.18560	-0.4835	1591.10	33.3171	-10.7059	1.1872

0.8022	1.19613	-0.3563	1618.75	31.9053	-7.4011	1.1618
0.9024	1.20492	-0.1974	1639.95	30.8589	-3.7696	1.1426
1.0000	1.21214	0.0000	1656.23	30.0750	0.0000	1.1280

$T = 303.15$ K

0.0000	0.98303	0.0000	1129.70	79.7091	0.0000	1.8531
0.0332	1.00709	-0.3636	1172.03	72.2857	-5.7931	1.7647
0.0693	1.02958	-0.6732	1221.26	65.1215	-11.1860	1.6749
0.1009	1.04641	-0.8599	1262.47	59.9595	-14.7950	1.6072
0.2007	1.08644	-1.0520	1364.79	49.4156	-20.4411	1.4590
0.3004	1.11507	-1.0130	1434.07	43.6072	-21.3544	1.3706
0.4005	1.13731	-0.9151	1483.71	39.9412	-20.1070	1.3117
0.5005	1.15531	-0.8135	1522.24	37.3538	-17.7844	1.2685
0.6014	1.16989	-0.6555	1554.58	35.3694	-14.8176	1.2344
0.7012	1.18210	-0.5114	1578.31	33.9595	-11.3280	1.2095
0.8022	1.19269	-0.3737	1606.16	32.501	-7.8258	1.1833
0.9024	1.20153	-0.2037	1627.48	31.4221	-3.9845	1.1635
1.0000	1.20881	0.0000	1643.75	30.6175	0.0000	1.1485

$T = 308.15$ K

0.0000	0.97764	0.0000	1111.29	82.8258	0.0000	1.9060
0.0332	1.00209	-0.3872	1154.39	74.8839	-6.2250	1.8123
0.0693	1.02488	-0.7143	1204.51	67.2523	-11.9914	1.7175
0.1009	1.04190	-0.9106	1246.35	61.7864	-15.8218	1.6462
0.2007	1.08233	-1.1141	1349.89	50.7043	-21.7460	1.4913
0.3004	1.11119	-1.0745	1419.92	44.6359	-22.6593	1.3992
0.4005	1.13359	-0.9709	1470.12	40.8168	-21.3042	1.3380
0.5005	1.15170	-0.8612	1509.03	38.1299	-18.8203	1.2932
0.6014	1.16637	-0.6932	1541.68	36.0726	-15.6635	1.2579
0.7012	1.17862	-0.5360	1565.63	34.6136	-11.9628	1.2322
0.8022	1.18927	-0.3868	1593.70	33.1061	-8.2462	1.2050
0.9024	1.19815	-0.2044	1615.15	31.9936	-4.1773	1.1846
1.0000	1.20554	0.0000	1632.44	31.1274	0.0000	1.1685

T = 313.15 K

0.0000	0.97225	0.0000	1092.80	86.1274	0.0000	1.9610
0.0332	0.99709	-0.4130	1136.85	77.5999	-6.7185	1.8614
0.0693	1.02018	-0.7590	1187.82	69.4737	-12.8792	1.7613
0.1009	1.03741	-0.9660	1230.27	63.6869	-16.9427	1.6863
0.2007	1.07822	-1.1835	1335.07	52.0337	-23.1609	1.5242
0.3004	1.10732	-1.1471	1405.86	45.6921	-24.0704	1.4283
0.4005	1.12987	-1.0400	1456.65	41.7119	-22.5985	1.3647
0.5005	1.14810	-0.9252	1495.95	38.9213	-19.9406	1.3183
0.6014	1.16285	-0.7496	1528.90	36.7890	-16.5786	1.2817
0.7012	1.17517	-0.5829	1553.10	35.2778	-12.6530	1.2551
0.8022	1.18587	-0.4250	1581.37	33.7208	-8.7053	1.2270
0.9024	1.19479	-0.2315	1603.00	32.5718	-4.3945	1.2060
1.0000	1.20212	0.0000	1621.16	31.6519	0.0000	1.1888

The plots of excess molar volume V_m^E against mole fraction of {[BMIM]$^+$[MeSO$_4$]$^-$ for the binary systems of {[BMIM]$^+$[MeSO$_4$]$^-$ + ethanoic or propanoic acid} at T = (293.15, 298.15, 303.15, 308.15 and 313.15) K have been presented in Figures 5.13 and 5.14 below:
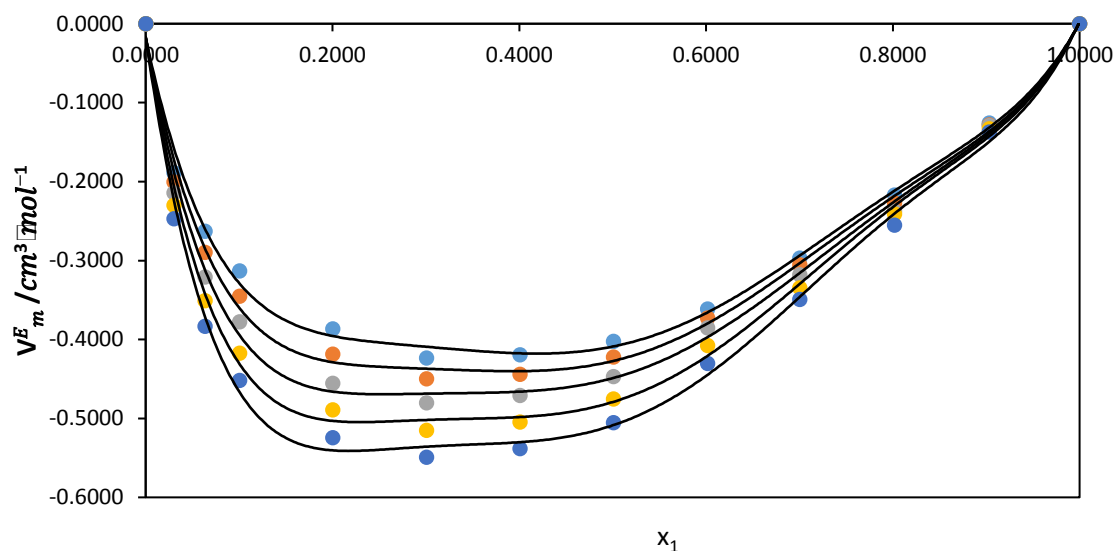
Figure 5.13 Excess molar volumes (V_m^E) for the binary mixture of ({[BMIM]$^+$[MeSO$_4$]$^-$ (x_1) + ethanoic acid (x_2)} as a function of the composition expressed in mole fraction of [BMIM]$^+$[MeSO$_4$]$^-$ at T = 293.15 K (●), 298.15 K (●), 303.15 K (●), 308.15 K (●), 313.15 K (●). The lines were generated using Redlich-Kister curve-fitting.
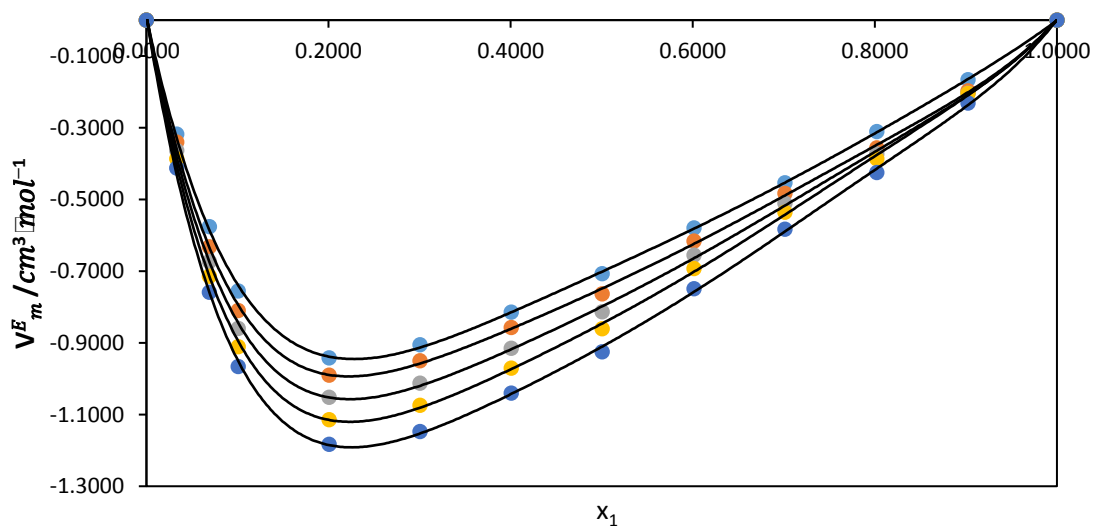
Figure 5.14 Excess molar volumes (V_m^E) for the binary mixture of {[BMIM]$^+$[MeSO$_4$]$^-$ (x_1)+ propanoic acid (x_2)} as a function of the composition expressed in mole fraction of [BMIM]$^+$[MeSO$_4$]$^-$ at T = 293.15 K (●), 298.15 K (●), 303.15 K (●), 308.15 K (●), 313.15 K (●). The lines were generated using Redlich-Kister curve-fitting.

The obtained results of V_m^E for two-component combinations of $\{[BMIM]^+[MeSO_4]^-$ (x_1) + ethanoic or propanoic acid (x_2) were presented in Tables 5.4 and 5.5 and are as well plotted in Figures 5.13 and 5.14. The excess molar volumes gave negative results for both systems studied, but at high concentration of propanoic acid, $\{[BMIM]^+[MeSO_4]^-$ (x_1) + propanoic acid (x_2) tend to decrease more sharply compared to $\{[BMIM]^+[MeSO_4]^-$ (x_1) + ethanoic acid (x_2). This is due to strong interaction by hydrogen bonding of the propanoic acid molecules, but when IL concentration increases, the self-association structure of the acid collapses. The minimum $V_{m,min}^E$ values for the ethanoic acid and propanoic acid binary mixtures gave -0.5493 cm^3·mol^{-1} and -1.1835 cm^3·mol^{-1} which occurred at $x_1 = 0.3008$ and 0.2007 respectively, for both systems studied respectively. This occurs because the carboxylic acid molecules in the ionic liquid interstices tend to be filled up when mixing of the components occur.

The isentropic compressibility, k_s of the two-component systems studied were reported in Table 5.4 and 5.5. k_s values were found to be positive for both studied systems which indicates that the binary mixture is compressible. In addition, k_s shows an increment with rise in temperature and a reduction occur with increasing concentration of IL. This increment in isentropic compressibility explains that, an increment in arbitrary directions associated with heat makes the mixture become further agitated (Zafarani-Moattar and Shekaari, 2005).

For the binary systems studied, the deviation in isentropic compressibility values shows negative results throughout the concentration and at the temperatures examined. This behaviour gave an indication that the binary mixtures are less compressible, this probably occurs because there is nearer approach of different molecules as well as strong interface between carboxylic acids and IL mixtures, leading to a reduction in compressibility of binary mixtures thereby giving a negative deviation in isentropic compressibility (Zafarani-Moattar and Shekaari, 2005; Gowrisankar, 2013). The minimum $\Delta k_{s,min}$ values for the two-component systems of $\{[BMIM]^+[MeSO_4]^-$ (x$_1$) + ethanoic or propanoic acid (x$_2$)$\}$ were found to be -25.2171 (10^8/Pa^{-1}) and -24.0704 (10^8/Pa^{-1}) which occurred at $x_1 = 0.2004$ and 0.3004 respectively.

The plots of deviation in isentropic compressibility for the binary systems are presented in Figures 5.15 and 5.16 below:
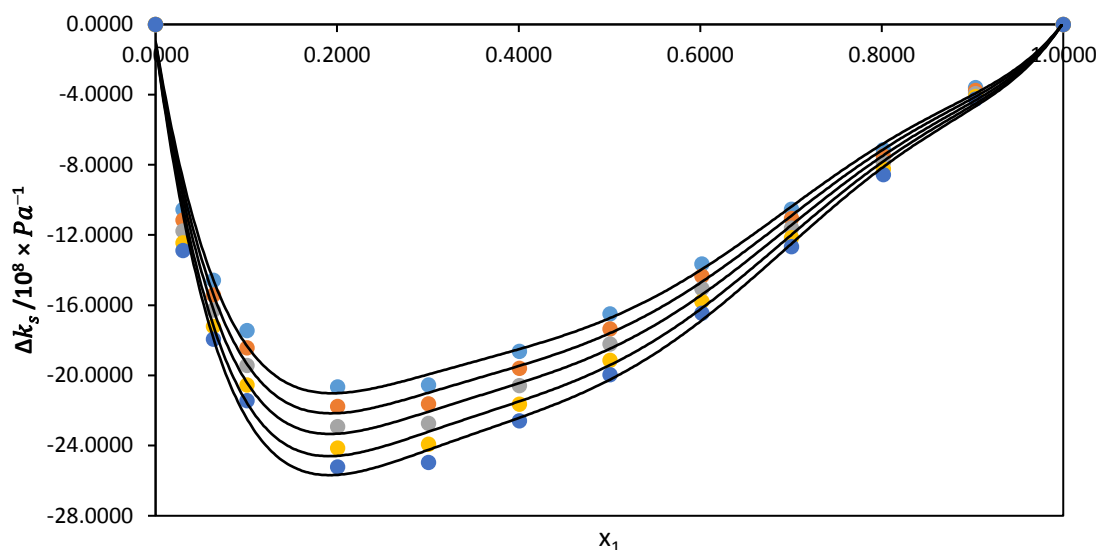
Figure 5.15 Deviation in isentropic compressibility (Δk_s) for the binary mixture of {[BMIM]$^+$[MeSO$_4$]$^-$ (x_1) + ethanoic acid (x_2)} as a function of the composition expressed in mole fraction of [BMIM]$^+$[MeSO$_4$]$^-$ at T = 293.15 K (●), 298.15 K (●), 303.15 K (●), 308.15 K (●), 313.15 K (●). The lines were generated using Redlich-Kister curve-fitting.
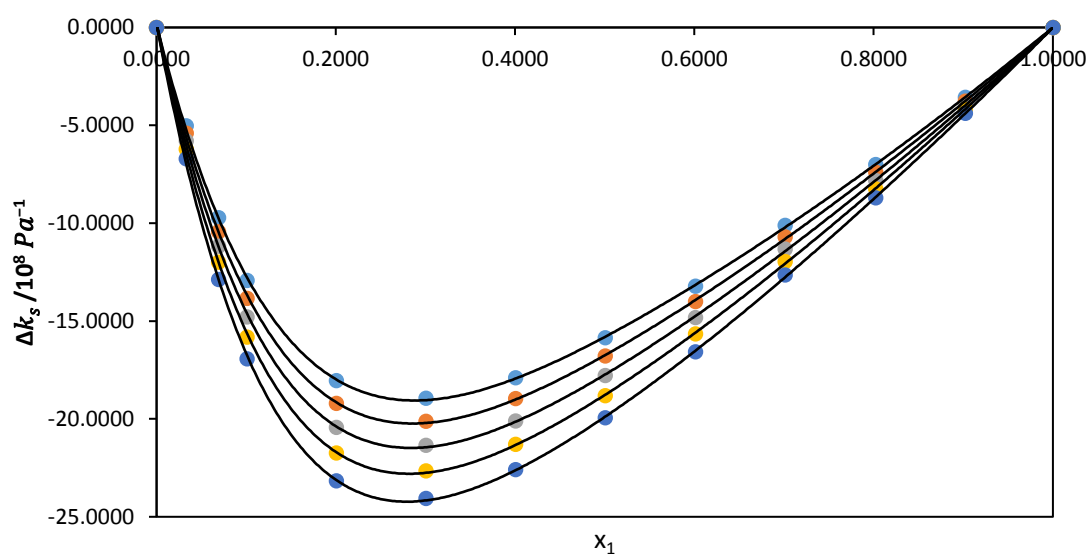
Figure 5.16 Deviation in isentropic compressibility (Δk_s) for the binary mixture of {[BMIM]$^+$[MeSO$_4$]$^-$ (x_1) + propanoic acid (x_2)} as a function of the composition expressed in mole fraction of [BMIM]$^+$[MeSO$_4$]$^-$ at T = 293.15 K (●), 298.15 K (●), 303.15 K (●), 308.15 K (●), 313.15 K (●). The lines were generated using Redlich-Kister curve-fitting.

Figures 5.17 and 5.18 presents the plots of intermolecular free length (L_f) against mole fraction for the binary systems of {[BMIM]$^+$[MeSO$_4$]$^-$ (x_1) + ethanoic or propanoic acid (x_2)} studied at T = (293.15, 298.15, 303.15, 308.15 and 313.15) K.
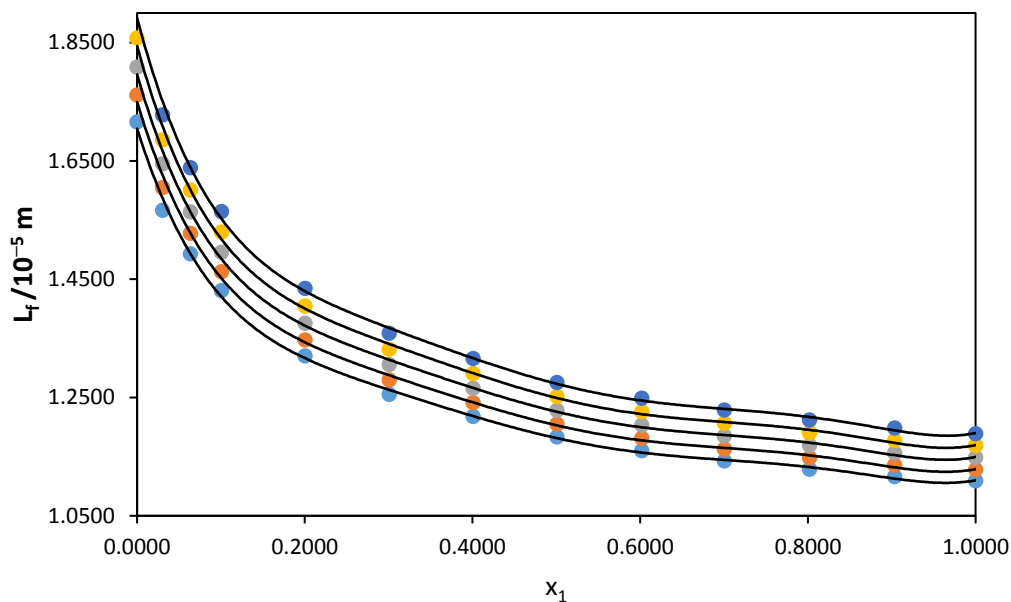
Figure 5.17   Intermolecular free length (L_f) for the binary mixture of {[BMIM]$^+$[MeSO$_4$]$^-$ (x_1) + ethanoic acid (x_2)} as a function of the composition expressed in mole fraction of [BMIM]$^+$[MeSO$_4$]$^-$ at T = 293.15 K (●), 298.15 K (●), 303.15 K (●), 308.15 K (●), 313.15 K (●). The lines were generated using Redlich-Kister curve-fitting.
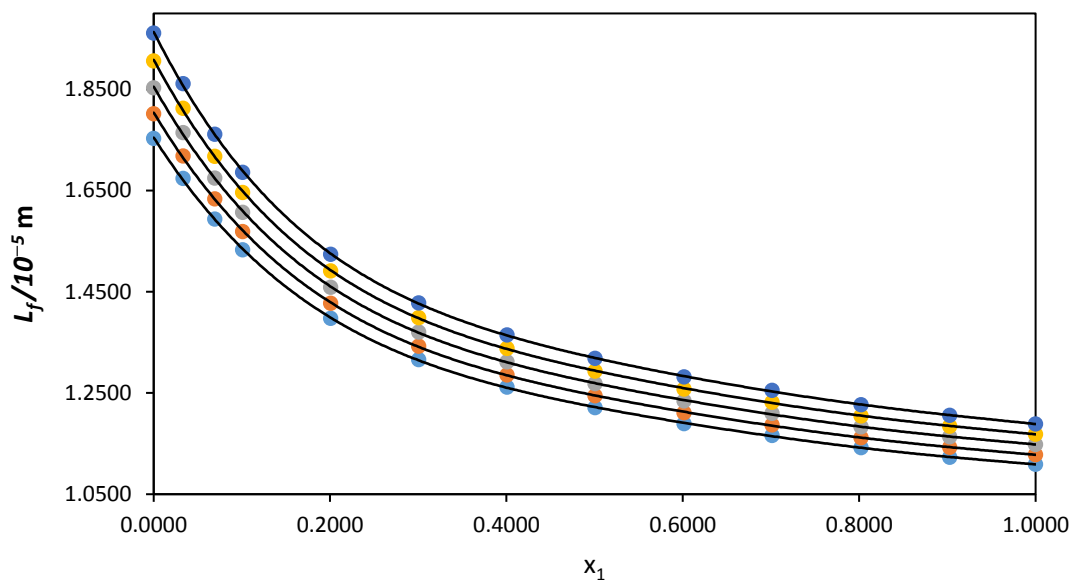
Figure 5.18   Intermolecular free length (L_f) for the binary mixture of $\{[BMIM]^+[MeSO_4]^-$ (x_1) + propanoic acid $(x_2)\}$ as a function of the composition expressed in mole fraction of $[BMIM]^+[MeSO_4]^-$ at $T = 293.15$ K (●), 298.15 K (●), 303.15 K (●), 308.15 K (●), 313.15 K (●). The lines were generated using Redlich-Kister curve-fitting.

Tables 5.4 and 5.5 present the values of intermolecular free length (L_f) for $\{[BMIM]^+[MeSO_4]^-$ (x_1) + ethanoic or propanoic acid $(x_2)\}$ two-component solution over the whole concentration of the binary solutions at several temperatures. Figures 5.17 and 5.18 show the plots of intermolecular free length against mole fraction (x_1). Intermolecular free length supports the determination of the length between centers of two different molecules in liquid solutions otherwise known as intermolecular forces.

The distance between two surface of molecules gives a description of a repulsive force while the centre of attraction of molecules with respect to the distance describes attractive force. The changes in speed of sound of liquid component combinations produce a vital part in defining the free length where the association between L_f and u are connected inversely. The length between two molecular surfaces is evidently known by an increment in intermolecular free length as well as a reduction in the speed of sound. This is a valued means for determining the existence of molecular contacts that occur between the component in the binary solutions. A closer look at Table 5.4 and 5.5 as well as Figures 5.17 and 5.18 clearly shows that u and L_f are related in an inverse manner but the L_f showed that it is directly proportional to temperature.

The Redlich-Kister fitting parameters were calculated from equation (4.2) given as:

$$X = x_1 x_2 \sum_{i=1}^{k} A_i (1 - 2x_i)^{i-1} \tag{4.2}$$

where X represents V_m^E, Δk_s and x_1 represents the concentration of ([BMIM]$^+$[MeSO$_4$]$^-$), x_2 represents the concentration of carboxylic acids, k is the number of coefficients of the polynomial expansion, and A_i represents the Redlich-Kister parameters obtained using least-square method. The standard error σ, was obtained using the equation given below:

$$\sigma(X) = \sum_{i=1}^{n} \left[\frac{X_{exp} - X_{calc}}{N-k} \right]^{1/2} \tag{4.3}$$

where N is the number of measured data points, k is the number of coefficients utilized in the Redlich-Kister equation, X_{exp} and X_{calc} are the results of the experimental and calculated excess parameters.

The Redlich-Kister parameters and the standard deviation errors for the binary systems studied are given in Table 5.6 below:

Table 5.6   Redlich- Kister fitting coefficients and standard deviation, σ, for binary systems of {[BMIM]$^+$[MeSO$_4$]$^-$ (x_1) + ethanoic or propanoic acid (x_2)} studied at T = (293.15, 298.15, 303.15, 308.15 and 313.15) K.

	T/(K)	A_0	A_1	A_2	A_3	σ
		{[BMIM]$^+$[MeSO$_4$]$^-$ (x_1) + ethanoic acid (x_2)}				
V_m^E/cm^3·mol^{-1}	293.15	-1.548	-0.362	-1.327	-1.781	0.020
	298.15	-1.615	-0.438	-1.511	-1.962	0.021
	303.15	-1.696	-0.513	-1.690	-2.196	0.022
	308.15	-1.802	-0.578	-1.820	-2.485	0.024
	313.15	-1.908	-0.637	-1.982	-2.736	0.026
Δk_s/10^8 × Pa^{-1}	293.15	-62.958	-37.894	-82.809	-106.787	0.999
	298.15	-66.154	-39.849	-87.703	-113.495	1.058
	303.15	-69.443	-41.871	-92.735	-120.198	1.118
	308.15	-72.905	-44.028	-98.104	-128.009	1.185
	313.15	-76.081	-46.287	-102.054	-132.957	1.213

$L_f/10^{-5}$ m	293.15	3.952	-2.185	14.993	12.068	0.597
	298.15	4.021	-2.238	15.315	12.411	0.611
	303.15	4.095	-2.294	15.653	12.766	0.626
	308.15	4.170	-2.351	15.999	13.129	0.642
	313.15	4.246	-2.410	16.351	13.507	0.657
		{[BMIM]$^+$[MeSO$_4$]$^-$ (x_1) + propanoic acid (x_2)}				
V_m^E/cm$^3\cdot$mol^{-1}	293.15	-2.764	-2.285	-3.375	-2.695	0.010
	298.15	-2.918	-2.281	-3.816	-2.977	0.016
	303.15	-3.112	-2.445	-3.987	-3.196	0.017
	308.15	-3.299	-2.611	-4.134	-3.477	0.018
	313.15	-3.546	-2.732	-4.431	-3.614	0.019
$\Delta k_s/10^8 \times$ Pa^{-1}	293.15	-63.104	-48.716	-42.563	-22.482	0.097
	298.15	-66.796	-51.621	-46.103	-25.555	0.106
	303.15	-70.698	-54.754	-49.873	-28.579	0.116
	308.15	-74.776	-58.111	-53.797	-32.254	0.125
	313.15	-79.173	-61.668	-58.229	-36.474	0.134
$L_f/10^{-5}$ m	293.15	4.080	-2.14	15.555	13.027	0.604
	298.15	4.152	-2.198	15.911	13.439	0.620
	303.15	4.228	-2.261	16.285	13.866	0.636
	308.15	4.305	-2.325	16.668	14.309	0.652
	313.15	4.384	-2.392	17.061	14.768	0.669

Standard uncertainties u are $u(T) = \pm 0.01$ K and the combined expanded uncertainty U_c in density and speed of sound measurements were less than $U_c (\rho) = \pm 2 \times 10^{-4}$ g$\cdot$cm^{-3} and $U_c(u) = 0.6$ m$\cdot$s^{-1} respectively (0.95 level of confidence)

5.1.3 Ionic liquid {[EPMpyr]$^+$[SAL]$^-$ with ethanoic or propanoic acid}

The experimental densies of pure liquid component [EPMpyr]$^+$[SAL]$^-$, ethanoic acid, propanoic acid as well as their two-component combinations {[EPMpyr]$^+$[SAL]$^-$ (x_1) + ethanoic or propanoic acid (x_2)} were measured at studied temperatures T = (293.15, 298.15, 303.15, 308.15 and 313.15) K. The obtained results are presented in Table 5.7 and 5.8 while the plot of density versus concentration of [EPMpyr]$^+$[SAL]$^-$ are shown in Figure 5.19 and 5.20 for both systems. It can be observed from the results that density showed an increase in a non-linear manner with increase in concentration of IL while density decreases whenever there is rise in temperature This can be attributed to the occurrence of intermolecular interactions in IL and carboxylic acids molecules of the mixtures (Vasanthakumar et al. 2016).
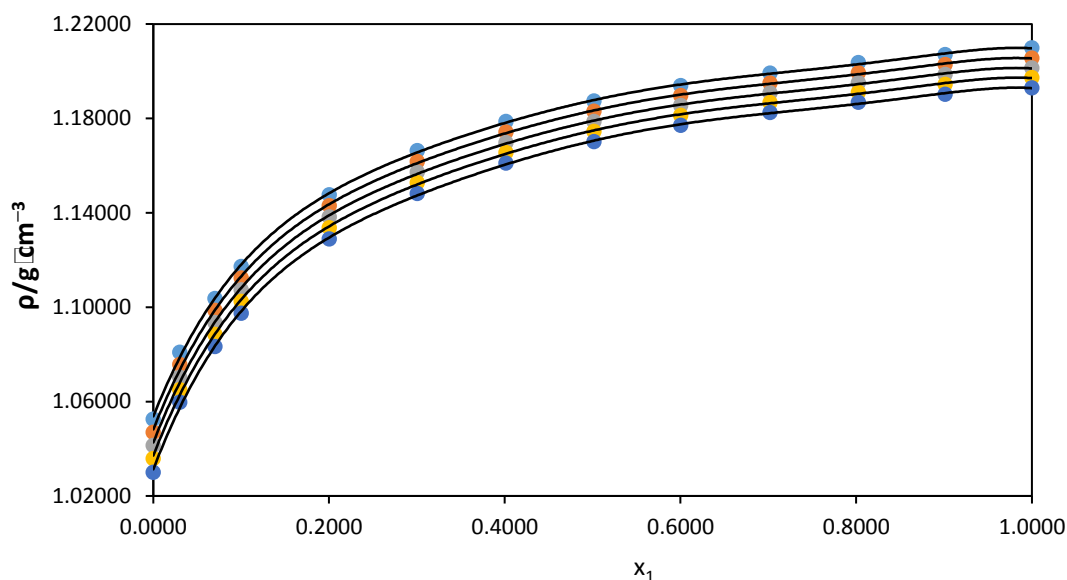
Figure 5.19   Density (ρ) for the binary mixture of {[EPMpyr]$^+$[SAL]$^-$ (x_1) + ethanoic acid (x_2)} plotted against mole fraction of [EPMpyr]$^+$[SAL]$^-$at T = 293.15 K (●), 298.15 K (●), 303.15 K (●), 308.15 K (●), 313.15 K (●). The line represents the smoothness of the data.
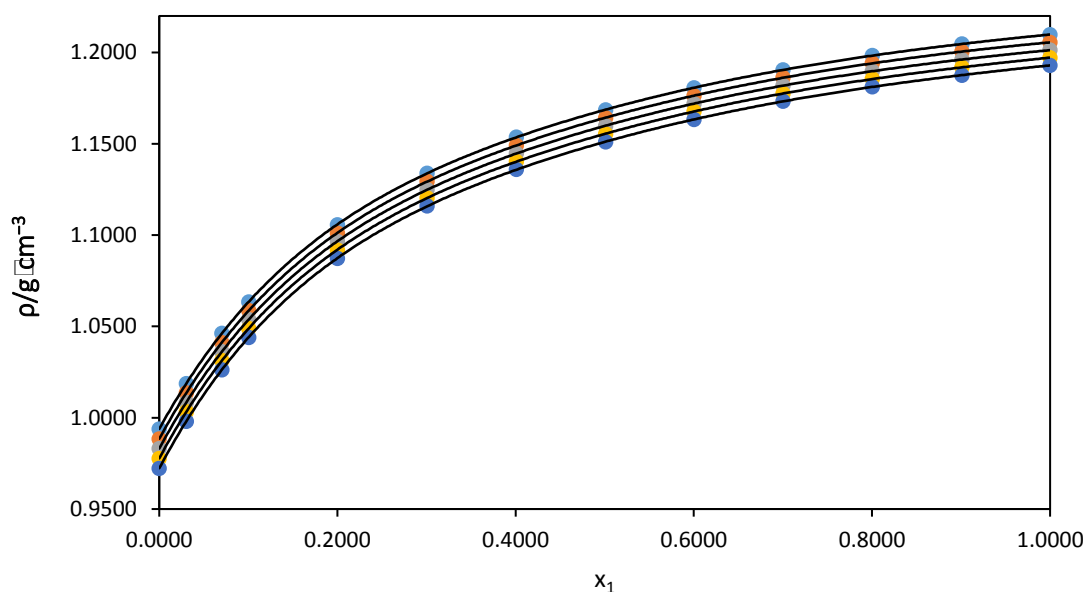
Figure 5.20   Density (ρ) for the binary mixture of {[EPMpyr]$^+$[SAL]$^-$ (x_1) + propanoic acid (x_2)} plotted against mole fraction of [EPMpyr]$^+$[SAL]$^-$ at T = 293.15 K (●), 298.15 K (●), 303.15 K (●), 308.15 K (●), 313.15 K (●). The line represents the smoothness of the data.

The experimental values of speed of sound u for pure liquid components and the two-component solutions of {[EPMpyr]$^+$[SAL]$^-$ (x_1) + ethanoic acid or propanoic acid (x_2)} at temperatures T = (293.15, 298.15, 303.15, 308.15 and 313.15) K have been determined throughout the concentration of [EPMpyr]$^+$[SAL]$^-$ under atmospheric pressure of 0.1MPa. Table 5.7 and 5.8 reports the results of u obtained from the measured two-component solutions. Figure 5.21 and 5.22 show the plots of u against the concentration of {[EPMpyr]$^+$[SAL]$^-$. It can be seen from the results that speed of sound values increases with increase in concentration of IL and also decreases with temperature rise for both systems.
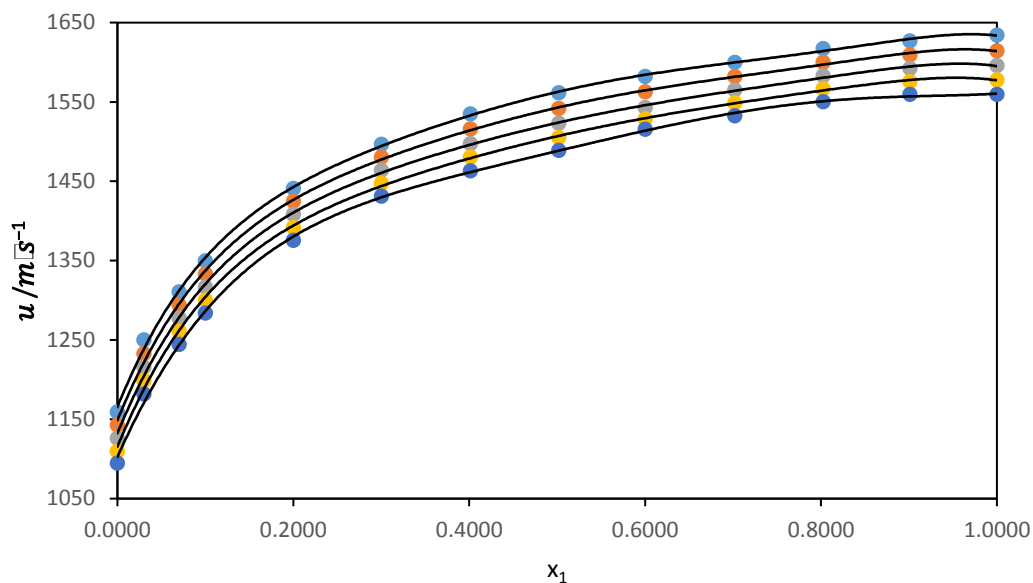
Figure 5.21 Speed of sound (u) for the binary mixture of $\{[\text{EPMpyr}]^+[\text{SAL}]^-$ (x_1) + ethanoic acid (x_2)$\}$ plotted against mole fraction of $[\text{EPMpyr}]^+[\text{SAL}]^-$ at $T = 293.15$ K (●), 298.15 K (●), 303.15 K (●), 308.15 K (●), 313.15 K (●). The line represents the smoothness of the data.
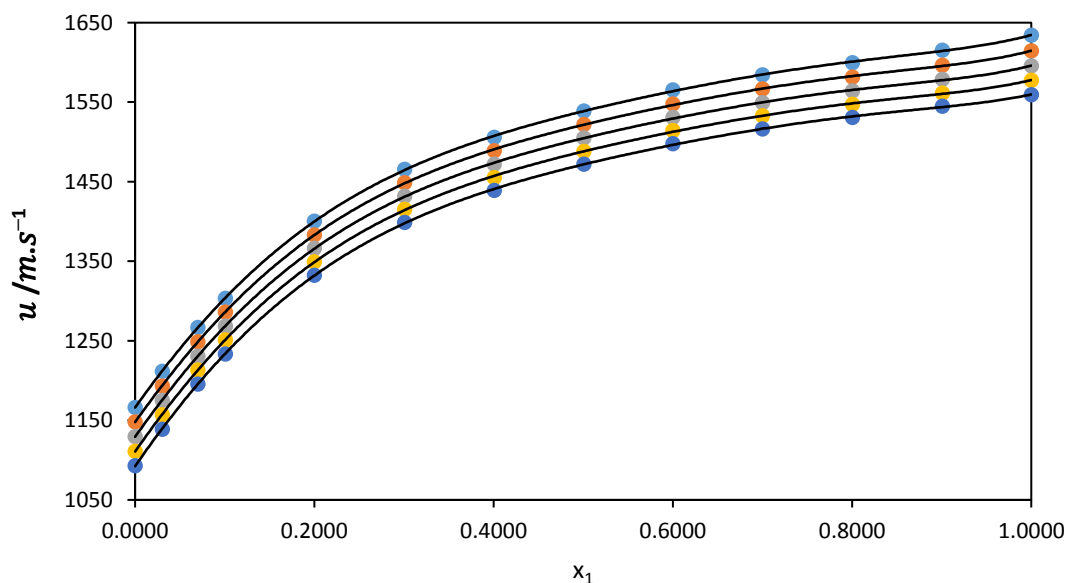
Figure 5.22 Speed of sound (u) for the binary mixture of $\{[\text{EPMpyr}]^+[\text{SAL}]^-$ (x_1) + propanoic acid (x_2)$\}$ plotted against mole fraction of $[\text{EPMpyr}]^+[\text{SAL}]^-$ at $T = 293.15$ K (●), 298.15 K (●), 303.15 K (●), 308.15 K (●), 313.15 K (●). The line represents the smoothness of the data.

Table 5.7 – 5.8 shows the results of excess molar volume V_m^E for the binary mixtures of {[EPMpyr]$^+$[SAL]$^-$ (x_1) + ethanoic or propanoic acid (x_2)} at all investigated temperatures.

Table 5.7 Density (ρ), excess molar volume (V_m^E), speed of sound (u), isentropic compressibility (k_s), deviation in isentropic compressibility (Δk_s) and intermolecular free length (L_f) for the binary system {[EPMpyr]$^+$[SAL]$^-$ (x_1) + ethanoic acid (x_2)} from T = (293.15 – 313.15) K.

x_1	ρ/g·cm^{-3}	V_m^E /cm^3·mol^{-1}	u/m·s^{-1}	k_s/10^8 × Pa^{-1}	Δk_s/10^8 × Pa^{-1}	L_f/10^{-5} m
			T = 293.15 K			
0.0000	1.05247	0.0000	1159.31	70.6951	0.0000	1.7136
0.0301	1.08090	-0.5859	1249.97	59.2127	-10.2875	1.5683
0.0701	1.10366	-0.8266	1310.72	52.7406	-15.1699	1.4801
0.1001	1.11723	-0.9650	1349.65	49.1376	-17.5798	1.4286
0.2001	1.14764	-1.1546	1441.02	41.9617	-20.7785	1.3202
0.3003	1.16626	-1.1751	1496.69	38.2772	-20.4838	1.2609
0.4013	1.17867	-1.0848	1535.05	36.0050	-18.7416	1.2229
0.5017	1.18734	-0.9245	1561.36	34.5477	-16.2083	1.1979
0.6002	1.19389	-0.7581	1582.19	33.4593	-13.3797	1.1789
0.7019	1.19914	-0.5624	1599.97	32.5765	-10.2215	1.1632
0.8024	1.20358	-0.4033	1617.35	31.7627	-7.0406	1.1486
0.9010	1.20700	-0.2090	1626.79	31.3061	-3.5776	1.1403
1.0000	1.20984	0.0000	1634.23	30.9489	0.0000	1.1338
			T = 298.15 K			
0.0000	1.04695	0.0000	1142.78	73.1393	0.0000	1.7590
0.0301	1.07561	-0.5990	1232.74	61.1789	-10.7183	1.6088
0.0701	1.09859	-0.8478	1294.03	54.3597	-15.8852	1.5165
0.1001	1.11229	-0.9909	1333.15	50.5854	-18.4192	1.4629
0.2001	1.14296	-1.1879	1424.62	43.1093	-21.7613	1.3505
0.3003	1.16172	-1.2094	1480.21	39.2874	-21.4470	1.2892
0.4013	1.17420	-1.1165	1515.76	37.0678	-19.4939	1.2523

0.5017	1.18297	-0.9583	1541.79	35.5612	-16.8524	1.2265
0.6002	1.18960	-0.7929	1562.55	34.4297	-13.9124	1.2069
0.7019	1.19491	-0.5991	1581.98	33.4397	-10.7021	1.1894
0.8024	1.19930	-0.4253	1599.97	32.5723	-7.4172	1.1739
0.9010	1.20275	-0.2283	1609.25	32.1053	-3.8100	1.1654
1.0000	1.20554	0.0000	1614.45	31.8252	0.0000	1.1603

$T = 303.15$ K

0.0000	1.04140	0.0000	1126.27	75.7006	0.0000	1.8059
0.0301	1.07032	-0.6127	1215.52	63.2359	-11.1715	1.6505
0.0701	1.09352	-0.8695	1277.27	56.0544	-16.6330	1.5540
0.1001	1.10734	-1.0167	1316.54	52.1015	-19.2946	1.4982
0.2001	1.13828	-1.2192	1408.13	44.3064	-22.7860	1.3816
0.3003	1.15717	-1.2399	1463.70	40.3366	-22.4497	1.3182
0.4013	1.16974	-1.1434	1497.41	38.1268	-20.3156	1.2816
0.5017	1.17867	-0.9931	1523.20	36.5675	-17.5565	1.2551
0.6002	1.18537	-0.8292	1542.92	35.4371	-14.4483	1.2356
0.7019	1.19073	-0.6333	1565.21	34.2799	-11.2326	1.2152
0.8024	1.19508	-0.4439	1583.00	33.3918	-7.7979	1.1994
0.9010	1.19856	-0.2425	1592.25	32.9093	-4.0390	1.1907
1.0000	1.20131	0.0000	1595.74	32.6903	0.0000	1.1867

$T = 308.15$ K

0.0000	1.03584	0.0000	1109.56	78.4165	0.0000	1.8546
0.0301	1.06501	-0.6260	1198.57	65.3612	-11.7067	1.6932
0.0701	1.08843	-0.8899	1260.74	57.8027	-17.4714	1.5923
0.1001	1.10239	-1.0410	1300.11	53.6668	-20.2608	1.5342
0.2001	1.13359	-1.2473	1391.81	45.5392	-23.9002	1.4133
0.3003	1.15273	-1.2760	1447.47	41.4052	-23.5435	1.3476
0.4013	1.16546	-1.1843	1480.22	39.1606	-21.2578	1.3106
0.5017	1.17447	-1.0325	1504.89	37.5966	-18.3184	1.2842
0.6002	1.18128	-0.8731	1528.53	36.2326	-15.2621	1.2606
0.7019	1.18668	-0.6734	1548.76	35.1318	-11.8027	1.2413

0.8024	1.19096	-0.4645	1566.53	34.2156	-8.2106	1.2250
0.9010	1.19446	-0.2574	1575.68	33.7205	-4.2826	1.2162
1.0000	1.19719	0.0000	1577.58	33.5625	0.0000	1.2133

T = 313.15 K

0.0000	1.02996	0.0000	1094.85	80.9975	0.0000	1.9017
0.0301	1.05969	-0.6569	1181.84	67.5623	-12.0362	1.7369
0.0701	1.08334	-0.9287	1244.42	59.6075	-18.1300	1.6314
0.1001	1.09743	-1.0835	1283.90	55.2793	-21.0614	1.5711
0.2001	1.12880	-1.2862	1375.69	46.8105	-24.8742	1.4457
0.3003	1.14808	-1.3111	1431.01	42.5348	-24.4913	1.3781
0.4013	1.16098	-1.2216	1463.07	40.2389	-22.0875	1.3404
0.5017	1.17014	-1.0747	1488.82	38.5549	-19.0996	1.3121
0.6002	1.17699	-0.9090	1515.38	36.9986	-16.0703	1.2853
0.7019	1.18249	-0.7144	1532.63	36.0020	-12.3361	1.2679
0.8024	1.18675	-0.4890	1550.38	35.0563	-8.6050	1.2511
0.9010	1.19016	-0.2548	1559.50	34.5482	-4.5245	1.2420
1.0000	1.19296	0.0000	1559.52	34.4661	0.0000	1.2405

Table 5.8 Density (ρ), excess molar volume (V_m^E), speed of sound (u), isentropic compressibility (k_s), deviation in isentropic compressibility (Δk_s) and intermolecular free length (L_f) for the binary system {[EPMpyr]$^+$[SAL]$^-$ (x_1) + propanoic acid (x_2)} from T = (293.15 – 313.15) K.

x_1	ρ/g·cm^{-3}	V_m^E /cm^3·mol^{-1}	u/m·s^{-1}	k_s/10^8 × Pa^{-1}	Δk_s/10^8 × Pa^{-1}	L_f/10^{-5} m
			T = 293.15 K			
0.0000	0.99378	0.0000	1166.35	73.9694	0.0000	1.7528
0.0303	1.01875	-0.3951	1211.89	66.8354	-5.8318	1.6662
0.0701	1.04618	-0.8113	1266.69	59.5734	-11.3782	1.5731
0.1006	1.06344	-1.0332	1303.51	55.3423	-14.2981	1.5162
0.2000	1.10571	-1.4698	1400.32	46.1214	-19.2427	1.3841
0.3007	1.13394	-1.5634	1465.81	41.0444	-19.9882	1.3057
0.4009	1.15364	-1.4537	1505.74	38.2321	-18.4902	1.2602
0.5010	1.16858	-1.2757	1538.85	36.1367	-16.2801	1.2252
0.6002	1.18064	-1.1176	1565.39	34.5650	-13.5830	1.1982
0.7002	1.19049	-0.9344	1584.49	33.4575	-10.3906	1.1789
0.8005	1.19835	-0.6767	1599.72	32.6083	-6.9213	1.1638
0.9010	1.20461	-0.3422	1615.39	31.8126	-3.3951	1.1495
1.0000	1.20984	0.0000	1634.23	30.9489	0.0000	1.1338
			T = 298.15 K			
0.0000	0.98841	0.0000	1148.13	76.7504	0.0000	1.8019
0.0303	1.01357	-0.4092	1193.40	69.2747	-6.1158	1.7119
0.0701	1.04121	-0.8405	1248.69	61.5959	-12.0031	1.6142
0.1006	1.05859	-1.0699	1286.04	57.1169	-15.1129	1.5545
0.2000	1.10108	-1.5183	1383.27	47.4643	-20.2998	1.4170
0.3007	1.12943	-1.6133	1448.95	42.1731	-21.0677	1.3357
0.4009	1.14919	-1.4996	1488.91	39.2528	-19.4869	1.2886
0.5010	1.16419	-1.3182	1521.86	37.0874	-17.1562	1.2526
0.6002	1.17631	-1.1579	1547.77	35.4867	-14.2992	1.2253
0.7002	1.18621	-0.9726	1566.76	34.3425	-10.9530	1.2053

0.8005	1.19408	-0.7068	1581.66	33.4764	-7.3094	1.1900
0.9010	1.20044	-0.3802	1596.41	32.6866	-3.5860	1.1759
1.0000	1.20554	0.0000	1614.45	31.8252	0.0000	1.1603

$T = 303.15$ K

0.0000	0.98303	0.0000	1129.70	79.7089	0.0000	1.8531
0.0303	1.00839	-0.4241	1175.00	71.8280	-6.4576	1.7591
0.0701	1.03624	-0.8699	1230.82	63.7015	-12.7092	1.6566
0.1006	1.05374	-1.1068	1268.48	58.9795	-15.9982	1.5940
0.2000	1.09646	-1.5660	1366.14	48.8671	-21.4368	1.4509
0.3007	1.12493	-1.6615	1432.01	43.3494	-22.2204	1.3666
0.4009	1.14476	-1.5424	1472.04	40.3131	-20.5458	1.3178
0.5010	1.15980	-1.3527	1504.95	38.0692	-18.0841	1.2281
0.6002	1.17196	-1.1855	1530.94	36.4060	-15.0819	1.2523
0.7002	1.18189	-0.9929	1549.51	35.2397	-11.5486	1.2321
0.8005	1.18980	-0.7199	1564.16	34.3530	-7.7155	1.2165
0.9010	1.19608	-0.3663	1578.57	33.5515	-3.7935	1.2022
1.0000	1.20131	0.0000	1595.74	32.6903	0.0000	1.1867

$T = 308.15$ K

0.0000	0.97764	0.0000	1111.29	82.8259	0.0000	1.9060
0.0303	1.00322	-0.4394	1156.83	74.4845	-6.8502	1.8075
0.0701	1.03127	-0.8994	1213.19	65.8822	-13.4880	1.6999
0.1006	1.04888	-1.1428	1251.11	60.9092	-16.9596	1.6345
0.2000	1.09184	-1.6111	1349.20	50.3142	-22.6577	1.4855
0.3007	1.12043	-1.7050	1415.27	44.5593	-23.4525	1.3980
0.4009	1.14033	-1.5793	1455.41	41.3998	-21.6762	1.3475
0.5010	1.15542	-1.3812	1488.36	39.0700	-19.0757	1.3091
0.6002	1.16761	-1.2042	1514.29	37.3493	-15.9083	1.2799
0.7002	1.17758	-1.0009	1532.71	36.1485	-12.1851	1.2592
0.8005	1.18550	-0.7162	1547.26	35.2348	-8.1537	1.2432
0.9010	1.19182	-0.3528	1561.46	34.4135	-4.0259	1.2286
1.0000	1.19719	0.0000	1577.58	33.5625	0.0000	1.2133

T = 313.15 K

0.0000	0.97225	0.0000	1092.8	86.1273	0.0000	1.961
0.0303	0.99804	-0.4557	1138.91	77.2456	-7.3179	1.8572
0.0701	1.02631	-0.9310	1195.81	68.1395	-14.3639	1.7443
0.1006	1.04402	-1.1813	1233.65	62.9371	-17.9918	1.6764
0.2000	1.08721	-1.6610	1332.50	51.8028	-23.9908	1.5209
0.3007	1.11592	-1.7558	1398.73	45.8033	-24.7887	1.4301
0.4009	1.13591	-1.6254	1438.98	42.5156	-22.9004	1.3778
0.5010	1.15105	-1.4214	1472.00	40.0949	-20.1509	1.338
0.6002	1.16328	-1.2369	1497.93	38.3118	-16.8079	1.3079
0.7002	1.17327	-1.0251	1516.33	37.0693	-12.8868	1.2865
0.8005	1.18121	-0.7300	1530.79	36.1279	-8.6424	1.2701
0.9010	1.18754	-0.3568	1544.90	35.2817	-4.2986	1.2551
1.0000	1.19296	0.0000	1559.52	34.4661	0.0000	1.2405

The plot of excess molar volume V_m^E against concentration of {[EPMpyr]$^+$[SAL]$^-$ for the binary systems of {[EPMpyr]$^+$[SAL]$^-$ + ethanoic or propanoic acid} at T = (293.15, 298.15, 303.15, 308.15 and 313.15) K were presented in Figures 5.23 – 5.24 below:
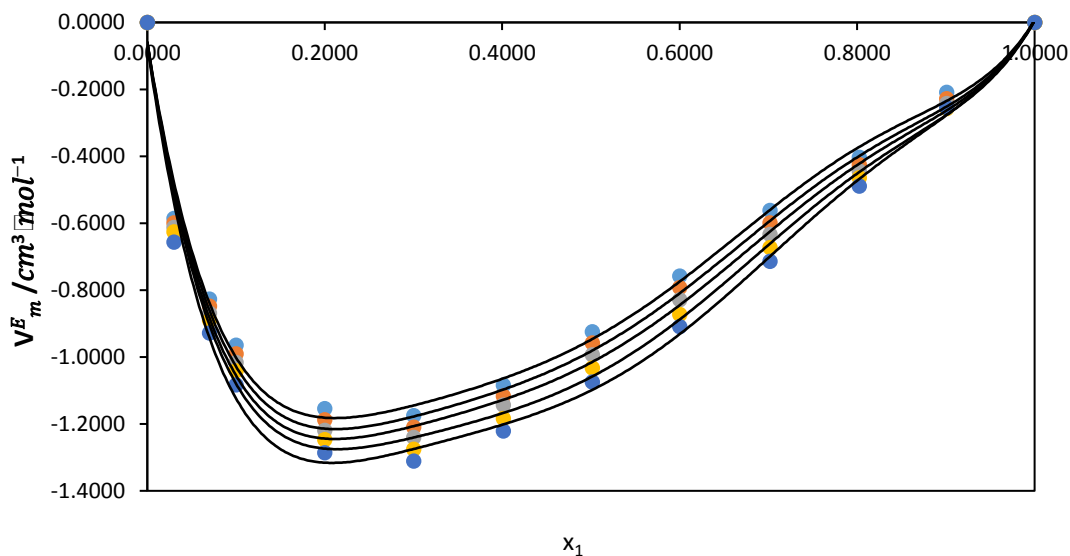
Figure 5.23 Excess molar volumes (V_m^E) for the binary mixture of {[EPMpyr]$^+$[SAL]$^-$ (x_1) + ethanoic acid (x_2)} as a function of the composition expressed in mole fraction of [EPMpyr]$^+$[SAL]$^-$ at T = 293.15 K (●), 298.15 K (●), 303.15 K (●), 308.15 K (●), 313.15 K (●). The lines were generated using Redlich-Kister curve-fitting.
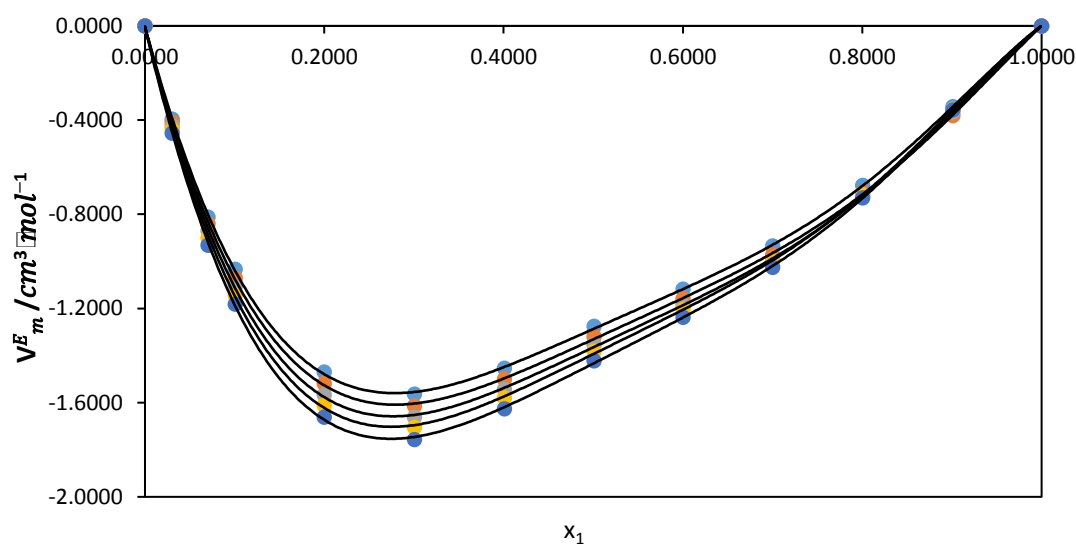
Figure 5.24 Excess molar volumes (V_m^E) for the binary mixture of {[EPMpyr]$^+$[SAL]$^-$ (x_1) + propanoic acid (x_2)} as a function of the composition expressed in mole fraction of [EPMpyr]$^+$[SAL]$^-$ at T = 293.15 K (●), 298.15 K (●), 303.15 K (●), 308.15 K (●), 313.15 K (●). The lines were generated using Redlich-Kister curve-fitting.

Excess molar volume results were computed using the measured values of density for two-component combinations of {[EPMpyr]$^+$[SAL]$^-$ (x_1) + ethanoic or propanoic acid (x_2) presented in tables 5.7 – 5.8 and as well plotted in Figures 5.23 – 5.24. An observation of the results presented in Tables 5.7 and 5.8 as well as in Figures 5.23 and 5.24 showed that V_m^E were negative for both studied systems throughout the entire concentration of IL. The $V_{m,min}^E$ values were found to be -1.3111 cm$^3\cdot$mol^{-1} and -1.7558 cm$^3\cdot$mol^{-1} which occurred at $x_1 = 0.3003$ and 0.3007 for ethanoic and propanoic acid systems respectively. This occurrence suggest the presence of ion-dipole connections in the molecules of [EPMpyr]$^+$ and [SAL]$^-$ and carboxylic acid molecules. In addition, V_m^E values tends to decrease with rise in temperature and increases with concentration. This can be ascribed to association of weak bonds that occur when IL and carboxylic molecules react.

The isentropic compressibility, k_s for the two-component systems of {[EPMpyr]$^+$[SAL]$^-$ (x_1) + ethanoic or propanoic acid (x_2)} were estimated from the density and speed of sound values using equation (3.5). It was observed from the results presented in Tables 5.7 and 5.8 that k_s shows increase with temperature rise and a decrease with increasing concentration of the IL. This increase in k_s explains that random association occurs with heat are more pronounced which in turn makes the solution to be further compressible (Zafarani-Moattar and Shekaari 2005). The positive results of isentropic compressibility indicate that the binary solution is compressible.

Deviation in isentropic compressibility Δk_s values were tabulated in Table 5.7 and 5.8 for both studied systems. These values were negative results throughout the entire composition and at all temperatures examined. The plots of deviation in isentropic compressibility for the two-component solutions were given in Figures 5.25 and 5.26. From close inspection of these results, it can be said that the negativity of deviation in isentropic compressibility can be ascribed to specific interactions that occur in the molecules of the liquid components. The minimum $\Delta k_{s,min}$ values for the two-component systems of {[EPMpyr]$^+$[SAL]$^-$ (x_1) + ethanoic or propanoic acid (x_2)} were found to be -24.8742 (10^8/ Pa^{-1}) and -24.7887 (10^8/Pa^{-1}) which occurred at $x_1 = 0.2001$ and 0.3007 respectively. Likewise, the Δk_s negative values could also be explained in terms of differences in molecular size of IL and carboxylic acids molecules.

The plots of deviation in isentropic compressibility for the binary systems have been given in Figures 5.25 – 5.26 below:
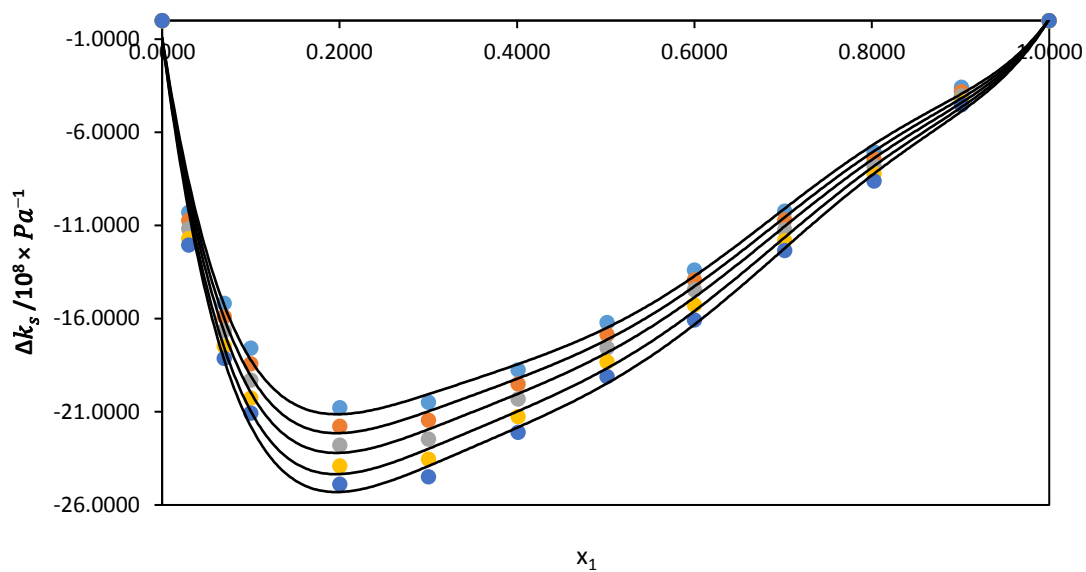
Figure 5.25   Deviation in isentropic compressibility (Δk_s) for the binary mixture of $\{[EPMpyr]^+[SAL]^-\ (x_1)$ + ethanoic acid $(x_2)\}$ as a function of the composition expressed in mole fraction of $[EPMpyr]^+[SAL]^-$ at T = 293.15 K (●), 298.15 K (●), 303.15 K (●), 308.15 K (●), 313.15 K (●). The lines were generated using Redlich-Kister curve-fitting.
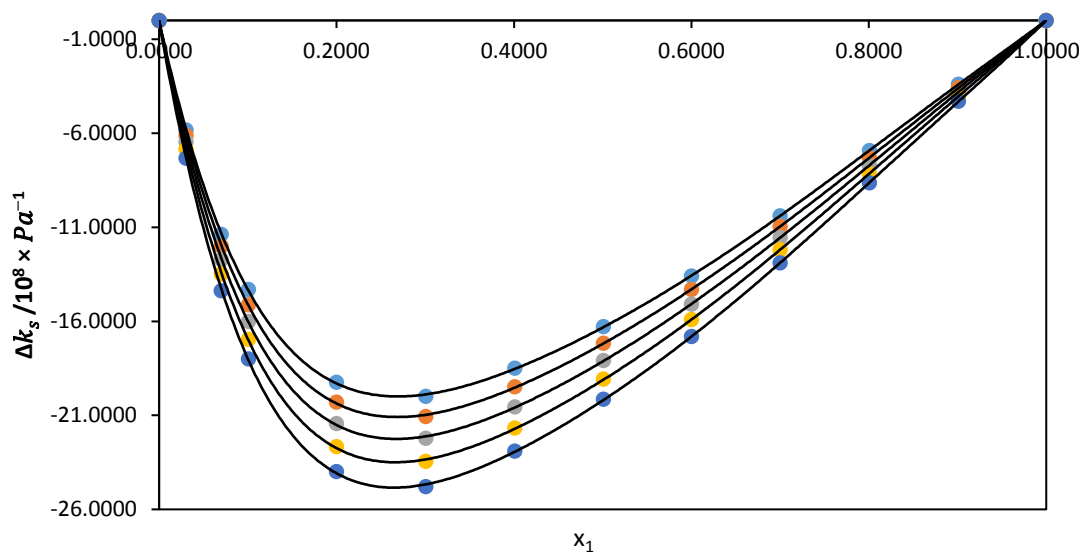
Figure 5.26   Deviation in isentropic compressibility (Δk_s) for the binary mixture of {[EPMpyr]$^+$[SAL]$^-$ (x_1) + propanoic acid (x_2)} as a function of the composition expressed in mole fraction of [EPMpyr]$^+$[SAL]$^-$ at T = 293.15 K (●), 298.15 K (●), 303.15 K (●), 308.15 K (●), 313.15 K (●). The lines were generated using Redlich-Kister curve-fitting.

Figures 5.27 – 5.28 presents the plots of intermolecular free length (L_f) against mole fraction for the binary systems of {[EPMpyr]$^+$[SAL]$^-$ (x_1) + ethanoic or propanoic acid (x_2)} studied at T = (293.15, 298.15, 303.15, 308.15 and 313.15) K.
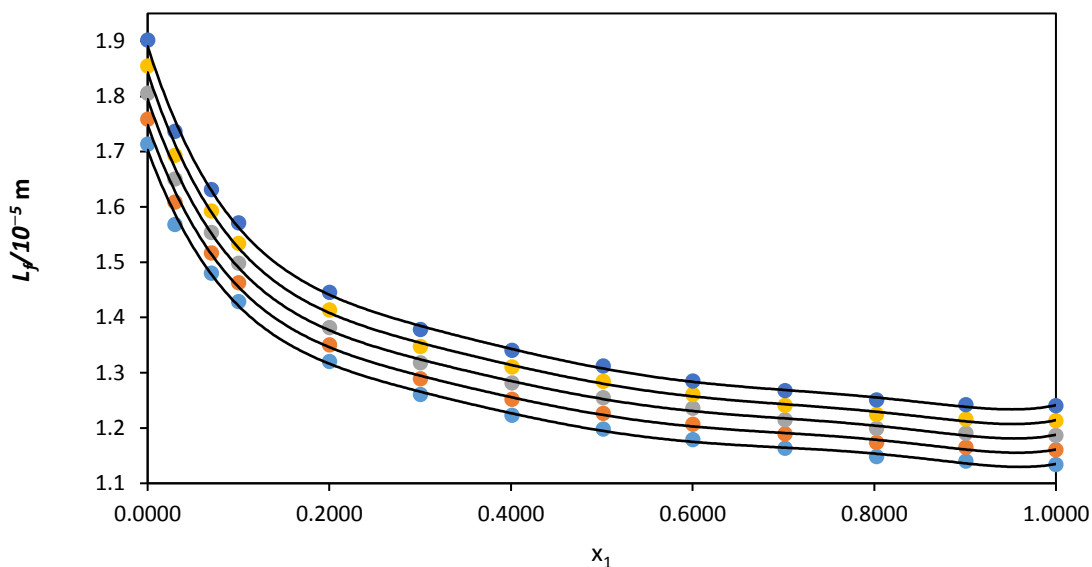
Figure 5.27   Intermolecular free length (L_f) for the binary mixture of $\{[\text{EPMpyr}]^+[\text{SAL}]^-$ (x_1) + ethanoic acid $(x_2)\}$ as a function of the composition expressed in mole fraction of $[\text{EPMpyr}]^+[\text{SAL}]^-$ at T = 293.15 K (●), 298.15 K (●), 303.15 K (●), 308.15 K (●), 313.15 K (●). The lines were generated using Redlich-Kister curve-fitting.
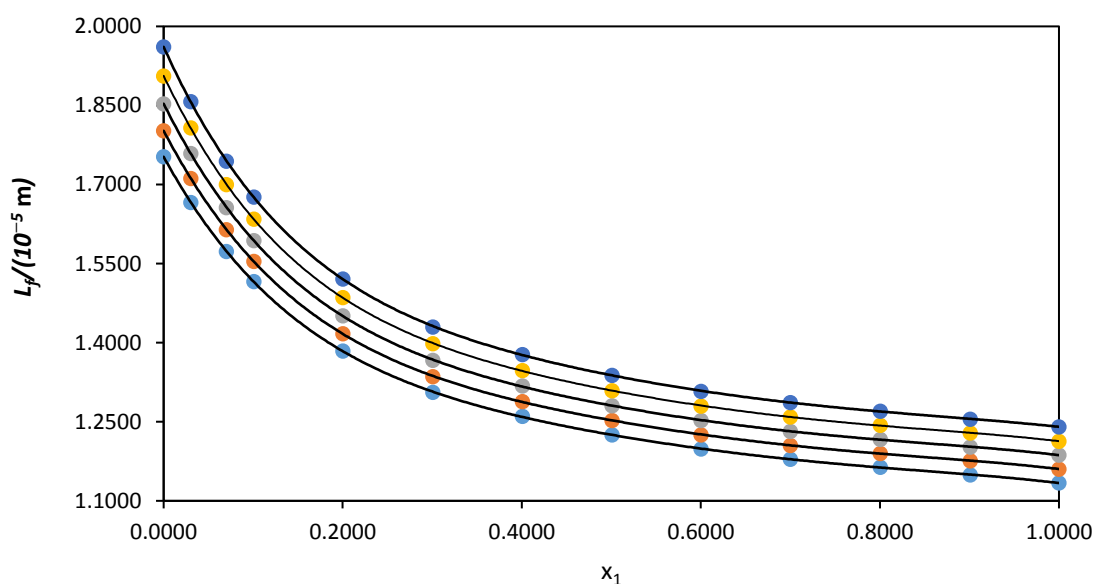
Figure 5.28   Intermolecular free length (L_f) for the binary mixture of $\{[\text{EPMpyr}]^+[\text{SAL}]^-$ (x_1) + propanoic acid $(x_2)\}$ as a function of the composition expressed in mole fraction of $[\text{EPMpyr}]^+[\text{SAL}]^-$ at T = 293.15 K (●), 298.15 K (●), 303.15 K (●), 308.15 K (●), 313.15 K (●). The lines were generated using Redlich-Kister curve-fitting.

Intermolecular free length (L_f) for the two-component systems {[EPMpyr]$^+$[SAL]$^-$ (x_1) + ethanoic or propanoic acid (x_2)} throughout the concentration of [EPMpyr]$^+$[SAL]$^-$ were calculated at temperatures T = (293.15, 298.15, 303.15, 308.15 and 313.15) K using the Jacobson empirical formula and isentropic compressibility values. The formula is given as:

$$L_f = k_j(k_s)^{1/2} \tag{5.1}$$

where k_j denotes the Jacobson's temperature dependent variable which is (93.875 + 0.375 T) $\times 10^{-8}$ and k_s represent the isentropic compressibility. The plots of L_f against the mole fraction x_1 were presented in Figures 5.27 and 5.28. Additionally, the results of the binary mixtures of {[EPMpyr]$^+$[SAL]$^-$ (x_1) + ethanoic or propanoic acid (x_2)} were reported in Tables 5.7 and 5.8. A closer look at the results of L_f in Tables 5.7 and 5.8 as well as in Figures 5.27 and 5.28, it can be seen that L_f and u values are inversely related, also the L_f values increase slightly with rise in temperature but decreases throughout the concentration of IL across all temperatures for both binary solutions. This can be ascribed to the attractive and repulsive forces that occurs in the binary combinations.

The Redlich-Kister fitting parameters were calculated from equation (4.2) and the coefficients and standard errors for the binary systems studied are given in Table 5.9 below:

Table 5.9   Redlich- Kister fitting coefficients and standard deviation, σ, for binary systems of {[EPMpyr]$^+$[SAL]$^-$ (x_1) + ethanoic or propanoic acid (x_2)} studied at T = (293.15, 298.15, 303.15, 308.15 and 313.15) K.

	T/(K)	A_0	A_1	A_2	A_3	σ
		{[EPMpyr]$^+$[SAL]$^-$ (x_1) + ethanoic acid (x_2)}				
V_m^E/cm^3·mol^{-1}	293.15	-3.574	-2.559	-4.463	-4.945	0.058
	298.15	-3.708	-2.533	-4.621	-5.101	0.058
	303.15	-3.840	-2.468	-4.735	-5.379	0.059
	308.15	-4.007	-2.415	-4.777	-5.604	0.060
	313.15	-4.162	-2.276	-4.915	-6.306	0.063

$\Delta k_s/10^8 \times Pa^{-1}$	293.15	-62.350	-40.944	-83.218	-101.357	0.922
	298.15	-64.854	-42.985	-88.635	-105.093	0.945
	303.15	-67.548	-45.137	-94.035	-109.076	0.972
	308.15	-70.770	-46.755	-99.265	-115.228	1.010
	313.15	-73.900	-48.025	-102.894	-119.785	1.018
$L_f/10^{-5}$ m	293.15	4.033	-2.197	14.789	11.620	0.598
	298.15	4.128	-2.260	15.125	11.953	0.613
	303.15	4.223	-2.324	15.472	12.299	0.629
	308.15	4.313	-2.378	15.837	12.632	0.530
	313.15	4.403	-2.428	16.218	12.963	0.662

{[EPMpyr]$^+$[SAL]$^-$ (x_1) + propanoic acid (x_2)}

$V_m^E/cm^3 \cdot mol^{-1}$	293.15	-5.206	-3.417	-4.074	-2.015	0.011
	298.15	-5.368	-3.513	-4.393	-1.918	0.010
	303.15	-5.518	-3.618	-4.433	-2.232	0.012
	308.15	-5.634	-3.785	-4.461	-2.498	0.012
	313.15	-5.793	-3.913	-4.580	-2.678	0.012
$\Delta k_s/10^8 \times Pa^{-1}$	293.15	-64.647	-49.475	-50.789	-42.456	0.128
	298.15	-68.100	-52.212	-53.861	-44.693	0.130
	303.15	-71.770	-54.983	-57.337	-47.731	0.139
	308.15	-75.660	-57.911	-61.321	-51.191	0.155
	313.15	-79.866	-60.972	-65.930	-55.159	0.177
$L_f/10^{-5}$ m	293.15	4.100	-2.237	15.497	12.749	0.613
	298.15	4.189	-2.305	15.892	13.131	0.629
	303.15	4.212	-2.356	16.487	13.468	0.645
	308.15	4.371	-2.440	16.707	13.941	0.664
	313.15	4.464	-2.510	17.127	14.370	0.682

Standard uncertainties u are $u(T) = \pm0.01$ K and the combined expanded uncertainty Uc in density and speed of sound measurements were less than Uc $(\rho) = \pm 2 \times 10^{-4}$ g$\cdot$cm^{-3} and Uc$(u)=$ 0.6 m$\cdot$s^{-1} respectively (0.95 level of confidence).

5.1.4 Ionic liquid {[EPMpyr]$^+$[OAC]$^-$ with propanoic or butanoic acid}

Table 5.10 and 5.11 presents the density (ρ) values obtained on the measured pure liquids and two-component combinations of {[EPMpyr]$^+$[OAC]$^-$ (x_1) + propanoic or butanoic acid (x_2)} at T = (293.15, 298.15, 303.15, 308.15 and 313.15) K under atmospheric pressure of 0.1 MPa. A graphical representation of density (ρ) versus mole fraction of [EPMpyr]$^+$[OAC]$^-$ for both two-component combinations were plotted in Fig 5.29 and 5.30 throughout the examined temperatures. It can be deduced from the results in Table 5.10 and 5.11, likewise in Figure 5.29 and 5.30, that density values decreases with temperature increase, and increases upon concentration increase of the IL which are more dominant at the IL rich region in both systems. This can be explained as a result of weak dispersion and intermolecular interactions that occurred between the two-component liquid compositions.
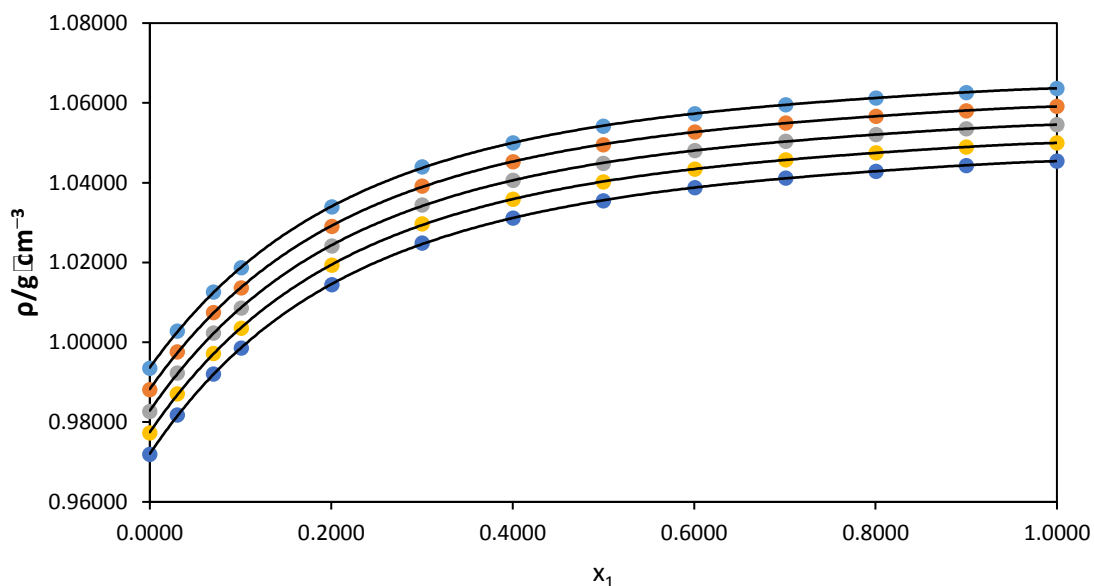
Figure 5.29   Density (ρ) for the binary mixture of {[EPMpyr]$^+$[OAC]$^-$ (x_1) + propanoic acid (x_2)} plotted against mole fraction of [EPMpyr]$^+$[OAC]$^-$ at T = 293.15 K (●), 298.15 K (●), 303.15 K (●), 308.15 K (●), 313.15 K (●). The line represents the smoothness of the data.
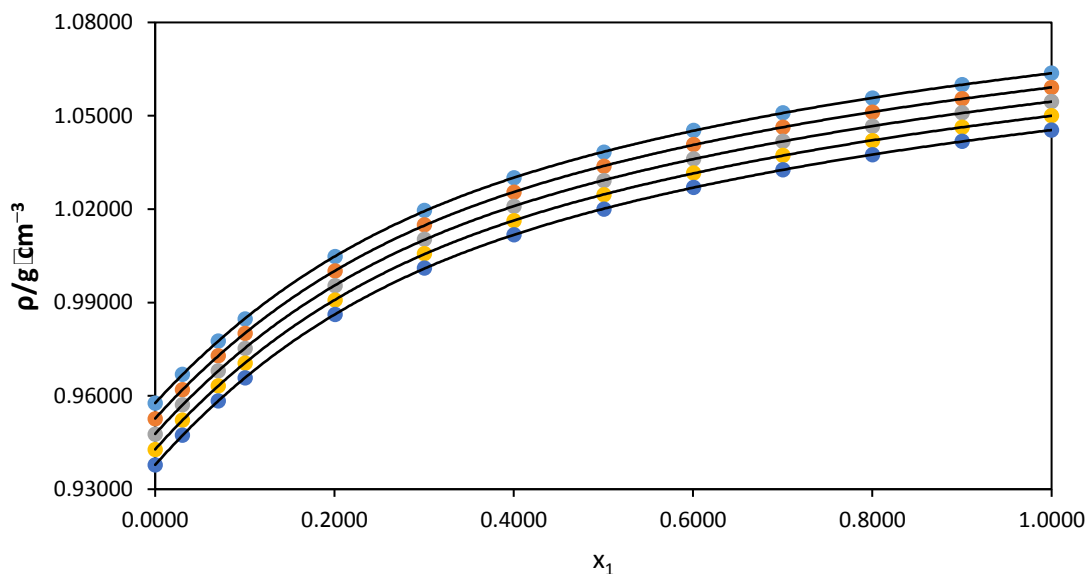
Figure 5.30 Density (ρ) for the binary mixture of {[EPMpyr]$^+$[OAC]$^-$ (x_1) + butanoic acid (x_2)} plotted against mole fraction of [EPMpyr]$^+$[OAC]$^-$ at T = 293.15 K (●), 298.15 K (●), 303.15 K (●), 308.15 K (●), 313.15 K (●). The line represents the smoothness of the data.

The speed of sound u data for pure liquids [EPMpyr]$^+$[OAC]$^-$, propanoic acid, butanoic acid and their two-component solutions {[EPMpyr]$^+$[OAC]$^-$ (x_1) + propanoic acid or butanoic acid (x_2)} were investigated at T = (293.15, 298.15, 303.15, 308.15 and 313.15) K. The experimental results for the measured speed of sound u are reported in Table 5.10 and 5.11 while the plots of u against the concentration of [EPMpyr]$^+$[OAC]$^-$ are shown in Figure 5.31 and 5.32. It was discovered from the data that there is an increment in speed of sound with an increasing concentration of IL. Also, u value decreases with rise in temperature for the two-component solutions.
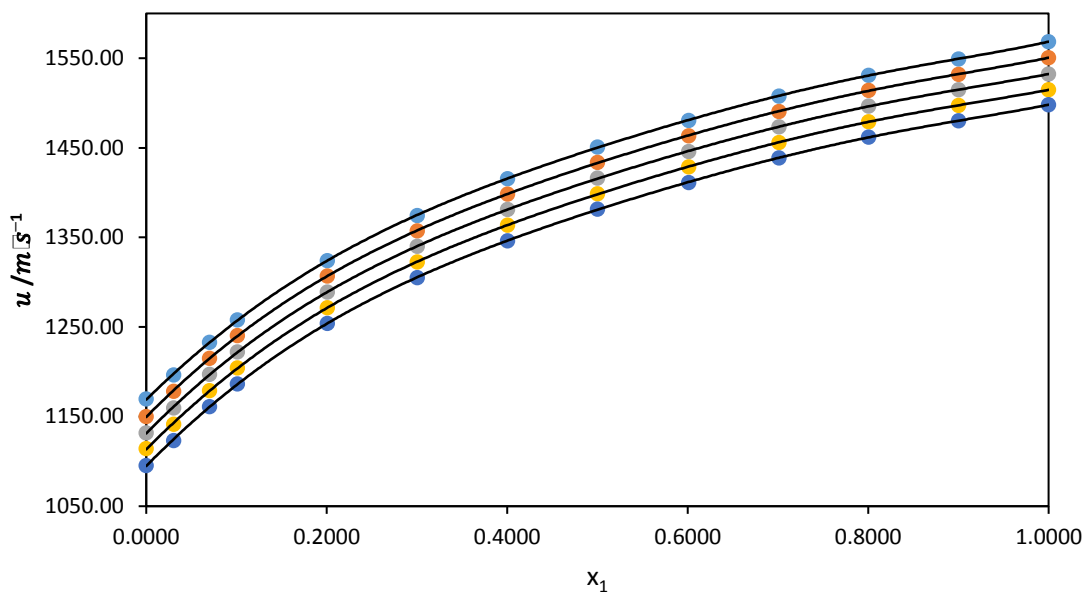
Figure 5.31 Speed of sound (u) for the binary mixture of $\{$[EPMpyr]$^+$[OAC]$^-$ (x_1) + propanoic acid (x_2)$\}$ plotted against mole fraction of [EPMpyr]$^+$[OAC]$^-$ at T = 293.15 K ($\bullet$), 298.15 K ($\bullet$), 303.15 K ($\bullet$), 308.15 K ($\bullet$), 313.15 K ($\bullet$). The line represents the smoothness of the data.
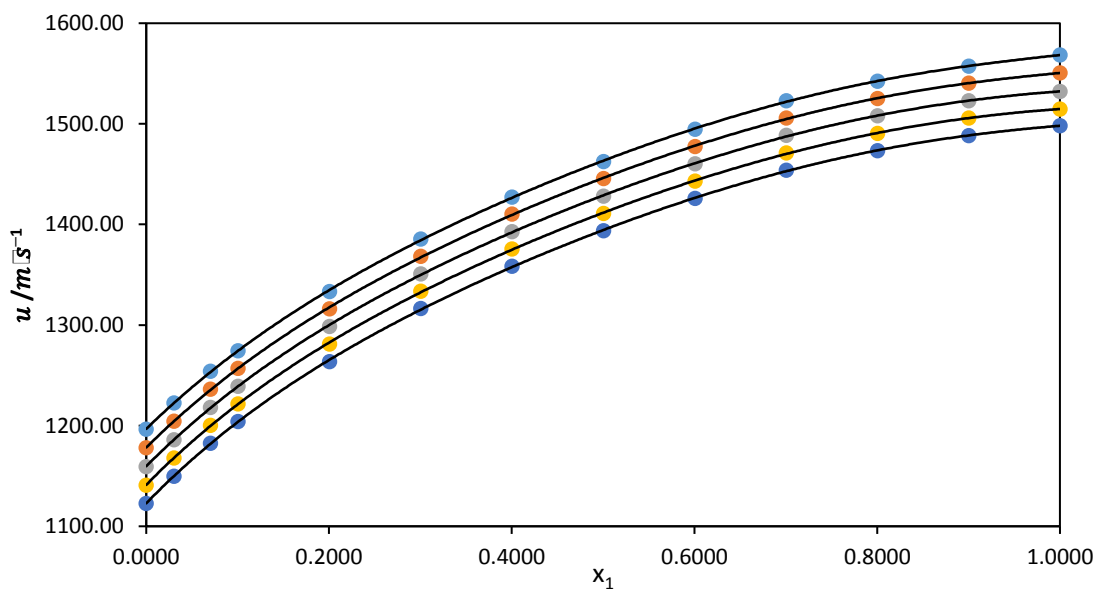
Figure 5.32 Speed of sound (u) for the binary mixture of $\{$[EPMpyr]$^+$[OAC]$^-$ (x_1) + butanoic acid (x_2)$\}$ plotted against mole fraction of [EPMpyr]$^+$[OAC]$^-$ at T = 293.15 K ($\bullet$), 298.15 K ($\bullet$), 303.15 K ($\bullet$), 308.15 K ($\bullet$), 313.15 K ($\bullet$). The line represents the smoothness of the data.

Table 5.10 – 5.11 shows the results of excess molar volume V_m^E for the binary mixtures of $\{[\text{EPMpyr}]^+[\text{OAC}]^-\ (x_1) +$ propanoic or butanoic acid $(x_2)\}$ at all investigated temperatures.

Table 5.10   Density (ρ), excess molar volume (V_m^E), speed of sound (u), isentropic compressibility (k_s), deviation in isentropic compressibility (Δk_s) and intermolecular free length (L_f) for the binary system $\{[\text{EPMpyr}]^+[\text{OAC}]^-\ (x_1) +$ propanoic acid $(x_2)\}$ from $T = (293.15 - 313.15)$ K.

x_1	$\rho/\text{g·cm}^{-3}$	$V_m^E\ /\text{cm}^3\text{·mol}^{-1}$	$u/\text{m·s}^{-1}$	$k_s/10^8 \times \text{Pa}^{-1}$	$\Delta k_s/10^8 \times \text{Pa}^{-1}$	$L_f/10^{-5}$ m
			$T = 293.15$ K			
0.0000	0.99350	0.0000	1169.75	73.5608	0.0000	1.7480
0.0302	1.00285	-0.3036	1196.34	69.6714	-2.8217	1.7012
0.0702	1.01258	-0.5889	1232.91	64.9696	-6.1086	1.6428
0.1009	1.01871	-0.7574	1258.05	62.0232	-7.9696	1.6051
0.2008	1.03393	-1.1615	1324.18	55.1589	-11.3044	1.5136
0.3003	1.04396	-1.3750	1374.61	50.6939	-12.2523	1.4511
0.4005	1.05000	-1.3507	1415.69	47.5197	-11.8856	1.4049
0.5001	1.05417	-1.2340	1450.96	45.0587	-10.8282	1.3681
0.6010	1.05731	-1.0651	1480.62	43.1429	-9.1768	1.3387
0.7010	1.05958	-0.8439	1507.83	41.5107	-7.2736	1.3131
0.8005	1.06125	-0.5808	1531.07	40.1969	-5.0713	1.2922
0.9001	1.06262	-0.3059	1549.22	39.2098	-2.5385	1.2762
1.0000	1.06367	0.0000	1568.45	38.2168	0.0000	1.2599
			$T = 298.15$ K			
0.0000	0.98811	0.0000	1150.14	76.5057	0.0000	1.7990
0.0302	0.99759	-0.3124	1178.17	72.2158	-3.1650	1.7479
0.0702	1.00745	-0.6063	1215.10	67.2282	-6.6620	1.6864
0.1009	1.01367	-0.7798	1240.43	64.1150	-8.6317	1.6469
0.2008	1.02907	-1.1930	1306.89	56.8957	-12.1325	1.5514
0.3003	1.03920	-1.4093	1357.43	52.2236	-13.0992	1.4864

0.4005	1.04530	-1.3835	1398.55	48.9107	-12.6817	1.4385
0.5001	1.04951	-1.2633	1433.61	46.3608	-11.5248	1.4005
0.6010	1.05269	-1.0902	1463.46	44.3545	-9.7728	1.3698
0.7010	1.05498	-0.8636	1490.73	42.6536	-7.7490	1.3433
0.8005	1.05667	-0.5945	1513.97	41.2883	-5.4101	1.3216
0.9001	1.05806	-0.3130	1532.11	40.2635	-2.7265	1.3051
1.0000	1.05911	0.0000	1550.61	39.2693	0.0000	1.2889

$T = 303.15$ K

0.0000	0.98271	0.0000	1131.80	79.4393	0.0000	1.8499
0.0302	0.99233	-0.3217	1159.74	74.9247	-3.3348	1.7966
0.0702	1.00233	-0.6247	1197.06	69.624	-7.0721	1.7319
0.1009	1.00863	-0.8030	1222.25	66.3667	-9.1300	1.6909
0.2008	1.02420	-1.2253	1289.02	58.7621	-12.8344	1.5911
0.3003	1.03443	-1.4448	1339.99	53.8387	-13.8715	1.5229
0.4005	1.04059	-1.4169	1381.10	50.3812	-13.4164	1.4732
0.5001	1.04485	-1.2935	1416.17	47.7215	-12.1883	1.4338
0.6010	1.04806	-1.1157	1446.05	45.6295	-10.3385	1.4020
0.7010	1.05038	-0.8833	1473.34	43.8578	-8.2037	1.3745
0.8005	1.05209	-0.6080	1496.59	42.4369	-5.7394	1.3521
0.9001	1.05349	-0.3205	1514.75	41.3701	-2.9167	1.3350
1.0000	1.05456	0.0000	1532.35	40.3845	0.0000	1.3190

$T = 308.15$ K

0.0000	0.97731	0.0000	1114.23	82.4173	0.0000	1.9013
0.0302	0.98706	-0.3312	1141.41	77.7632	-3.4183	1.8468
0.0702	0.99720	-0.6436	1179.09	72.1312	-7.4126	1.7787
0.1009	1.00358	-0.8270	1204.43	68.6886	-9.5990	1.7357
0.2008	1.01933	-1.2585	1271.49	60.6822	-13.5201	1.6314
0.3003	1.02966	-1.4806	1322.57	55.5226	-14.6089	1.5605
0.4005	1.03588	-1.4513	1363.71	51.9093	-14.1239	1.5089
0.5001	1.04018	-1.3240	1398.87	49.1287	-12.8321	1.4679
0.6010	1.04343	-1.1414	1428.68	46.9535	-10.8784	1.4351

0.7010	1.04577	-0.9036	1455.99	45.1073	-8.6326	1.4066
0.8005	1.04749	-0.6221	1479.24	43.6286	-6.0417	1.3833
0.9001	1.04892	-0.3278	1497.37	42.5208	-3.0754	1.3657
1.0000	1.04999	0.0000	1514.74	41.5086	0.0000	1.3493

$T = 313.15$ K

0.0000	0.97191	0.0000	1095.58	85.7207	0.0000	1.9564
0.0302	0.98179	-0.3407	1123.20	80.7361	-3.6826	1.8987
0.0702	0.99207	-0.6625	1161.18	74.758	-7.9353	1.8270
0.1009	0.99853	-0.8511	1186.68	71.1165	-10.2532	1.7820
0.2008	1.01445	-1.2922	1254.02	62.6845	-14.3811	1.6730
0.3003	1.02488	-1.5170	1305.19	57.2769	-15.4998	1.5992
0.4005	1.03116	-1.4857	1346.39	53.4971	-14.9616	1.5455
0.5001	1.03551	-1.3549	1381.59	50.5927	-13.5755	1.5030
0.6010	1.03878	-1.1669	1411.39	48.3262	-11.4919	1.4689
0.7010	1.04115	-0.9235	1438.72	46.4018	-9.1052	1.4394
0.8005	1.04289	-0.6357	1461.96	44.8631	-6.3561	1.4153
0.9001	1.04433	-0.3342	1480.11	43.7095	-3.2174	1.3970
1.0000	1.04542	0.0000	1498.12	42.6202	0.0000	1.3795

Table 5.11 Density (ρ), excess molar volume (V_m^E), speed of sound (u), isentropic compressibility (k_s), deviation in isentropic compressibility (Δk_s) and intermolecular free length (L_f) for the binary system $\{[\text{EPMpyr}]^+[\text{OAC}]^-$ (x_1) + butanoic acid (x_2)$\}$ from $T =$ (293.15 – 313.15) K.

x_1	ρ/g·cm^{-3}	V_m^E /cm^3·mol^{-1}	u/m·s^{-1}	$k_s/10^8 \times$ Pa^{-1}	$\Delta k_s/10^8 \times$ Pa^{-1}	$L_f/10^{-5}$ m
			$T = 293.15$ K			
0.0000	0.95761	0.0000	1196.58	72.9337	0.0000	1.7405
0.0303	0.96690	-0.2431	1222.45	69.2079	-2.6726	1.6955
0.0703	0.97764	-0.5003	1253.99	65.0477	-5.4441	1.6437
0.1003	0.98476	-0.6566	1274.52	62.5139	-6.9387	1.6114
0.2006	1.00475	-1.0717	1333.24	55.9917	-9.9790	1.5250
0.3004	1.01954	-1.2789	1385.41	51.1020	-11.4014	1.4569
0.4004	1.03008	-1.2388	1427.29	47.6547	-11.3772	1.4069
0.5005	1.03834	-1.1018	1462.61	45.0200	-10.5364	1.3675
0.6006	1.04529	-0.9464	1494.80	42.8151	-9.2692	1.3336
0.7004	1.05092	-0.7278	1522.90	41.0289	-7.5887	1.3055
0.8003	1.05572	-0.4894	1542.29	39.8216	-5.3297	1.2861
0.9002	1.06002	-0.2596	1557.43	38.8930	-2.7877	1.2710
1.0000	1.06367	0.0000	1568.45	38.2168	0.0000	1.2599
			$T = 298.15$ K			
0.0000	0.95265	0.0000	1178.07	75.6350	0.0000	1.7888
0.0303	0.96202	-0.2507	1204.37	71.6633	-2.8685	1.7412
0.0703	0.97284	-0.5161	1236.21	67.2629	-5.8142	1.6869
0.1003	0.98008	-0.6853	1256.98	64.5776	-7.4109	1.6529
0.2006	1.00010	-1.1027	1316.01	57.7348	-10.6065	1.5628
0.3004	1.01494	-1.3133	1368.31	52.6248	-12.0845	1.4921
0.4004	1.02550	-1.2714	1410.21	49.0341	-12.0389	1.4403
0.5005	1.03377	-1.1306	1445.55	46.2925	-11.1399	1.3994
0.6006	1.04073	-0.9708	1477.54	44.0133	-9.7822	1.3645
0.7004	1.04636	-0.7471	1505.81	42.1481	-8.0160	1.3353

0.8003	1.05117	-0.5027	1525.23	40.8937	-5.6395	1.3153
0.9002	1.05546	-0.2663	1540.34	39.9323	-2.9655	1.2997
1.0000	1.05911	0.0000	1550.61	39.2693	0.0000	1.2889

_T_ = 303.15 K

0.0000	0.94769	0.0000	1159.43	78.4952	0.0000	1.8389
0.0303	0.95713	-0.2587	1186.06	74.2703	-3.0688	1.7887
0.0703	0.96803	-0.5328	1218.24	69.6057	-6.2089	1.7316
0.1003	0.97525	-0.6997	1239.23	66.7695	-7.9042	1.6960
0.2006	0.99545	-1.1345	1298.54	59.5761	-11.2754	1.6020
0.3004	1.01033	-1.3483	1350.97	54.2306	-12.8147	1.5285
0.4004	1.02091	-1.3046	1392.89	50.4867	-12.7477	1.4748
0.5005	1.02920	-1.1601	1428.24	47.6320	-11.7872	1.4325
0.6006	1.03617	-0.9956	1460.18	45.2645	-10.3433	1.3964
0.7004	1.04181	-0.7664	1488.48	43.3239	-8.4782	1.3662
0.8003	1.04662	-0.5161	1507.87	42.0228	-5.9741	1.3455
0.9002	1.05091	-0.2731	1522.99	41.0243	-3.1627	1.3294
1.0000	1.05456	0.0000	1532.35	40.3845	0.0000	1.3190

_T_ = 308.15 K

0.0000	0.94273	0.0000	1140.94	81.4869	0.0000	1.8905
0.0303	0.95224	-0.2671	1167.87	76.9952	-3.2790	1.8377
0.0703	0.96322	-0.5499	1200.38	72.0503	-6.6247	1.7777
0.1003	0.97050	-0.7221	1221.59	69.0487	-8.4294	1.7403
0.2006	0.99078	-1.1669	1281.12	61.4953	-11.9734	1.6423
0.3004	1.00572	-1.3836	1333.65	55.9037	-13.5722	1.5659
0.4004	1.01632	-1.3383	1375.61	51.9970	-13.4814	1.5102
0.5005	1.02462	-1.1897	1410.94	49.0254	-12.4507	1.4664
0.6006	1.03160	-1.0207	1442.98	46.5554	-10.9225	1.4290
0.7004	1.03724	-0.7856	1471.16	44.5454	-8.9403	1.3978
0.8003	1.04205	-0.5294	1490.56	43.1929	-6.3012	1.3764
0.9002	1.04635	-0.2806	1505.67	42.1566	-3.3410	1.3598
1.0000	1.04999	0.0000	1514.74	41.5086	0.0000	1.3493

T = 313.15 K

0.0000	0.93777	0.0000	1122.60	84.6167	0.0000	1.9437
0.0303	0.94735	-0.2752	1149.84	79.8389	-3.5038	1.8881
0.0703	0.95841	-0.5667	1182.61	74.6047	-7.0581	1.8251
0.1003	0.96573	-0.7445	1204.03	71.4280	-8.9775	1.7859
0.2006	0.98611	-1.1992	1263.80	63.4916	-12.7020	1.6837
0.3004	1.00110	-1.4192	1316.40	57.6433	-14.3560	1.6043
0.4004	1.01173	-1.3723	1358.39	53.5659	-14.2340	1.5465
0.5005	1.02003	-1.2198	1393.72	50.4702	-13.1255	1.5012
0.6006	1.02702	-1.0457	1425.78	47.8980	-11.4976	1.4624
0.7004	1.03266	-0.8047	1453.96	45.8076	-9.3943	1.4301
0.8003	1.03748	-0.5424	1473.34	44.4033	-6.6055	1.4081
0.9002	1.04177	-0.2867	1488.42	43.3288	-3.4817	1.3909
1.0000	1.04542	0.0000	1498.12	42.6202	0.0000	1.3795

The plot of excess molar volume V_m^E against mole fraction of {[EPMpyr]$^+$[OAC]$^-$ for the binary systems of {[EPMpyr]$^+$[OAC]$^-$ + propanoic or butanoic acid} at T = (293.15, 298.15, 303.15, 308.15 and 313.15) K have been graphically presented in Figures 5.33 – 5.34 below:
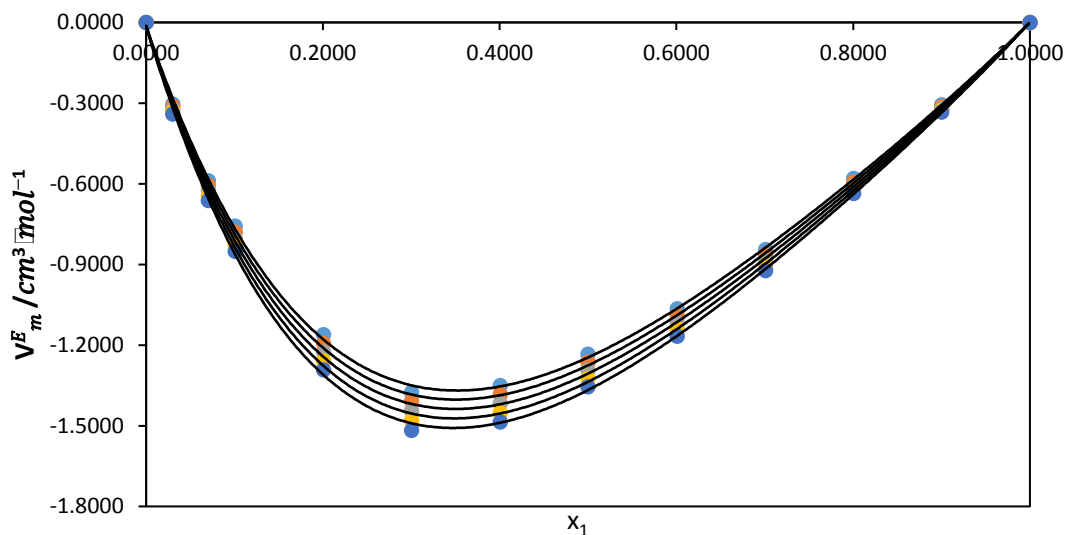
Figure 5.33 Excess molar volumes (V_m^E) for the binary mixture of ({[EPMpyr]$^+$[OAC]$^-$ (x_1) + propanoic acid (x_2)} as a function of the composition expressed in mole fraction of [EPMpyr]$^+$[OAC]$^-$ at T = 293.15 K (●), 298.15 K (●), 303.15 K (●), 308.15 K (●), 313.15 K (●). The lines were generated using Redlich-Kister curve-fitting.
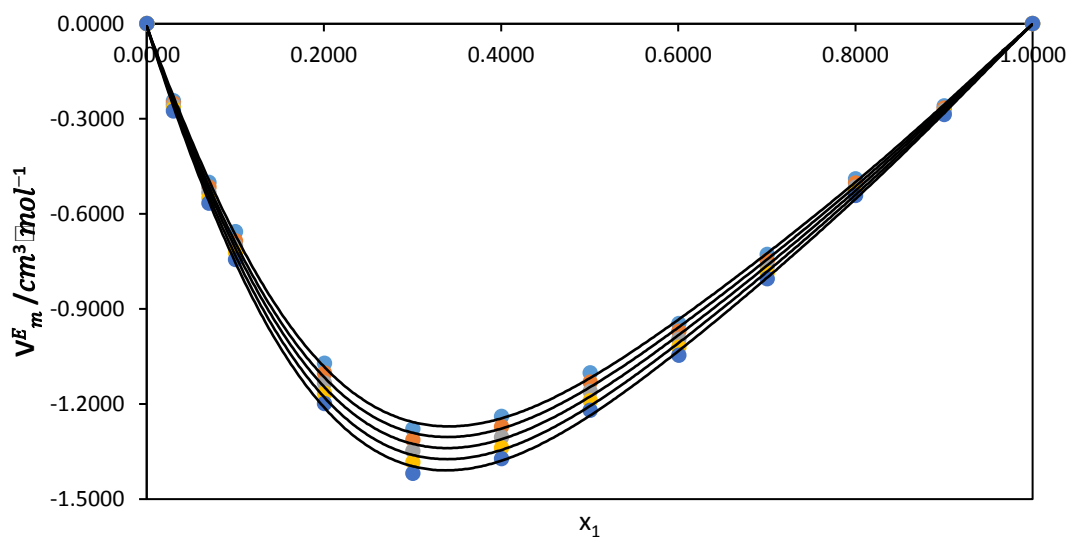
Figure 5.34 Excess molar volumes (V_m^E) for the binary mixture of ({[EPMpyr]$^+$[OAC]$^-$ (x_1) + butanoic acid (x_2)} as a function of the composition expressed in mole fraction of [EPMpyr]$^+$[OAC]$^-$ at T = 293.15 K (●), 298.15 K (●), 303.15 K (●), 308.15 K (●), 313.15 K (●). The lines were generated using Redlich-Kister curve-fitting.

Tables 5.10 and 5.11 present the tabulated values of V_m^E for the two-component solutions of {[EPMpyr]$^+$[OAC]$^-$ (x_1) + propanoic or butanoic acid (x_2) and the corresponding plots of V_m^E versus mole fraction of IL were depicted in Figures 5.33 and 5.34. It was noticed that with every rise in temperature, the V_m^E values decreases and increases with increasing mole fraction. The $V_{m,min}^E$ values obtained for the two-component solutions of {[EPMpyr]$^+$[OAC]$^-$ (x_1) + propanoic acid (x_2) and {[EPMpyr]$^+$[OAC]$^-$ (x_1) + butanoic acid (x_2) were found to be -1.5170 cm^3·mol^{-1} and -1.4192 cm^3·mol^{-1} which occurred at x_1 = 0.3003 and 0.3004 respectively. The negative values observed for the excess molar volumes may be due to accommodation or interaction of different molecules in the liquid components.

Table 5.10 and 5.11 presents the results of isentropic compressibility k_s and deviation in isentropic compressibility Δk_s for the two-component combinations of {[EPMpyr]$^+$[OAC]$^-$ (x_1) + propanoic or butanoic acid (x_2)}. The k_s values were found to increase with rise in temperature but was decreased across the concentration of IL for both binary systems. This can be linked to the occurrence of thermal agitation of the liquid solutions leading to compressibility. Figure 5.35 and 5.36 show the plots of deviation in compressibility Δk_s against the mole fraction of IL. The negative values of Δk_s depicts stronger interactions in the molecules of the IL and carboxylic acid mixtures. This behaviour specifies a lesser compressibility in the two-component solutions. However, there is closeness in the molecules of carboxylic acids and IL mixtures which in turn leads to a reduction in compressibility of binary solutions thereby giving a negative deviation in isentropic compressibility (Zafarani-Moattar and Shekaari 2005; Gowrisankar. 2013). The minimum $\Delta k_{s,min}$ values for the two-component combinations of {[EPMpyr]$^+$[OAC]$^-$ (x_1) + propionic or butyric acid (x_2)} were found to be are -15.4998 (10^8/ Pa^{-1}) and -14.3560 (10^8/Pa^{-1}) which occurred at x_1 = 0.3003 and 0.3004 respectively.

The plots of deviation in isentropic compressibility for the binary systems have been plotted in Figures 5.35 – 5.36 below:
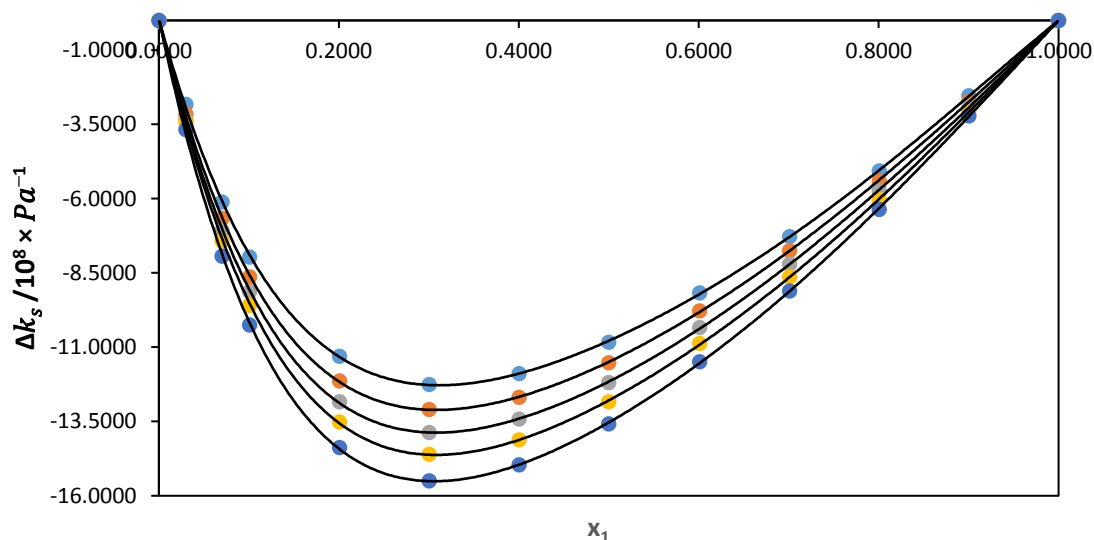
Figure 5.35 Deviation in isentropic compressibility (Δk_s) for the binary mixture of {[EPMpyr]$^+$[OAC]$^-$ (x_1) + propanoic acid (x_2)} as a function of the composition expressed in mole fraction of [EPMpyr]$^+$[OAC]$^-$ at T = 293.15 K (●), 298.15 K (●), 303.15 K (●), 308.15 K (●), 313.15 K (●). The lines were generated using Redlich-Kister curve-fitting.
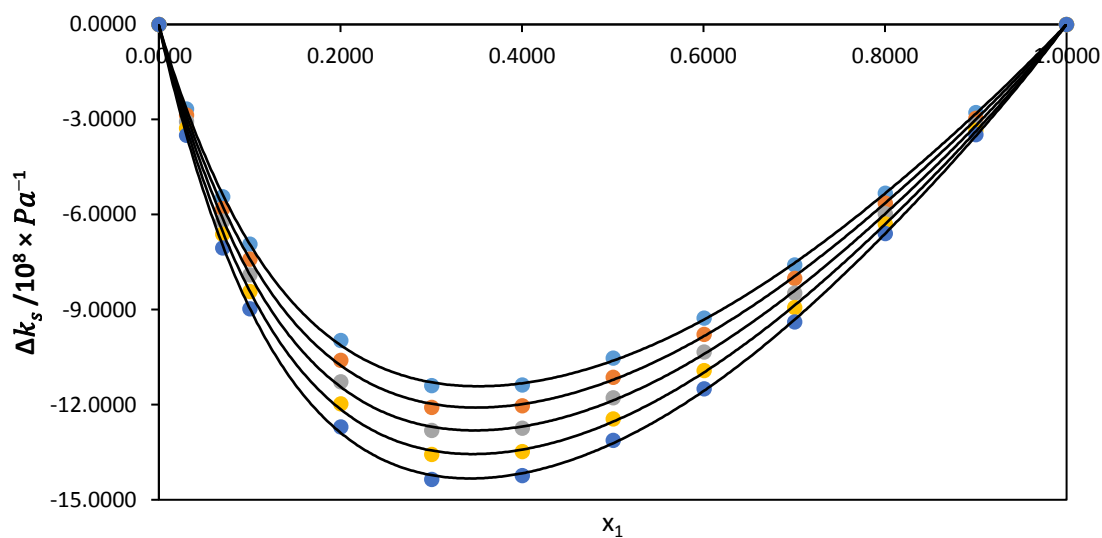
Figure 5.36 Deviation in isentropic compressibility (Δk_s) for the binary mixture of ({[EPMpyr]$^+$[OAC]$^-$ (x_1) + butanoic acid (x_2)}) as a function of the composition expressed in mole fraction of [EPMpyr]$^+$[OAC]$^-$ at T = 293.15 K (●), 298.15 K (●), 303.15 K (●), 308.15 K (●), 313.15 K (●). The lines were generated using Redlich-Kister curve-fitting.

Figures 5.37 – 5.38 presents the plots of intermolecular free length (L_f) against mole fraction for the binary systems of {[EPMpyr]$^+$[OAC]$^-$ (x_1) + propanoic or butanoic acid (x_2)} studied at T = (293.15, 298.15, 303.15, 308.15 and 313.15) K.
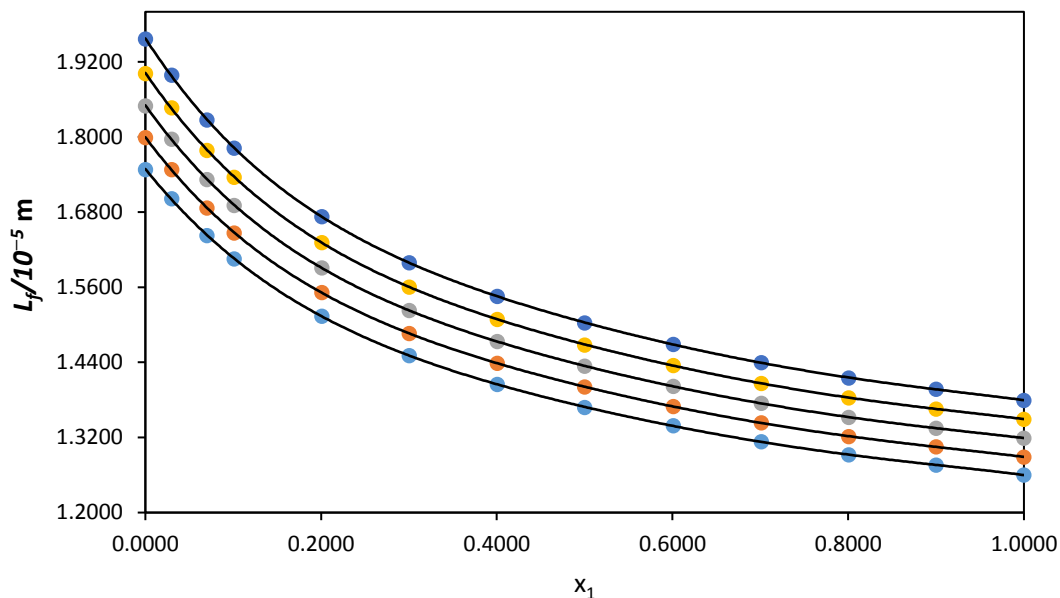
Figure 5.37 Intermolecular free length (L_f) for the binary mixture of ({[EPMpyr]$^+$[OAC]$^-$ (x_1) + propanoic acid (x_2)} as a function of the composition expressed in mole fraction of [EPMpyr]$^+$[OAC]$^-$ at T = 293.15 K (●), 298.15 K (●), 303.15 K (●), 308.15 K (●), 313.15 K (●). The lines were generated using Redlich-Kister curve-fitting.
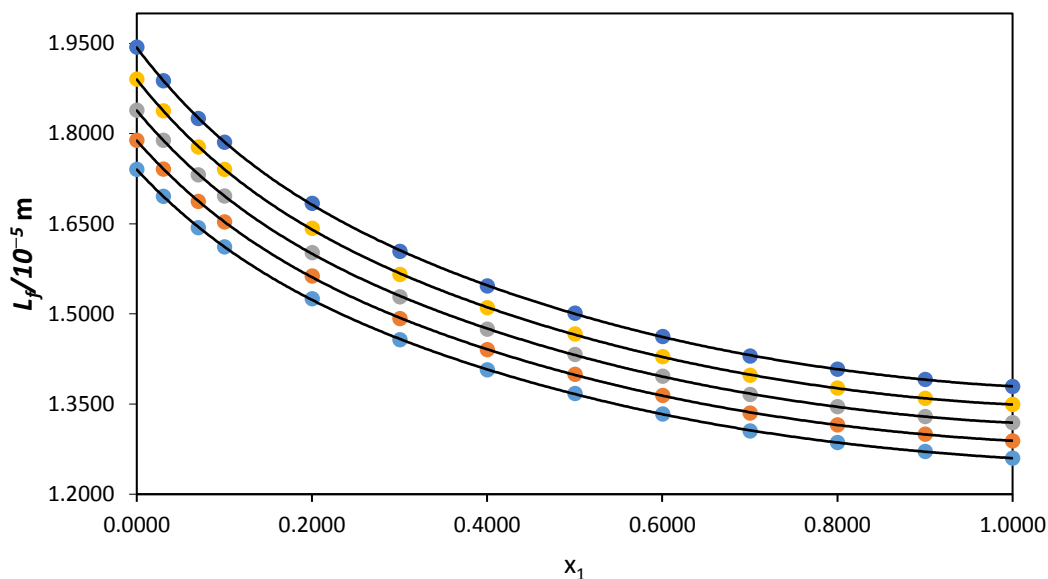
Figure 5.38   Intermolecular free length (L_f) for the binary mixture of ({[EPMpyr]$^+$[OAC]$^-$ (x_1) + butanoic acid (x_2)} as a function of the composition expressed in mole fraction of [EPMpyr]$^+$[OAC]$^-$ at T = 293.15 K (●), 298.15 K (●), 303.15 K (●), 308.15 K (●), 313.15 K (●). The lines were generated using Redlich-Kister curve-fitting.

The calculated values of L_f for the two-component combinations of {[EPMpyr]$^+$[OAC]$^-$ (x_1) + ethanoic or propanoic acid (x_2)} at T = (293.15, 298.15, 303.15, 308.15 and 313.15) K throughout the concentration of IL were reported in Table 5.10 and 5.11. These L_f values have been calculated from equation (5.1). The plots of L_f against the mole fraction of IL were presented in Figures 5.37 and 5.38. As seen from the results, Tables 5.10 and 5.11 as well as in Figures 5.37 and 5.38 showed that L_f increases with increase in temperature, while an increment in concentration of IL results in the decrease in L_f values throughout the binary mixtures studied. Similarly, the relationship that exist between speed of sound u and intermolecular free length L_f indicates a decrease in L_f as the corresponding u values increases. Intermolecular free length L_f explains the distance that occur between the surface of two molecules leading to a corresponding decrease in the speed of sound; L_f explains better the nature of intermolecular interactions that occur in the liquid mixtures.

The Redlich-Kister fitting parameters were calculated from equation (4.2) and the standard deviation σ, was calculated using equation (4.3). The resultant values for the binary systems studied are given in Table 5.12 below:

Table 5.12 Redlich- Kister fitting coefficients and standard deviation, σ, for binary systems of $\{[EPMpyr]^+[OAC]^-\ (x_1)$ + propanoic or butanoic acid $(x_2)\}$ studied at $T = (293.15,\ 298.15,\ 303.15,\ 308.15$ and $313.15)$ K.

	$T/(K)$	A_0	A_1	A_2	A_3	σ
		$\{[EPMpyr]^+[OAC]^-\ (x_1)$ + propanoic acid $(x_2)\}$				
$V_m^E/cm^3 \cdot mol^{-1}$	293.15	-4.976	-2.968	-1.515	-0.368	0.016
	298.15	-5.094	-3.046	-1.585	-0.413	0.016
	303.15	-5.213	-3.129	-1.660	-0.458	0.016
	308.15	-5.335	-3.212	-1.738	-0.510	0.017
	313.15	-5.458	-3.299	-1.811	-0.564	0.017
$\Delta k_s/10^8 \times Pa^{-1}$	293.15	-43.060	-27.110	-22.737	-15.242	0.066
	298.15	-45.797	-28.766	-25.699	-18.151	0.062
	303.15	-48.434	-30.495	-27.485	-18.852	0.071
	308.15	-51.008	-32.388	-28.755	-18.893	0.085
	313.15	-53.938	-34.480	-30.965	-21.196	0.090
$L_f/10^{-5}$ m	293.15	4.649	-2.113	16.334	12.326	0.813
	298.15	4.756	-2.170	16.749	12.703	0.835
	303.15	4.867	-2.230	17.184	13.101	0.857
	308.15	4.980	-2.292	17.629	13.509	0.880
	313.15	5.097	-2.355	18.087	13.933	0.904
		$\{[EPMpyr]^+[OAC]^-\ (x_1)$ + butanoic acid $(x_2)\}$				
$V_m^E/cm^3 \cdot mol^{-1}$	293.15	-4.509	-3.293	-1.081	-0.758	0.016
	298.15	-4.624	-3.371	-1.165	-0.692	0.015
	303.15	-4.744	-3.467	-1.205	-0.717	0.016
	308.15	-4.863	-3.559	-1.275	-0.698	0.016
	313.15	-4.984	-3.651	-1.332	-0.671	0.016

$\Delta k_s/10^8 \times Pa^{-1}$	293.15	-42.213	-20.035	-17.804	-13.947	0.098
	298.15	-44.587	-21.355	-19.582	-15.103	0.108
	303.15	-47.147	-22.739	-21.431	-16.251	0.118
	308.15	-49.786	-24.204	-23.243	-17.765	0.128
	313.15	-52.473	-25.830	-24.925	-19.641	0.137
$L_f/10^{-5}$ m	293.15	4.644	-2.009	16.362	12.251	0.809
	298.15	4.751	-2.063	16.774	12.618	0.831
	303.15	4.861	-2.118	17.202	12.999	0.853
	308.15	4.973	-2.175	17.642	13.393	0.875
	313.15	5.089	-2.233	18.094	13.799	0.899

Standard uncertainties u are $u(T) = \pm 0.01$ K and the combined expanded uncertainty U_c in density and speed of sound measurements were less than $U_c\,(\rho) = \pm\,2$ x 10^{-4} g·cm^{-3} and $U_c(u) = 0.6$ m·s^{-1} respectively (0.95 level of confidence)

5.1.5 Ionic liquid {[PYR-PDO]⁺[Cl]⁻ with ethanoic or propanoic or butanoic acid}

Densities (ρ) were measured for pure liquids [PYR-PDO]$^+$[Cl]$^-$, ethanoic acid, propanoic acid and butanoic acid as well as their two-component systems {[PYR-PDO]$^+$[Cl]$^-$ (x_1) + ethanoic or propanoic or butanoic acid (x_2)} at temperature T = (293.15, 298.15, 303.15, 308.15 and 313.15) K, and at p = 0.1 MPa. The results were reported in Table 5.13 − 5.15. The plots of density (ρ) versus mole fraction of [PYR-PDO]$^+$[Cl]$^-$ at the examined temperatures were shown in Figure 5.39 − 5.41 for the three two-component systems. It can be seen from Table 5.13 − 5.15 that an increment in temperature decreases ρ values but increases when concentration of IL is increased. This occurrence can be linked to the stronger interactions between the component molecules when combined. The density values of the three binary systems follow the sequence: ethanoic acid > propanoic acid > butanoic acid. It can be deduced from the results that density decreases as the alkyl chain length increases at the same concentration for the two-component combinations (Vasanthakumar et al. 2016).
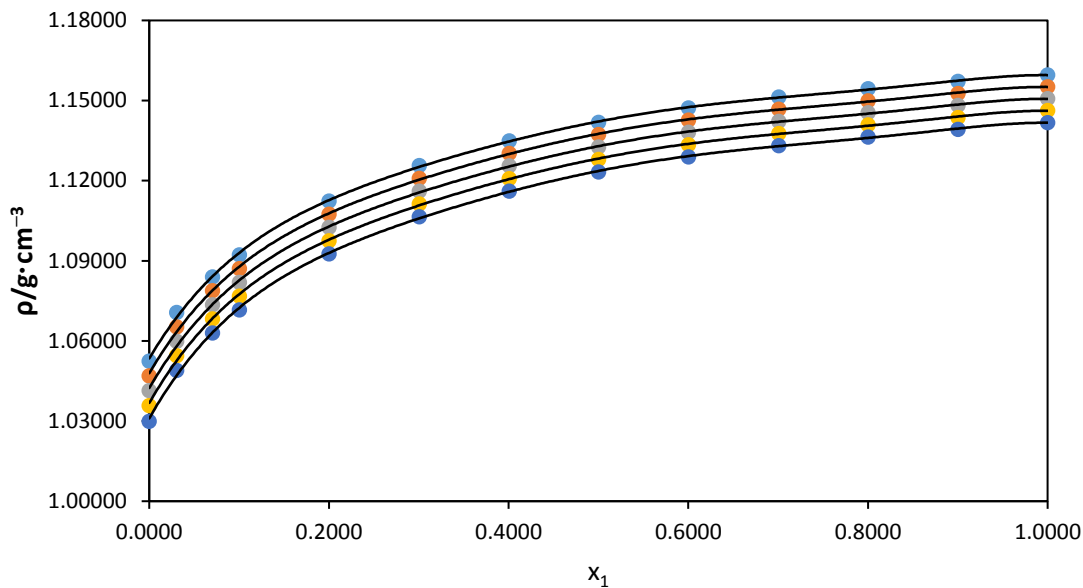
Figure 5.39 Density (ρ) for the binary mixture of {[PYR-PDO]$^+$[Cl]$^-$ (x_1) + ethanoic acid (x_2)} plotted against mole fraction of [PYR-PDO]$^+$[Cl]$^-$ at T = 293.15 K (●), 298.15 K (●), 303.15 K (●), 308.15 K (●), 313.15 K (●). The line represents the smoothness of the data.

Figure 5.40 Density (ρ) for the binary mixture of {[PYR-PDO]$^+$[Cl]$^-$ (x_1) + propanoic acid (x_2)} plotted against mole fraction of [PYR-PDO]$^+$[Cl]$^-$ at T = 293.15 K (●), 298.15 K (●), 303.15 K (●), 308.15 K (●), 313.15 K (●). The line represents the smoothness of the data.

107
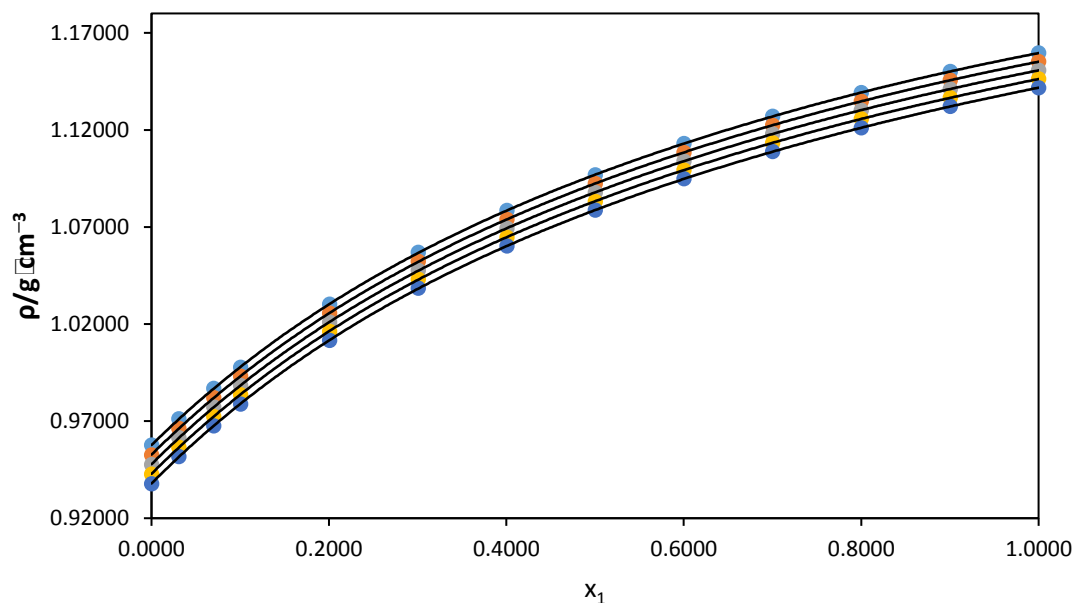
Figure 5.41 Density (ρ) for the binary mixture of {[PYR-PDO]$^+$[Cl]$^-$ (x_1) + butanoic acid (x_2)} plotted against mole fraction of [PYR-PDO]$^+$[Cl]$^-$ at T = 293.15 K (●), 298.15 K (●), 303.15 K (●), 308.15 K (●), 313.15 K (●). The line represents the smoothness of the data.

Speed of sound u measurements for the two-component solutions of {[PYR-PDO]$^+$[Cl]$^-$ (x_1) + ethanoic acid or propanoic acid or butanoic acid (x_2)} were determined at T = (293.15, 298.15, 303.15, 308.15 and 313.15) K. The plots of u versus the mole concentration of IL (x_1) of the two-component systems studied were presented in Figures 5.42 − 5.44 and the values of u have been recorded in Table 5.13 − 5.15. The speed of sound is a parameter that helps to understand the behaviour of solute-solute, solute-solvent and solvent-solvent interactions in liquid component solutions. In this regard, the results obtained from Table 5.13 − 5.15 and plotted in Figure 5.42 − 5.44 for the three two-component systems showed that u value decreases with rise in temperature and increases as concentration of the IL increases.
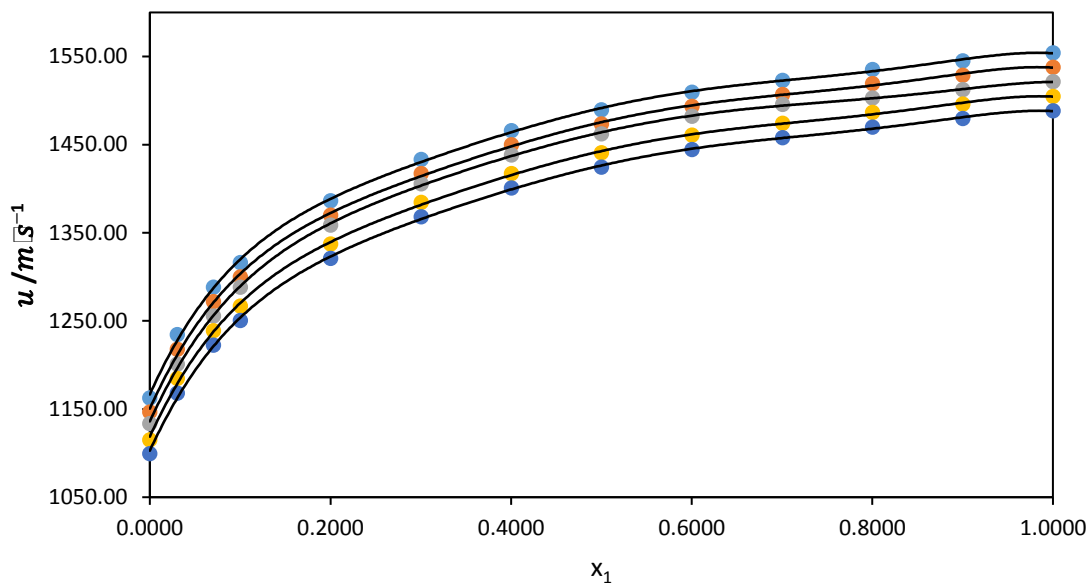
Figure 5.42 Speed of sound (u) for the binary mixture of {[PYR-PDO]$^+$[Cl]$^-$ (x_1) + ethanoic acid (x_2)} plotted against mole fraction of [PYR-PDO]$^+$[Cl]$^-$ at T = 293.15 K (●), 298.15 K (●), 303.15 K (●), 308.15 K (●), 313.15 K (●). The line represents the smoothness of the data.
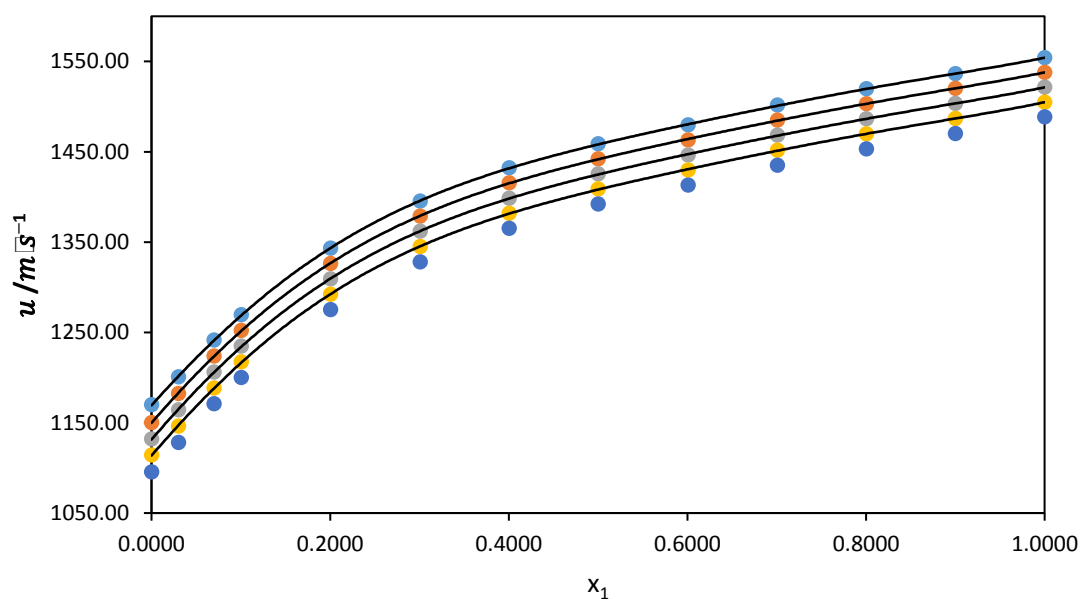
Figure 5.43 Speed of sound (u) for the binary mixture of {[PYR-PDO]$^+$[Cl]$^-$ (x_1) + propanoic acid (x_2)} plotted against mole fraction of [PYR-PDO]$^+$[Cl]$^-$ at T = 293.15 K (●), 298.15 K (●), 303.15 K (●), 308.15 K (●), 313.15 K (●). The line represents the smoothness of the data.
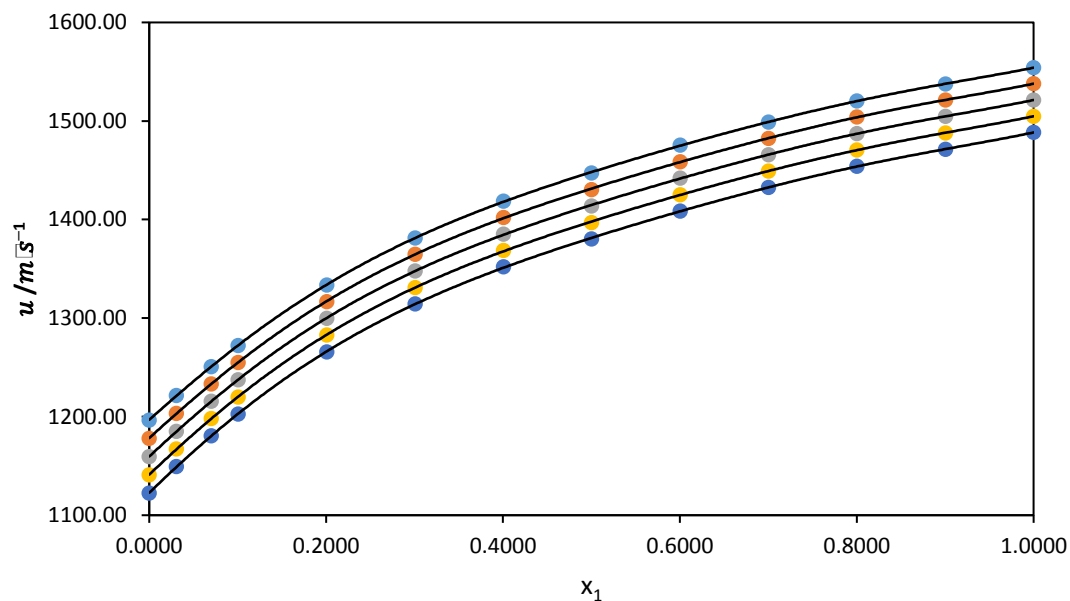
Figure 5.44 Speed of sound (u) for the binary mixture of $\{[\text{PYR-PDO}]^+[\text{Cl}]^-\ (x_1) + \text{butanoic}$ acid $(x_2)\}$ plotted against mole fraction of $[\text{PYR-PDO}]^+[\text{Cl}]^-$ at $T = 293.15$ K (●), 298.15 K (●), 303.15 K (●), 308.15 K (●), 313.15 K (●). The line represents the smoothness of the data.

Table 5.13 – 5.15 shows the results of excess molar volume V_m^E for the binary mixtures of $\{[\text{PYR-PDO}]^+[\text{Cl}]^-\ (x_1) + \text{ethanoic or propanoic or butanoic acid }(x_2)\}$ at all investigated temperatures.

Table 5.13   Density (ρ), excess molar volume (V_m^E), speed of sound (u), isentropic compressibility (k_s), deviation in isentropic compressibility (Δk_s) and intermolecular free length (L_f) for the binary system {[PYR-PDO]$^+$[Cl]$^-$ (x_1) + ethanoic acid (x_2)} from $T = $ (293.15 − 313.15) K.

x_1	ρ/g·cm^{-3}	V_m^E/cm^3·mol^{-1}	u/m·s^{-1}	$k_s/10^8 \times$ Pa^{-1}	$\Delta k_s/10^8 \times$ Pa^{-1}	$L_f/10^{-5}$ m
			T = 293.15 K			
0.0000	1.05247	0.0000	1162.54	70.3028	0.0000	1.7088
0.0305	1.07062	-0.4792	1234.60	61.2789	-7.9684	1.5954
0.0704	1.08401	-0.6560	1288.45	55.5689	-12.3001	1.5193
0.1002	1.09222	-0.7505	1316.20	52.8500	-13.9857	1.4816
0.2001	1.11238	-0.9216	1386.16	46.7864	-16.5921	1.3940
0.3005	1.12567	-0.9572	1433.12	43.2538	-16.6527	1.3404
0.4006	1.13490	-0.9073	1465.75	41.0132	-15.4312	1.3052
0.5002	1.14186	-0.8271	1489.64	39.4661	-13.5318	1.2804
0.6002	1.14723	-0.7137	1509.59	38.2500	-11.2876	1.2605
0.7007	1.15130	-0.5519	1523.03	37.4452	-8.6161	1.2471
0.8003	1.15443	-0.3581	1535.41	36.7438	-5.8719	1.2354
0.9001	1.15713	-0.1683	1545.00	36.2043	-2.9578	1.2263
1.0000	1.15960	0.0000	1554.07	35.7067	0.0000	1.2178
			T = 298.15 K			
0.0000	1.04695	0.0000	1146.68	72.6426	0.0000	1.7530
0.0305	1.06523	-0.4871	1217.98	63.2814	-8.2618	1.6362
0.0704	1.07877	-0.6687	1272.11	57.2826	-12.8248	1.5567
0.1002	1.08707	-0.7655	1299.94	54.4372	-14.5938	1.5175
0.2001	1.10745	-0.9412	1370.03	48.1079	-17.3218	1.4266
0.3005	1.12088	-0.9781	1417.05	44.4294	-17.3835	1.3710
0.4006	1.13021	-0.9274	1449.71	42.0997	-16.1068	1.3345
0.5002	1.13726	-0.8475	1473.57	40.4947	-14.1217	1.3089
0.6002	1.14267	-0.7292	1493.49	39.2353	-11.7765	1.2883
0.7007	1.14677	-0.5636	1506.91	38.4015	-8.9891	1.2746

111

0.8003	1.14994	-0.3656	1519.27	37.6752	-6.1261	1.2625
0.9001	1.15267	-0.1717	1528.80	37.1188	-3.0850	1.2531
1.0000	1.15516	0.0000	1537.84	36.6045	0.0000	1.2444

T = 303.15 K

0.0000	1.04140	0.0000	1133.51	74.7366	0.0000	1.7943
0.0305	1.05984	-0.4961	1201.28	65.3841	-8.2179	1.6783
0.0704	1.07353	-0.6828	1255.55	59.0908	-13.0296	1.5955
0.1002	1.08192	-0.7822	1288.43	55.6781	-15.3315	1.5487
0.2001	1.10252	-0.9630	1358.62	49.1380	-18.1552	1.4549
0.3005	1.11609	-1.0010	1405.70	45.3436	-18.2175	1.3976
0.4006	1.12551	-0.9490	1438.37	42.9447	-16.8948	1.3602
0.5002	1.13264	-0.8673	1462.24	41.2926	-14.8420	1.3337
0.6002	1.13809	-0.7463	1482.11	40.0002	-12.4149	1.3127
0.7007	1.14223	-0.5763	1495.50	39.1447	-9.5336	1.2986
0.8003	1.14543	-0.3744	1502.81	38.6565	-6.3178	1.2905
0.9001	1.14819	-0.1758	1512.34	38.0792	-3.1827	1.2808
1.0000	1.15071	0.0000	1521.34	37.5476	0.0000	1.2718

T = 308.15 K

0.0000	1.03584	0.0000	1115.22	77.6225	0.0000	1.8452
0.0305	1.05443	-0.5049	1184.69	67.5733	-8.8564	1.7216
0.0704	1.06826	-0.6966	1239.02	60.9769	-13.8950	1.6354
0.1002	1.07674	-0.7986	1266.95	57.8587	-15.8455	1.5930
0.2001	1.09757	-0.9843	1337.25	50.9500	-18.8470	1.4949
0.3005	1.11128	-1.0237	1384.35	46.9553	-18.9179	1.4351
0.4006	1.12080	-0.9708	1417.04	44.4333	-17.5273	1.3960
0.5002	1.12799	-0.8869	1440.89	42.7005	-15.3650	1.3685
0.6002	1.13350	-0.7630	1460.74	41.3459	-12.8090	1.3467
0.7007	1.13768	-0.5887	1474.10	40.4507	-9.7755	1.3320
0.8003	1.14091	-0.3829	1486.40	39.6712	-6.6608	1.3191
0.9001	1.14370	-0.1798	1495.88	39.0747	-3.3544	1.3091
1.0000	1.14624	0.0000	1504.86	38.5241	0.0000	1.2999

T = 313.15 K

0.0000	1.02996	0.0000	1099.47	80.3182	0.0000	1.8937
0.0305	1.04900	-0.5309	1168.14	69.8608	-9.2131	1.7662
0.0704	1.06299	-0.7268	1222.52	62.9450	-14.5040	1.6765
0.1002	1.07156	-0.8312	1250.48	59.6801	-16.5507	1.6324
0.2001	1.09260	-1.0203	1320.90	52.4563	-19.6988	1.5304
0.3005	1.10645	-1.0589	1368.04	48.2913	-19.7707	1.4684
0.4006	1.11607	-1.0033	1400.76	45.6648	-18.3157	1.4279
0.5002	1.12333	-0.9153	1424.62	43.8627	-16.0547	1.3995
0.6002	1.12890	-0.7871	1444.43	42.4574	-13.3806	1.3769
0.7007	1.13311	-0.6066	1457.76	41.5295	-10.2104	1.3617
0.8003	1.13638	-0.3951	1470.03	40.7215	-6.9562	1.3484
0.9001	1.13919	-0.1854	1479.50	40.1029	-3.5035	1.3381
1.0000	1.14176	0.0000	1488.45	39.5329	0.0000	1.3286

Table 5.14 Density (ρ), excess molar volume (V_m^E), speed of sound (u), isentropic compressibility (k_s), deviation in isentropic compressibility (Δk_s) and intermolecular free length (L_f) for the binary system {[PYR-PDO]$^+$[Cl]$^-$ (x_1) + propanoic acid (x_2)} from T = (293.15 – 313.15) K.

x_1	ρ/g·cm^{-3}	V_m^E /cm^3·mol^{-1}	u/m·s^{-1}	k_s/10^8 × Pa^{-1}	Δk_s/10^8 × Pa^{-1}	L_f/10^{-5} m
			T = 293.15 K			
0.0000	0.99378	0.0000	1169.75	73.5398	0.0000	1.7477
0.0302	1.00771	-0.1763	1200.52	68.8520	-3.5440	1.6911
0.0702	1.02366	-0.3382	1241.27	63.4032	-7.4818	1.6228
0.1004	1.03460	-0.4525	1269.46	59.9779	-9.7644	1.5784
0.2004	1.06435	-0.7086	1343.07	52.0858	-13.8718	1.4709
0.3007	1.08670	-0.8089	1395.43	47.2579	-14.9038	1.4011
0.4004	1.10343	-0.7558	1431.98	44.1958	-14.1949	1.3549
0.5001	1.11702	-0.6645	1458.55	42.0819	-12.5377	1.3221
0.6010	1.12846	-0.5503	1479.55	40.4815	-10.3208	1.2967
0.7009	1.13811	-0.4341	1501.45	38.9756	-8.0456	1.2724
0.8003	1.14640	-0.3143	1519.50	37.7802	-5.4801	1.2527
0.9002	1.15359	-0.1820	1536.44	36.7214	-2.7617	1.2350
1.0000	1.15960	0.0000	1554.07	35.7067	0.0000	1.2178
			T = 298.15 K			
0.0000	0.98841	0.0000	1150.14	76.4823	0.0000	1.7988
0.0302	1.00246	-0.1833	1182.32	71.3616	-3.9164	1.7375
0.0702	1.01856	-0.3550	1223.76	65.5570	-8.1271	1.6653
0.1004	1.02958	-0.4738	1252.23	61.9401	-10.5395	1.6188
0.2004	1.05950	-0.7366	1326.24	53.6605	-14.8299	1.5067
0.3007	1.08195	-0.8369	1378.76	48.6201	-15.8691	1.4342
0.4004	1.09875	-0.7809	1415.43	45.4282	-15.0863	1.3863
0.5001	1.11249	-0.6965	1442.07	43.2248	-13.3147	1.3523
0.6010	1.12396	-0.5780	1463.11	41.5619	-10.9540	1.3260
0.7009	1.13364	-0.4559	1485.05	39.9984	-8.5321	1.3008

0.8003	1.14194	-0.3302	1503.10	38.7596	-5.8067	1.2805
0.9002	1.14915	-0.1915	1520.04	37.6628	-2.9221	1.2623
1.0000	1.15516	0.0000	1537.84	36.6045	0.0000	1.2444

T = 303.15 K

0.0000	0.98303	0.0000	1131.80	79.4136	0.0000	1.8496
0.0302	0.99722	-0.1927	1164.02	74.0100	-4.1392	1.7856
0.0702	1.01347	-0.3732	1206.04	67.8370	-8.6388	1.7095
0.1004	1.02456	-0.4967	1234.75	64.0181	-11.1932	1.6607
0.2004	1.05466	-0.7665	1309.14	55.3245	-15.6987	1.5438
0.3007	1.07720	-0.8675	1361.82	50.0568	-16.7658	1.4685
0.4004	1.09406	-0.8081	1398.59	46.7280	-15.9217	1.4188
0.5001	1.10785	-0.7193	1425.31	44.4325	-14.0440	1.3835
0.6010	1.11945	-0.6068	1446.39	42.6996	-11.5527	1.3563
0.7009	1.12916	-0.4798	1468.36	41.0751	-8.9932	1.3302
0.8003	1.13749	-0.3484	1486.42	39.7896	-6.1168	1.3092
0.9002	1.14471	-0.2033	1503.38	38.6515	-3.0750	1.2904
1.0000	1.15071	0.0000	1521.34	37.5476	0.0000	1.2718

T = 308.15 K

0.0000	0.97764	0.0000	1114.23	82.3893	0.0000	1.9010
0.0302	0.99197	-0.2021	1145.95	76.7665	-4.2980	1.8350
0.0702	1.00836	-0.3913	1188.38	70.2222	-9.0891	1.7550
0.1004	1.01954	-0.5194	1217.31	66.1904	-11.7960	1.7039
0.2004	1.04980	-0.7964	1292.07	57.0589	-16.5393	1.5820
0.3007	1.07244	-0.8980	1344.92	51.5506	-17.6465	1.5037
0.4004	1.08947	-0.8464	1381.78	48.0738	-16.7510	1.4521
0.5001	1.10330	-0.7535	1408.57	45.6826	-14.7698	1.4155
0.6010	1.11494	-0.6363	1429.71	43.8788	-12.1477	1.3873
0.7009	1.12467	-0.5039	1451.70	42.1910	-9.4516	1.3604
0.8003	1.13302	-0.3658	1469.75	40.8580	-6.4240	1.3387
0.9002	1.14026	-0.2144	1486.72	39.6771	-3.2254	1.3192
1.0000	1.14624	0.0000	1504.86	38.5241	0.0000	1.2999

T = 313.15 K

0.0000	0.97225	0.0000	1095.58	85.6909	0.0000	1.9560
0.0302	0.98671	-0.2117	1127.96	79.6568	-4.6401	1.8859
0.0702	1.00325	-0.4101	1170.79	72.7167	-9.7353	1.8019
0.1004	1.01450	-0.5430	1199.95	68.4574	-12.6004	1.7483
0.2004	1.04493	-0.8271	1275.04	58.8663	-17.5740	1.6212
0.3007	1.06767	-0.9290	1328.06	53.1043	-18.7049	1.5398
0.4004	1.08486	-0.8854	1365.04	49.4695	-17.7389	1.4862
0.5001	1.09873	-0.7885	1391.90	46.9778	-15.6296	1.4483
0.6010	1.11040	-0.6663	1413.08	45.1010	-12.8491	1.4191
0.7009	1.12017	-0.5283	1435.10	43.3464	-9.9907	1.3912
0.8003	1.12855	-0.3874	1453.15	41.9621	-6.7865	1.3688
0.9002	1.13578	-0.2257	1470.12	40.7379	-3.4022	1.3487
1.0000	1.14176	0.0000	1488.45	39.5329	0.0000	1.3286

Table 5.15   Density (ρ), excess molar volume (V_m^E), speed of sound (u), isentropic compressibility (k_s), deviation in isentropic compressibility (Δk_s) and intermolecular free length (L_f) for the binary system {[PYR-PDO]$^+$[Cl]$^-$ (x_1) + butanoic acid (x_2)} from T = (293.15 – 313.15) K.

x_1	ρ/g·cm^{-3}	V_m^E /cm^3·mol^{-1}	u/m·s^{-1}	k_s/10$^8 \times$ Pa^{-1}	Δk_s/10$^8 \times$ Pa^{-1}	L_f/10^{-5} m
			T = 293.15 K			
0.0000	0.95761	0.0000	1196.58	72.9337	0.0000	1.7405
0.0307	0.97118	-0.1706	1221.42	69.0193	-2.7730	1.6932
0.0700	0.98680	-0.3134	1250.83	64.7699	-5.5561	1.6402
0.1005	0.99783	-0.3909	1272.15	61.9249	-7.2681	1.6038
0.2007	1.03020	-0.6246	1333.63	54.5767	-10.8863	1.5056
0.3007	1.05689	-0.7589	1381.38	49.5844	-12.1535	1.4351
0.4006	1.07847	-0.7300	1418.66	46.0720	-11.9470	1.3834
0.5002	1.09687	-0.6651	1447.24	43.5276	-10.7841	1.3446
0.6002	1.11298	-0.5892	1475.36	41.2778	-9.3121	1.3094
0.7002	1.12699	-0.4827	1498.85	39.4970	-7.3710	1.2809
0.8001	1.13926	-0.3494	1520.32	37.9758	-5.1715	1.2559
0.9004	1.15010	-0.1888	1537.65	36.7746	-2.6384	1.2359
1.0000	1.15960	0.0000	1554.07	35.7067	0.0000	1.2178
			T = 298.15 K			
0.0000	0.95265	0.0000	1178.07	75.6350	0.0000	1.7888
0.0307	0.96630	-0.1784	1203.28	71.4751	-2.9632	1.7389
0.0700	0.98202	-0.3305	1233.31	66.9475	-5.9535	1.6829
0.1005	0.99310	-0.4123	1254.89	63.9432	-7.7699	1.6447
0.2007	1.02556	-0.6527	1316.81	56.2330	-11.5693	1.5424
0.3007	1.05230	-0.7879	1364.75	51.0217	-12.8750	1.4692
0.4006	1.07390	-0.7561	1402.14	47.3645	-12.6333	1.4155
0.5002	1.09232	-0.6871	1430.50	44.7376	-11.3732	1.3757
0.6002	1.10845	-0.6054	1458.67	42.4006	-9.8082	1.3393
0.7002	1.12246	-0.4924	1482.44	40.5391	-7.7673	1.3096

0.8001	1.13474	-0.3521	1503.94	38.9622	-5.4433	1.2839
0.9004	1.14558	-0.1840	1521.25	37.7200	-2.7702	1.2632
1.0000	1.15516	0.0000	1537.84	36.6045	0.0000	1.2444

$T = 303.15$ K

0.0000	0.94769	0.0000	1159.43	78.4952	0.0000	1.8389
0.0307	0.96143	-0.1881	1185.10	74.0578	-3.1819	1.7862
0.0700	0.97724	-0.3484	1215.60	69.2497	-6.3772	1.7272
0.1005	0.98837	-0.4345	1237.41	66.0776	-8.3031	1.6872
0.2007	1.02093	-0.6830	1299.74	57.9817	-12.2962	1.5805
0.3007	1.04771	-0.8193	1347.87	52.5366	-13.6438	1.5044
0.4006	1.06934	-0.7847	1385.35	48.7264	-13.3635	1.4488
0.5002	1.08777	-0.7102	1413.74	45.9963	-12.0158	1.4077
0.6002	1.10390	-0.6231	1441.93	43.5693	-10.3491	1.3700
0.7002	1.11793	-0.5043	1465.78	41.6339	-8.1904	1.3392
0.8001	1.13021	-0.3569	1487.25	40.0012	-5.7306	1.3127
0.9004	1.14106	-0.1810	1504.59	38.7129	-2.9113	1.2914
1.0000	1.15071	0.0000	1521.34	37.5476	0.0000	1.2718

$T = 308.15$ K

0.0000	0.94273	0.0000	1140.94	81.4869	0.0000	1.8905
0.0307	0.95656	-0.1977	1167.16	76.7411	-3.4286	1.8347
0.0700	0.97245	-0.3663	1197.99	71.6519	-6.8256	1.7728
0.1005	0.98363	-0.4568	1220.02	68.3025	-8.8674	1.7309
0.2007	1.01628	-0.7128	1282.74	59.8010	-13.0641	1.6196
0.3007	1.04311	-0.8503	1331.05	54.1105	-14.4556	1.5406
0.4006	1.06477	-0.8128	1368.61	50.1402	-14.1340	1.4830
0.5002	1.08321	-0.7338	1397.04	47.3008	-12.6949	1.4404
0.6002	1.09935	-0.6411	1425.28	44.7778	-10.9227	1.4014
0.7002	1.11339	-0.5159	1449.12	42.7706	-8.6344	1.3697
0.8001	1.12567	-0.3607	1470.61	41.0767	-6.0343	1.3423
0.9004	1.13652	-0.1775	1487.94	39.7423	-3.0590	1.3203
1.0000	1.14624	0.0000	1504.86	38.5241	0.0000	1.2999

T = 313.15 K

0.0000	0.93777	0.0000	1122.60	84.6167	0.0000	1.9437
0.0307	0.95168	-0.2071	1149.33	79.5462	-3.6881	1.8846
0.0700	0.96765	-0.3842	1180.50	74.1564	-7.3022	1.8196
0.1005	0.97888	-0.4792	1202.72	70.6225	-9.4641	1.7758
0.2007	1.01163	-0.7432	1265.83	61.6919	-13.8773	1.6597
0.3007	1.03850	-0.8815	1314.30	55.7449	-15.3130	1.5777
0.4006	1.06018	-0.8410	1351.93	51.6075	-14.9467	1.5180
0.5002	1.07864	-0.7574	1380.41	48.6528	-13.4117	1.4739
0.6002	1.09479	-0.6590	1408.69	46.0298	-11.5274	1.4336
0.7002	1.10882	-0.5268	1432.55	43.9459	-9.1038	1.4008
0.8001	1.12110	-0.3644	1454.00	42.1915	-6.3522	1.3725
0.9004	1.13205	-0.1883	1471.35	40.8038	-3.2175	1.3498
1.0000	1.14176	0.0000	1488.45	39.5329	0.0000	1.3286

The plots of excess molar volume V_m^E against mole fraction of {[PYR-PDO]$^+$[Cl]$^-$ for the binary systems of {[PYR-PDO]$^+$[Cl]$^-$ + ethanoic or propanoic or butanoic acid} at $T = (293.15,$ 298.15, 303.15, 308.15 and 313.15) K have been graphically presented in Figures 5.45 – 5.47 below:
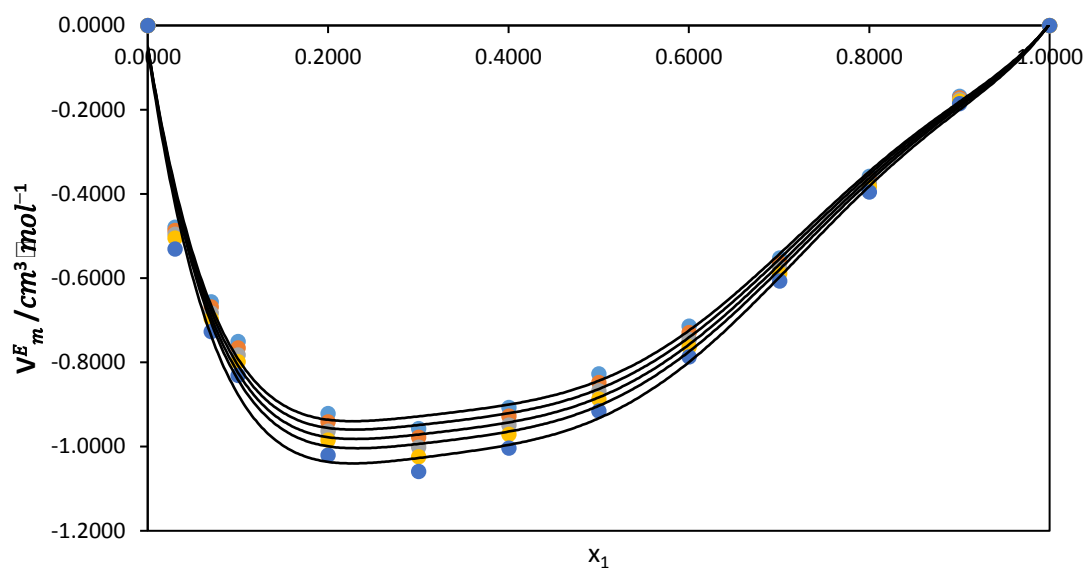
Figure 5.45 Excess molar volumes (V_m^E) for the binary mixture of {[PYR-PDO]$^+$[Cl]$^-$ (x_1) + ethanoic acid (x_2)} as a function of the composition expressed in mole fraction of [PYR-PDO]$^+$[Cl]$^-$ at $T = 293.15$ K (●), 298.15 K (●), 303.15 K (●), 308.15 K (●), 313.15 K (●). The lines were generated using Redlich-Kister curve-fitting.
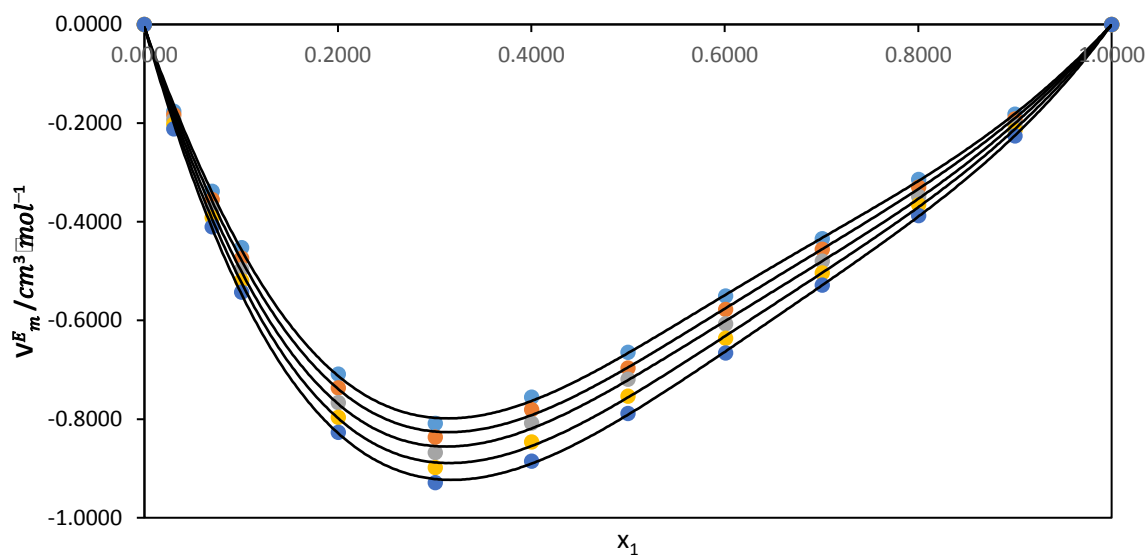
Figure 5.46 Excess molar volumes (V_m^E) for the binary mixture of {[PYR-PDO]$^+$[Cl]$^-$ (x_1) + propanoic acid (x_2)} as a function of the composition expressed in mole fraction of [PYR-PDO]$^+$[Cl]$^-$ at $T = 293.15$ K (●), 298.15 K (●), 303.15 K (●), 308.15 K (●), 313.15 K (●). The lines were generated using Redlich-Kister curve-fitting.
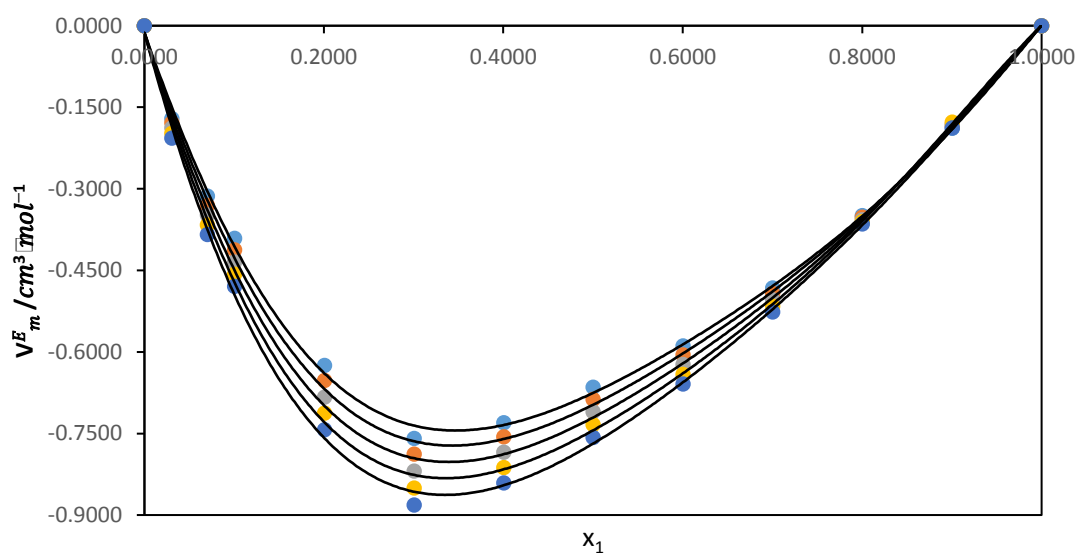
Figure 5.47 Excess molar volumes (V_m^E) for the binary mixture of {[PYR-PDO]$^+$[Cl]$^-$ (x_1) + butanoic acid (x_2)} as a function of the composition expressed in mole fraction of [PYR-PDO]$^+$[Cl]$^-$ at $T = 293.15$ K (●), 298.15 K (●), 303.15 K (●), 308.15 K (●), 313.15 K (●). The lines were generated using Redlich-Kister curve-fitting.

Excess molar volume V_m^E is a thermodynamic parameter which is derived from the measured density values. The calculated results of binary solutions of $\{$[PYR-PDO]$^+$[Cl]$^-$ (x_1) + ethanoic or propanoic or butanoic acid (x_2) were presented in Tables 5.13 to 5.15 while the plots of V_m^E against the mole fraction of IL were shown in Figures 5.45 to 5.47. As it can been seen from the tables and figures stated; the V_m^E values were negative all through the temperatures and compositions. The negative magnitude of these solutions with IL [PYR-PDO]$^+$[Cl]$^-$ follow the order:

Ethanoic acid < propanoic acid < butanoic acid

where the $V_{m,min}^E$ values for the two-component mixtures of IL with ethanoic or propanoic or butanoic acids were found to be -1.0589 cm^3·mol^{-1}, -0.9290 cm^3·mol^{-1} and -0.8815 cm^3·mol^{-1} which occurred at $x_1 = 0.3005$, 0.3007 and 0.3007 respectively. It was deduced from the above trend that as there is an increment in the alkyl chain length of these carboxylic acids utilized, the V_m^E values becomes more negative. This incidence may possibly be ascribed to the more filling outcome in the molecules of the carboxylic acid in the ionic liquid spaces (Patil and Dagade, 2018).

The thermodynamic derived parameters, k_s and Δk_s have been computed using the experimental values of densities and speed of sound for the two-component solutions of $\{$[PYR-PDO]$^+$[Cl]$^-$ + ethanoic or propanoic or butanoic acid$\}$ at different temperatures and concentrations. The results have been presented in Tables 5.13 to 5.15. k_s shows an increase with rise in temperature and a decrease with increment in concentration of IL. The increase in isentropic compressibility can be explained in terms of thermal stress that occur when the components are mixed. This in turn makes the solution to be more compressible (Zafarani-Moattar and Shekaari 2005).

For the two-component combinations studied, the deviation in isentropic compressibility values shows negative results throughout the entire composition and at all temperatures examined. The minimum $\Delta k_{s,min}$ values for the binary combinations of $\{$[PYR-PDO]$^+$[Cl]$^-$ (x_1) + acetic or propionic or butyric acid $(x_2)\}$ were found to be -19.7707 (10^8/ Pa^{-1}), -18.7049 (10^8/Pa^{-1}) and -15.3130 (10^8/Pa^{-1}) which occurred at $x_1 = 0.3005$, 0.3007 and 0.3007 respectively, and it follows the order:

ethanoic acid < propanoic acid < butanoic acid

This behaviour depicts that the binary solution are less compressible and as a result, there is closeness and strong connections in the molecules of the carboxylic acids and IL mixtures, leading to a reduction in compressibility of binary mixtures thereby giving a negative deviation in isentropic compressibility (Zafarani-Moattar and Shekaari 2005; Gowrisankar. 2013). The plots of deviation in isentropic compressibility for the binary systems have been plotted in Figures 5.48 – 5.50 below:
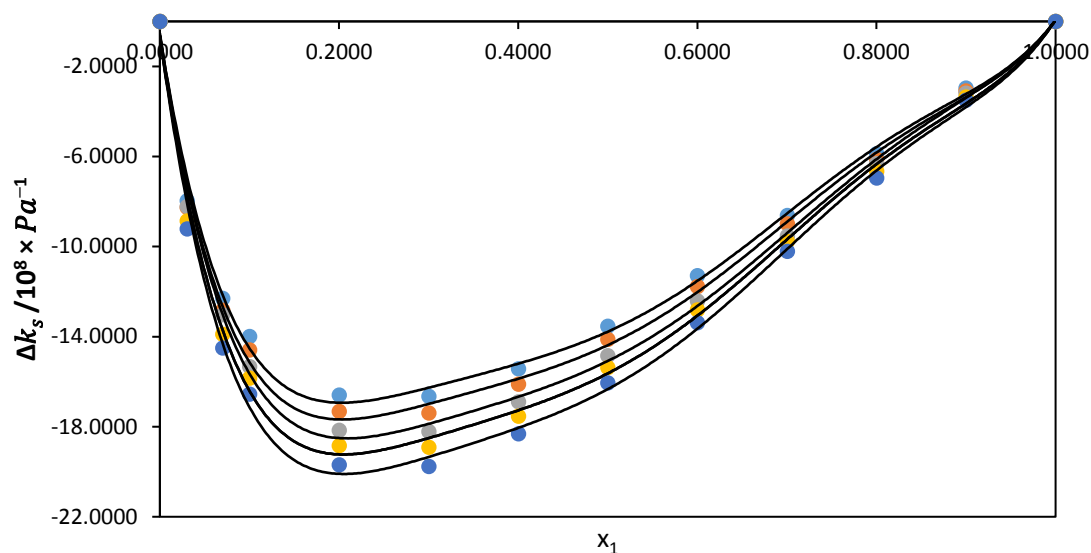
Figure 5.48 Deviation in isentropic compressibility (Δk_s) for the binary mixture of {[PYR-PDO]$^+$[Cl]$^-$ (x_1) + ethanoic acid (x_2)} as a function of the composition expressed in mole fraction of [PYR-PDO]$^+$[Cl]$^-$ at T = 293.15 K (●), 298.15 K (●), 303.15 K (●), 308.15 K (●), 313.15 K (●). The lines were generated using Redlich-Kister curve-fitting.
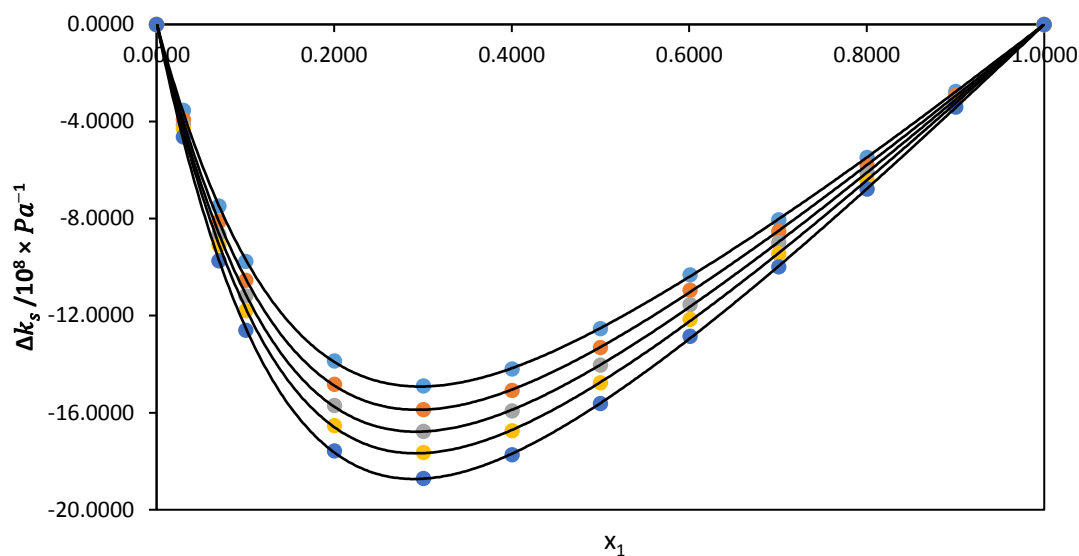
Figure 5.49   Deviation in isentropic compressibility (Δk_s) for the binary mixture of {[PYR-PDO]$^+$[Cl]$^-$ (x_1) + propanoic acid (x_2)} as a function of the composition expressed in mole fraction of [PYR-PDO]$^+$[Cl]$^-$ at T = 293.15 K (●), 298.15 K (●), 303.15 K (●), 308.15 K (●), 313.15 K (●). The lines were generated using Redlich-Kister curve-fitting.
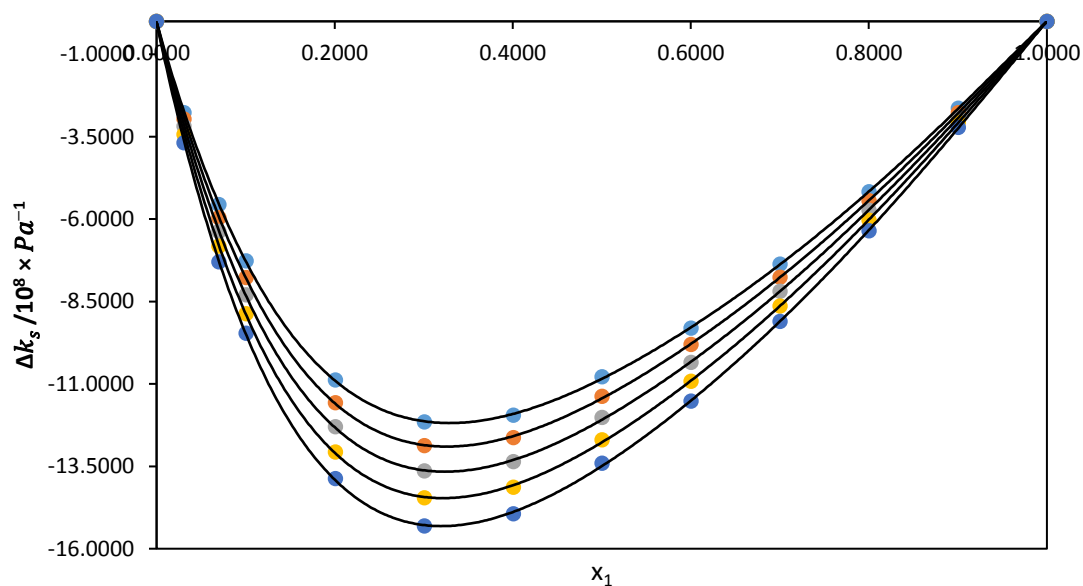
Figure 5.50   Deviation in isentropic compressibility (Δk_s) for the binary mixture of {[PYR-PDO]$^+$[Cl]$^-$ (x_1) + butanoic acid (x_2)} as a function of the composition expressed in mole fraction of [PYR-PDO]$^+$[Cl]$^-$ at T = 293.15 K (●), 298.15 K (●), 303.15 K (●), 308.15 K (●), 313.15 K (●). The lines were generated using Redlich-Kister curve-fitting.

Figures 5.51 – 5.53 presents the plots of intermolecular free length (L_f) against mole fraction for the binary systems of {[PYR-PDO]$^+$[Cl]$^-$ (x_1) + ethanoic or propanoic or butanoic acid (x_2)} studied at T = (293.15, 298.15, 303.15, 308.15 and 313.15) K.
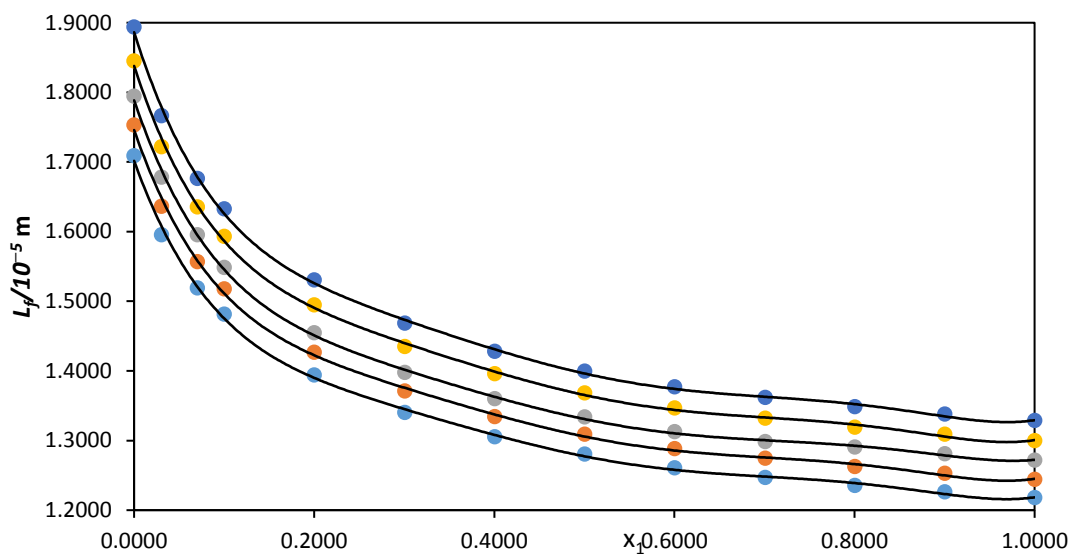
Figure 5.51 Intermolecular free length (L_f) for the binary mixture of {[PYR-PDO]$^+$[Cl]$^-$ (x_1) + ethanoic acid (x_2)} as a function of the composition expressed in mole fraction of [PYR-PDO]$^+$[Cl]$^-$ at T = 293.15 K (●), 298.15 K (●), 303.15 K (●), 308.15 K (●), 313.15 K (●). The lines were generated using Redlich-Kister curve-fitting.
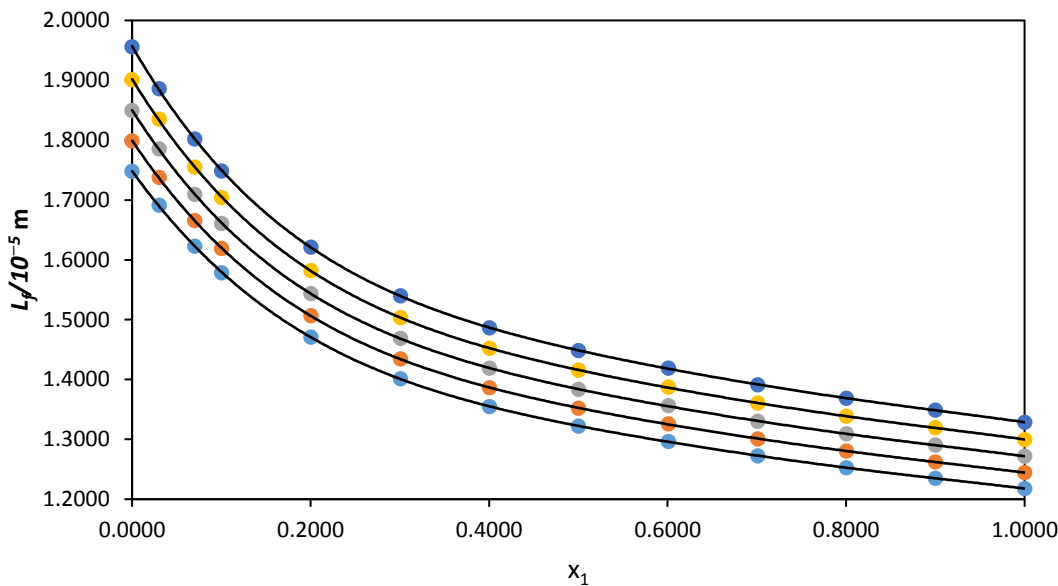
Figure 5.52 Intermolecular free length (L_f) for the binary mixture of {[PYR-PDO]$^+$[Cl]$^-$ (x_1) + propanoic acid (x_2)} as a function of the composition expressed in mole fraction of [PYR-PDO]$^+$[Cl]$^-$ at T = 293.15 K (●), 298.15 K (●), 303.15 K (●), 308.15 K (●), 313.15 K (●). The lines were generated using Redlich-Kister curve-fitting.
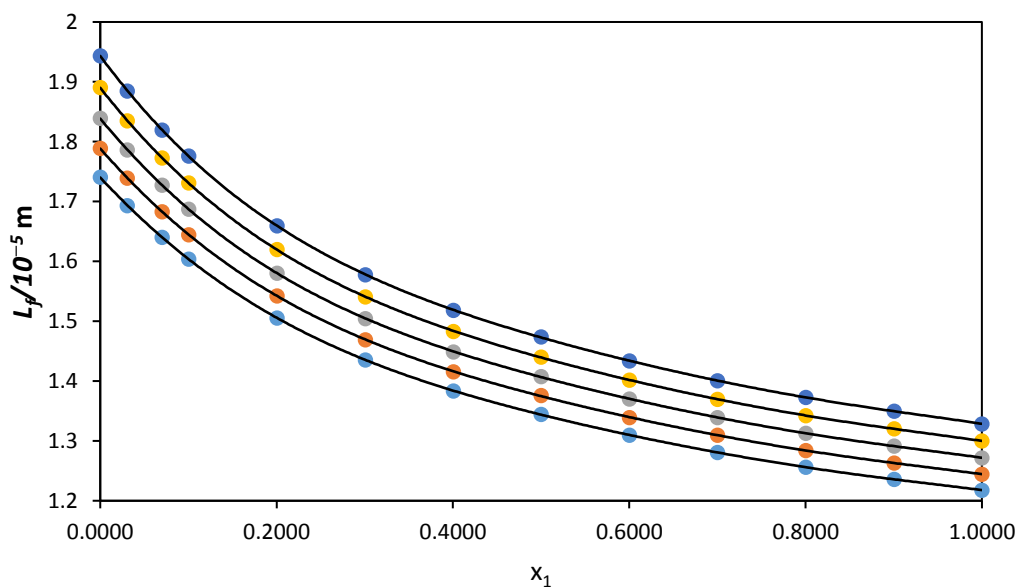
Figure 5.53 Intermolecular free length (L_f) for the binary mixture of {[PYR-PDO]$^+$[Cl]$^-$ (x_1) + butanoic acid (x_2)} as a function of the composition expressed in mole fraction of [PYR-PDO]$^+$[Cl]$^-$ at T = 293.15 K (●), 298.15 K (●), 303.15 K (●), 308.15 K (●), 313.15 K (●). The lines were generated using Redlich-Kister curve-fitting.

126

Intermolecular free length L_f is also regarded as intermolecular distance. Jacobson (1952) proposed an equation used in calculating L_f which is given in equation (5.1). L_f values are largely affected by change in concentration and temperature, and also the specific interactions that occur between the molecules of the component liquids, as a result, the molecules are dependent on hydrogen bond which binds the molecules. The two-component solutions of $\{$[PYR-PDO]$^+$[Cl]$^-$ (x_1) + ethanoic or propanoic or butanoic acid $(x_2)\}$ at T = (293.15, 298.15, 303.15, 308.15 and 313.15) K throughout the concentration of [PYR-PDO]$^+$[Cl]$^-$ for intermolecular free length L_f were estimated and presented in Table 5.13 to 5.15. The plots of these binary solutions have been presented in Figures 5.51 to 5.53. From the results obtained, L_f was found to increase with a rise in temperature but decrease across the increasing concentration of IL. However, speed of sound relates in an inverse manner to L_f during a close observation of the values in Tables 5.13 to 5.15 and as well in Figures 5.51 to 5.53.

The Redlich-Kister fitting parameters were calculated from equation (4.2) and standard deviation errors as well from equation (4.3). The values are presented in Table 5.16

Table 5.16 Redlich- Kister fitting coefficients and standard deviation, σ, for binary systems of $\{[PYR\text{-}PDO]^+[Cl]^-\ (x_1)$ + ethanoic or propanoic or butanoic acid $(x_2)\}$ studied at T = (293.15, 298.15, 303.15, 308.15 and 313.15) K.

	$T/(\text{K})$	A_0	A_1	A_2	A_3	σ
		$\{[PYR\text{-}PDO]^+[Cl]^-\ (x_1)$ + ethanoic acid $(x_2)\}$				
$V_m^E/\text{cm}^3\cdot\text{mol}^{-1}$	293.15	-3.207	-1.425	-2.899	-4.891	0.060
	298.15	-3.281	-1.465	-2.938	-4.966	0.061
	303.15	-3.359	-1.507	-2.997	-5.048	0.062
	308.15	-3.435	-1.552	-3.052	-5.123	0.063
	313.15	-3.542	-1.597	-3.215	-5.397	0.067
$\Delta k_s/10^8 \times \text{Pa}^{-1}$	293.15	-52.067	-31.629	-62.717	-81.677	0.911
	298.15	-54.350	-33.168	-65.352	-84.788	0.936
	303.15	-57.369	-35.382	-65.896	-85.850	0.838
	308.15	-59.175	-36.469	-70.657	-90.870	0.985
	313.15	-61.841	-38.257	-73.721	-94.524	1.019
$L_f/10^{-5}\,\text{m}$	293.15	4.344	-2.148	15.381	11.289	0.786
	298.15	4.439	-2.203	15.749	11.604	0.805
	303.15	4.517	-2.268	16.134	11.902	0.825
	308.15	4.637	-2.319	16.521	12.269	0.846
	313.15	4.740	-2.379	16.923	12.618	0.867
		$\{[PYR\text{-}PDO]^+[Cl]^-\ (x_1)$ + propanoic acid $(x_2)\}$				
$V_m^E/\text{cm}^3\cdot\text{mol}^{-1}$	293.15	-2.684	-2.266	-1.410	0.598	0.009
	298.15	-2.797	-2.274	-1.481	0.471	0.009
	303.15	-2.902	-2.288	-1.617	0.364	0.009
	308.15	-3.034	-2.330	-1.677	0.295	0.008
	313.15	-3.169	-2.367	-1.756	0.227	0.006
$\Delta k_s/10^8 \times \text{Pa}^{-1}$	293.15	-49.992	-38.670	-29.613	-14.402	0.056
	298.15	-53.011	-40.874	-32.823	-17.920	0.062
	303.15	-55.904	-43.208	-35.125	-19.594	0.071

	T/K					
	308.15	-58.808	-45.659	-36.952	-20.368	0.082
	313.15	-62.186	-48.261	-39.992	-23.204	0.091
$L_f/10^{-5}$ m	293.15	4.471	-2.204	16.078	12.588	0.805
	298.15	4.570	-2.265	16.481	12.972	0.827
	303.15	4.673	-2.328	16.899	13.373	0.849
	308.15	4.778	-2.394	17.330	13.786	0.871
	313.15	4.886	-2.461	17.772	14.214	0.895

$\{[\text{PYR-PDO}]^+[\text{Cl}]^-\ (x_1) + \text{butanoic acid}\ (x_2)\}$

	T/K					
$V_m^E/\text{cm}^3\cdot\text{mol}^{-1}$	293.15	-2.717	-1.541	-0.993	0.101	0.015
	298.15	-2.805	-1.633	-1.006	-0.026	0.015
	303.15	-2.901	-1.731	-1.038	-0.140	0.016
	308.15	-2.997	-1.824	-1.059	-0.269	0.016
	313.15	-3.085	-1.954	-1.162	-0.238	0.016
$\Delta k_s/10^8 \times \text{Pa}^{-1}$	293.15	-43.444	-27.057	-18.523	-7.701	0.038
	298.15	-45.822	-28.823	-20.283	-8.899	0.040
	303.15	-48.385	-30.633	-22.080	-10.362	0.043
	308.15	-51.091	-32.518	-23.993	-12.019	0.048
	313.15	-53.945	-34.518	-26.037	-13.765	0.056
$L_f/10^{-5}$ m	293.15	4.558	-2.041	16.170	12.565	0.801
	298.15	4.660	-2.096	16.572	12.944	0.822
	303.15	4.766	-2.153	16.990	13.336	0.843
	308.15	4.874	-2.212	17.420	13.739	0.866
	313.15	4.985	-2.272	17.861	14.155	0.889

Standard uncertainties u are $u(T) = \pm0.01$ K and the combined expanded uncertainty U_c in density and speed of sound measurements were less than $U_c\ (\rho) = \pm 2\ \text{x}\ 10^{-4}\ \text{g}\cdot\text{cm}^{-3}$ and $U_c(u) = 0.6\ \text{m}\cdot\text{s}^{-1}$ respectively (0.95 level of confidence)

CONCLUSION

Density and speed of sound were measured as a function of temperature and composition for the corresponding binary mixtures of $\{[EMIM]^+[EtSO_4]^- +$ pentanoic acid or 2-methylpropanoic acid$\}$, $\{[BMIM]^+[MeSO_4]^- +$ ethanoic acid or propanoic acid$\}$, $\{[EPMpyr]^+[SAL]^- +$ ethanoic acid or propanoic acid$\}$, $\{[EPMpyr]^+[OAC]^- +$ propanoic acid

or butanoic acid}, {[PYR-PDO]$^+$[Cl]$^-$ + ethanoic acid or propanoic acid or butanoic acid} under the same experimental conditions. The derived thermodynamic parameters such as excess molar volumes V_m^E, isentropic compressibility k_s, deviation in isentropic compressibility Δk_s and intermolecular free length L_f were calculated from the experimental values of density and speed of sound.

The experimental data for density and speed of sound of all the binary systems studied were evaluated and were found to decrease with an increase in temperature for all binary systems studied and increases with an increase in concentration of the ionic liquids. The data on these thermophysical properties could be used in gaining valuable insights on how chemical structures of ionic liquids are related to the thermophysical properties. Also, with the study on density and speed of sound of the binary liquid mixtures, this study have been able to explicate the interactions that occur between the molecules of the components of the liquid mixture utilized i.e. the molecules in the ionic liquids and carboxylic acid molecules.

Furthermore, the derived thermodynamic parameters like excess molar volume and deviation in isentropic compressibility were found to be negative throughout the entire range of concentrations. This is as a result of ion-dipole interaction or packing effects between the carboxylic acids and the ionic liquids. This results also help to understand the nature of these parameters with respect to the composition and temperature effects. Additionally, the increasing chain of the carboxylic acids utilized can influence the sign and magnitude of these parameters. The results were also analyzed on the basis of intermolecular interactions between the components of the binary liquid mixtures.

The isentropic compressibility values were found to be positive for the entire composition but increases with increasing temperature and decreases with an increase in concentration of the mole fraction of the IL. This positive result were ascribed to the effect of solutes on solvent intrinsic compression which creates free space thereby having the binary solution to be more compressed.

In comparing the effectiveness of the ionic liquids with the carboxylic acids utilized, it is notable to conclude that the pyrrolidinium based ILs interacts more with the molecules of carboxylic acids than imidazolium based cation. This is so because V_m^E and Δk_s negative values

increases as the alkyl chain length of the acids increases which in turn results in increase in compressibility of the liquid mixtures. It can also be concluded that stronger association of molecules in pyrrolidinium-based cations occur than in imidazolium based cations when mixed with the carboxylic acids.

Furthermore, in all binary systems studied, Redlich–Kister polynomial were used to correlate the obtained values of excess molar volumes, deviation in isentropic compressibility and intermolecular free length. The results were found to be satisfactory for all systems studied.

REFERENCES

Altuwaim, M.S., Alkhaldi, K.H., Al-Jimaz, A.S. and Mohammad, A.A., 2012. Comparative study of physico-chemical properties of binary mixtures of N, N-dimethylformamide with 1-alkanols at different temperatures. *Journal of Chemical Thermodynamics*, 48: 39-47.

Alvarez, V.H., Mattedi, S., Martin-Pastor, M., Aznar, M. and Iglesias, M., 2011. Thermophysical properties of binary mixtures of {ionic liquid 2-hydroxy ethylammonium

acetate+ (water, methanol, or ethanol)}. *Journal of Chemical Thermodynamics*, 43(7): 997-1010.

Anastas, P.T. and Warner, J.C., 2000. *Green chemistry: theory and practice*. volume 30, Oxford university press.

Andretta, A.E., Arce, A., Rodil, E. and Soto, A., 2009. Physical and excess properties of (methyl acetate+ methanol+ 1-octyl-3-methyl-imidazolium bis (trifluoromethylsulfonyl) imide) and its binary mixtures at T= 298.15 K and atmospheric pressure. *Journal of Chemical Thermodynamics*, 41(12): 1317-1323.

Anouti, M., Jones, J., Boisset, A., Jacquemin, J., Caillon-Caravanier, M. and Lemordant, D., 2009. Aggregation behavior in water of new imidazolium and pyrrolidinium alkycarboxylates protic ionic liquids. *Journal of colloid and interface science*, *340*(1):104-111.

Anouti, M., Vigeant, A., Jacquemin, J., Brigouleix, C. and Lemordant, D., 2010. Volumetric properties, viscosity and refractive index of the protic ionic liquid, pyrrolidinium octanoate, in molecular solvents. *Journal of Chemical Thermodynamics*, 42(7): 834-845.

Arce, A., Rodil, E. and Soto, A., 2006. Volumetric and viscosity study for the mixtures of 2-ethoxy-2-methylpropane, ethanol, and 1-ethyl-3-methylimidazolium ethyl sulfate ionic liquid. *Journal of Chemical & Engineering Data*, 51(4): 1453-1457.

Arumugam, V., Redhi, G.G. and Gengan, R.M., 2017. Synthesis, characterization and thermophysical properties of novel 2′, 3′-N-epoxypropyl-N-methyl-2-oxopyrrolidinium acetate ionic liquid and their binary mixtures with water or methanol. *Journal of Molecular Liquids*, 242: 1215-1227.

Ausländer, D. and Onitiu, L., 1971. On the ultrasound velocity and the adiabatic compressibility in aqueous solutions of certain halides–V. alkaline metals fluorides. *Acta Acustica united with Acustica*, 24(4): 205-210.

Azevedo, R.G., Szydlowski, J., Pires, P.F., Esperança, J.M.S.S., Guedes, H.J.R. and Rebelo, L.P.N., 2004. A novel non-intrusive microcell for sound-speed measurements in liquids. Speed of sound and thermodynamic properties of 2-propanone at pressures up to 160 MPa. *Journal of Chemical Thermodynamics*, 36(3): 211-222.

Aziz, R.A., Bowman, D.H. and Lim, C.C., 1972. An examination of the relationship between sound velocity and density in liquids. *Canadian Journal of Physics*, 50(7): 646-654.

Bahadur I., 2010, *PhD thesis, Durban University of Technology, Durban*.

Bahadur, I., Deenadayalu, N., Naidoo, P. and Ramjugernath, D., 2013. Density, speed of sound, and refractive index measurements for the binary systems (butanoic acid+ propanoic acid, or 2-methyl-propanoic acid) at T=(293.15 to 313.15) K. *Journal of Chemical Thermodynamics*, 57: 203-211.

Bahadur, I., Singh, S., Deenadayalu, N., Naidoo, P. and Ramjugernath, D., 2014. Influence of alkyl group and temperature on thermophysical properties of carboxylic acid and their binary mixtures. *Thermochimica Acta*, 590: 151-159.

Bhattacharjee, A., Varanda, C., Freire, M.G., Matted, S., Santos, L.M., Marrucho, I.M. and Coutinho, J.A., 2012. Density and viscosity data for binary mixtures of 1-alkyl-3-methylimidazolium alkylsulfates + water. *Journal of Chemical & Engineering Data*, 57(12): 3473-3482.

Bottomley, G.A. and Scott, R.L., 1974. A grease-free continuous dilution dilatometer; excess volumes for benzene+ carbon tetrachloride. *Journal of Chemical Thermodynamics*, 6(10): 973-981.

Brennecke, J.F. and Maginn, E.J., 2001. Ionic liquids: innovative fluids for chemical processing. *AIChE Journal*, 47(11): 2384-2389.

Cann, M.C. and Connelly, M.E., 2000. *Real-world cases in green chemistry*. American chemical society.

Chaudhary, G. R., Bansal, S., Mehta, S. K., Ahluwalia, A. S., 2012. Thermophysical and spectroscopic studies of room temperature ionic liquid, 1-butyl-3-methylimidazolium hexafluorophosphate in Tritons, *Journal of Chemical Thermodynamics* 50: 63-70.

Chen, J., Chen, L., Lu, Y. and Xu, Y., 2014. Physicochemical properties of aqueous solution of 1-methylimidazolium acetate ionic liquid at several temperatures. *Journal of Molecular Liquids*, 197: 374-380.

Chiappe, C., Pieraccini, D.; 2003, Ionic liquids: solvent properties and organic reactivity, *Journal of Physical Organic Chemistry,* 18: 275-297.

Chiu, Y.H., Gaeta, G., Heine, T.R., Dressler, R.A. and Levandier, D.J., 2006, July. Analysis of the electrospray plume from the EMIM propellant externally wetted on a tungsten needle. In *Proceedings of the 42nd AIAA/ASME/SAE/ASEE Joint Propulsion Conference and Exhibit*, page: 5010.

Chum, H.L., Koch, V.R., Miller, L.L. and Osteryoung, R.A., 1975. Electrochemical scrutiny of organometallic iron complexes and hexamethylbenzene in a room temperature molten salt. *Journal of the American Chemical Society*, 97(11): 3264-3265.

Crowhurst, L., Mawdsley, P. R., Perez-Arlandis, J. M., Salter, P. A., Welton, T.; 2003; Solvent–solute interactions in ionic liquids, *Physical Chemistry Chemical Physics* 5: 2790-2794.

Cunha, D.L., Coutinho, J.A., Daridon, J.L., Reis, R.A. and Paredes, M.L., 2013. Experimental densities and speeds of sound of substituted phenols and their modeling with the Prigogine–Flory–Patterson model. *Journal of Chemical & Engineering Data*, 58(11): 2925-2931.

Deenadayalu, N., Sen, S. and Sibiya, P.N., 2009. Application of the PFV EoS correlation to excess molar volumes of (1-ethyl-3-methylimidazolium ethylsulphate + alkanols) at different temperatures. *Journal of Chemical Thermodynamics*, 41(4): 538-548.

Deosarkar, S.D., Pandhare, V.V. and Kattekar, P.S., 2013. Densities and Refractive Indices of Potassium Salt Solutions in Binary Mixture of Different Compositions. *Journal of Engineering*, 2013: Article ID 368576.

Domańska, U. and Laskowska, M., 2008. Phase equilibria and volumetric properties of (1-ethyl-3-methylimidazolium ethylsulfate + alcohol or water) binary systems. *Journal of Solution Chemistry*, 37(9): 1271-1287.

Domańska, U., 2006. Thermophysical properties and thermodynamic phase behavior of ionic liquids. *Thermochimica Acta*, 448(1): 19-30.

Domańska, U., Królikowski, M. and Paduszyński, K., 2009. Phase equilibria study of the binary systems (N-butyl-3-methylpyridinium tosylate ionic liquid+ an alcohol). *Journal of Chemical Thermodynamics*, 41(8): 932-938.

Dupont, J., de Souza, R.F. and Suarez, P.A., 2002. Ionic liquid (molten salt) phase organometallic catalysis. *Chemical Reviews*, 102(10): 3667-3692.

Earle, M.J. and Seddon, K.R., 2000. Ionic liquids. Green solvents for the future. *Pure and applied chemistry*, 72(7): 1391-1398.

FitzPatrick M. A., 2011. *Master of Applied Science (thesis), Queen's University, Canada*.

Flieger, J., Grushka, E.B. and Czajkowska-Żelazko, A., 2014. Ionic Liquids as solvents in separation processes. *Austin Journal of Analytical Pharmaceutical Chemistry*, 1(2): 1009.

Fortin, T.J., Laesecke, A., Freund, M. and Outcalt, S., 2013. Advanced calibration, adjustment, and operation of a density and sound speed analyzer. *Journal of Chemical Thermodynamics*, 57: 276-285.

Fredlake, C.P., Crosthwaite, J.M., Hert, D.G., Aki, S.N. and Brennecke, J.F., 2004. Thermophysical properties of imidazolium-based ionic liquids. *Journal of Chemical & Engineering Data*, 49(4): 954-964.

Freemantle, M., 2010. An introduction to ionic liquids. *Royal Society of chemistry*. Chapter 1: 1-10.

Gabriel, S. and Weiner, J., 1888. Ueber einige abkömmlinge des propylamins. *Berichte der deutschen chemischen Gesellschaft*, 21(2): 2669-2679.

Gale, R.J. and Osteryoung, R.A., 1979. Potentiometric investigation of dialuminium heptachloride formation in aluminium chloride-1-butylpyridinium chloride *mixtures. Inorganic Chemistry,* 18(6): 1603-1605.

Giridhar, P., Venkatesan, K.A., Srinivasan, T.G. and Rao, P.V., 2007. Electrochemical behaviour of uranium (VI) in 1-butyl-3-methylimidazolium chloride and thermal characterization of uranium oxide deposit. *Electrochimica Acta*, 52(9): 3006-3012.

Gómez, E., González, B., Calvar, N., Tojo, E. and Domínguez, Á., 2006. Physical properties of pure 1-ethyl-3-methylimidazolium ethylsulfate and its binary mixtures with ethanol and water at several temperatures. *Journal of Chemical and Engineering Data*, 51(6): 2096-2102.

Gonzalez, B., Domınguez, A. and Tojo, J., 2004. Dynamic Viscosities, Densities, and Speed of Sound and Derived Properties of the Binary Systems Acetic Acid with Water, Methanol, Ethanol, Ethyl Acetate and Methyl Acetate at T = (293.15, 298.15, and 303.15) K at Atmospheric Pressure, *Journal of Chemical and Engineering Data*. 49: 1590–1596.

González, E.J., Domínguez, Á. and Macedo, E.A., 2012. Excess properties of binary mixtures containing 1-hexyl-3-methylimidazolium bis (trifluoromethylsulfonyl) imide ionic liquid and polar organic compounds. *Journal of Chemical Thermodynamics*, 47: 300-311.

González, E.J., González, B., Calvar, N. and Domínguez, Á., 2007. Physical properties of binary mixtures of the ionic liquid 1-ethyl-3-methylimidazolium ethyl sulfate with several alcohols at T= (298.15, 313.15, and 328.15) K and atmospheric pressure. *Journal of Chemical and Engineering Data*, 52(5): 1641-1648.

Govinda, V., Attri, P., Venkatesu, P. and Venkateswarlu, P., 2011. Temperature effect on the molecular interactions between two ammonium ionic liquids and dimethylsulfoxide. *Journal of Molecular Liquids*, 164(3): 218-225.

Gowrisankar, M., Venkateswarlu, P., Sivakumar, K. and Sivarambabu, S., 2013. Ultrasonic studies on molecular interactions in binary mixtures of N-methyl aniline with methyl isobutylketone,+ 3-pentanone, and+ cycloalkanones at 303.15 K. *Journal of solution chemistry*, 42(5): 916-935.

Handa, Y.P. and Benson, G.C., 1979. Volume changes on mixing two liquids: A review of the experimental techniques and the literature data. *Fluid Phase Equilibria*, 3(2-3): 185-249.

Hoffman, T., Gołdon, A., Nevines, A. and Letcher, T.M., 2008. Densities, excess volumes, isobaric expansivity, and isothermal compressibility of the (1-ethyl-3-methylimidazolium ethylsulfate+ methanol) system at temperatures (283.15 to 333.15) K and pressures from (0.1 to 35) MPa. *Journal of Chemical Thermodynamics*, 40(4): 580-591.

Iglesias, M., Pineiro, M.M., Marino, G., Orge, B., Domınguez, M. and Tojo, J., 1999. Thermodynamic properties of the mixture benzene+ cyclohexane+ 2-methyl-2-butanol at the temperature 298.15 K: excess molar volumes prediction by application of cubic equations of state. *Fluid phase equilibria*, 154(1): 123-138.

Jacobson, B., 1951. Intermolecular free lengths in liquids in relation to compressibility, surface tension and viscosity. *Acta Chemica Scandinavica*, 5(7-8): 1214-1216.

Jacquemin, J., Anouti, M. and Lemordant, D., 2011. Physico-chemical properties of non-Newtonian shear thickening di-isopropyl-ethylammonium-based protic ionic liquids and their mixtures with water and acetonitrile. *Journal of Chemical & Engineering Data*, 56(3): 556-564.

137

Karkamkar, A., Aardahl, C. and Autrey, T., 2007. Recent developments on hydrogen release from ammonia borane. *Material Matters*, 2(2): 6-9.

Keyes, D.B. and Hildebrand, J.H., 1917. A study of the system aniline—hexane. *Journal of the American Chemical Society*, 39(10): 2126-2137.

Kittel, C., 1946. Ultrasonic propagation in liquids II. Theoretical study of the free volume model of the liquid state. *Journal of Chemical Physics*, 14(10): 614-624.

Kumaran, M.K. and McGlashan, M.L., 1977. An improved dilution dilatometer for measurements of excess volumes. *Journal of Chemical Thermodynamics*, 9(3): 259-267.

Kurnia, K.A., Mutalib, M.A., Murugesan, T. and Ariwahjoedi, B., 2011. Physicochemical properties of binary mixtures of the protic ionic liquid bis (2-hydroxyethyl) methylammonium formate with methanol, ethanol, and 1-propanol. *Journal of Solution Chemistry*, 40(5): 818-831.

Letcher, T. M., 1975. Volume changes on mixing two liquids: A review of the experimental techniques and the literature data, *Chemsa,* 226.

Letcher, T.M. and Redhi, G.G., 2002. Thermodynamic excess properties for binary mixtures of (benzonitrile+ a carboxylic acid) at T= 298.15 K. *Fluid phase equilibria*, 198(2): 257-266.

Lomba, L., Giner, B., Bandrés, I., Lafuente, C. and Pino, M.R., 2011. Physicochemical properties of green solvents derived from biomass. *Green chemistry*, 13(8): 2062-2070.

López-Lázaro, J.D.L.S., Iglesias-Silva, G.A., Estrada-Baltazar, A. and Barajas-Fernández, J., 2015. Density and surface tension of binary mixtures of 2, 2, 4-trimethylpentane + n-heptane, 2, 2, 4-trimethylpentane + n-octane, ethyl acetate + benzene, and butanenitrile + benzene from (293.15 to 323.15) K. *Journal of Chemical & Engineering Data*, 60(6): 1823-1834.

Mahajan, A.R., Mirgane, S.R. and Deshmukh, S.B., 2012. Thermo-acoustical studies of binary mixture n-octane, n-decane, n-dodecane and n-tetradecane with octan-2-ol and application of theories of sound speed. *Journal of Molecular Liquids*, 175: 44-50.

Maia, F.M., Calvar, N., González, E.J., Carneiro, A.P., Rodriguez, O. and Macedo, E.A., 2013. Modeling of ionic liquid systems: phase equilibria and physical properties. In *Ionic Liquids-New Aspects for the Future*. InTech.

Meindersma G. W., Podt A. J. G., de Haan A. B., 2005, Selection of ionic liquids for the extraction of aromatic hydrocarbons from aromatic/aliphatic mixtures. *Fuel Process Technology,* 87: 59–70.

Mercer-Chalmers J. D. 1992. *Degree of Doctor of Philosophy (thesis)*, *Rhodes University*.

Nduli M. B., 2016, *MTech thesis, Durban University of Technology, Durban*.

Nevines J.A. 1997. Thermodynamics of nonelectrolytes liquid mixtures, *PhD thesis, UKZN, Durban*, 78-80.

Nieto de Castro, C.A. and Santos, F., 2007. Measurement of ionic liquids properties. Are we doing it well?. *Chimica oggi*, 25(6): 20-23.

Nunes, V.M.B., Lourenço, M.J.V., Santos, F.J.V., Matos Lopes, M.L.S. and Nieto de Castro, C.A. 2010. Accurate measurements of physico-chemical properties on ionic liquids and molten salts, *In: Ionic Liquids and Molten Salts: Never the Twain*, John Wiley, USA. Seddon, K. R. & Gaune-Escard, M., (Eds.): 229-263.

Papovic, S., Bešter-Rogac, M., Vraneš, M. and Gadzuric, S., 2016. The effect of the alkyl chain length on physicochemical features of (ionic liquids+ c-butyrolactone) binary mixtures. *Journal of Chemical Thermodynamics* 99: 1–10.

Pârvulescu, V.I. and Hardacre, C., 2007. Catalysis in ionic liquids. *Chemical Reviews*, 107(6): 2615-2665.

Patel, H., Vaid, Z.S., More, U.U., Ijardar, S.P. and Malek, N.I., 2016. Thermophysical, acoustic and optical properties of binary mixtures of imidazolium based ionic liquids+ polyethylene glycol. *Journal of Chemical Thermodynamics*, 99: 40-53.

Patil, K. R. and Dagade D. H., 2018. Volumetric and compressibility studies of aqueous triethylammonium based protic ionic liquids at $T = 298.15$ K. *Journal of Molecular Liquids*, 249: 272-280.

Patil, P.P., Patil, S.R., Borse, A.U. and Hundiwale, D.G., 2011. Density, excess molar volume and apparent molar volume of binary liquid mixtures. *Rasayan Journal of Chemistry*, 4(3): 599-604.

Pereiro, A.B. and Rodriguez, A., 2007. Study on the phase behaviour and thermodynamic properties of ionic liquids containing imidazolium cation with ethanol at several temperatures. *Journal of Chemical Thermodynamics*, 39(6): 978-989.

Pereiro, A.B., Verdía, P., Tojo, E. and Rodríguez, A., 2007. Physical properties of 1-butyl-3-methylimidazolium methyl sulfate as a function of temperature. *Journal of Chemical & Engineering Data*, 52(2): 377-380.

Plechkova, N.V. and Seddon, K.R., 2008. Applications of ionic liquids in the chemical industry. *Chemical Society Reviews*, 37(1): 123-150.

Qian, W., Xu, Y., Zhu, H. and Yu, C., 2012. Properties of pure 1-methylimidazolium acetate ionic liquid and its binary mixtures with alcohols. *Journal of Chemical Thermodynamics*, 49: 87-94.

Rafiee, H.R. and Frouzesh, F., 2015. Volumetric properties for binary and ternary mixtures of allyl alcohol, 1, 3-dichloro-2-propanol and 1-ethyl-3-methyl imidazolium ethyl sulfate [Emim][EtSO$_4$] from T= 298.15 to 318.15 K at ambient pressure. *Thermochimica Acta*, 611: 36-46.

Rao, C.H., Venkatesan, K.A., Nagarajan, K. and Srinivasan, T.G., 2008. Dissolution of uranium oxides and electrochemical behaviour of U (VI) in task specific ionic liquid. *Radiochimica Acta*, 96(7): 403-409.

Rao, C.J., Venkatesan, K.A., Nagarajan, K., Srinivasan, T.G. and Rao, P.V., 2009. Electrochemical behaviour of europium (III) in N-butyl-N-methylpyrrolidinium bis (trifluoromethylsulfonyl)imide. *Electrochimica Acta*, 54(20): 4718-4725.

Rao, C.J., Venkatesan, K.A., Nagarajan, K., Srinivasan, T.G. and Rao, P.V., 2011. Electrodeposition of metallic uranium at near ambient conditions from room temperature ionic liquid. *Journal of Nuclear Materials*, 408(1): 25-29.

Rao, M. V. P., Naidu, P. R.; 1974 Excess Volumes of Binary Mixtures of Alcohols in Methylcyclohexane, *Canadian Journal of Chem*istry 52: 788-790.

Rao, S.G., Mohan, T.M., Krishna, T.V., Narendra, K. and Rao, B.S., 2015. Thermophysical properties of 1-butyl-3-methylimidazolium tetrafluoroborate and N-methyl-2-pyrrolidinone as a function of temperature. *Journal of Molecular Liquids*, 211: 1009-1017.

Rao, S.G., Mohan, T.M., Krishna, T.V., Raju, K.T.S.S. and Rao, B.S., 2015. Excess thermodynamic properties of ionic liquid 1-butyl-3-methylimidazolium tetrafluoroborate and N-octyl-2-pyrrolidone from T = (298.15 to 323.15) K at atmospheric pressure. *Journal of Chemical Thermodynamics*, 89: 286-295.

Reddy S., M., Raju, K.T.S., Md Nayeem, S., Bala Murali Krishna, K. and Bollikolla, H.B., 2017. Molecular interaction studies in the binary mixture of 1-ethyl-3-methylimidazolium trifluoromethanesulphonate+ 1-butanol from density, speed of sound and refractive index measurements. *Physics and Chemistry of Liquids*, 55(6): 775-795.

Reddy, M.S., Nayeem, S.M., Soumini, C., Raju, K.T.S. and Babu, B.H., 2016. Study of molecular interactions in binary liquid mixtures of [Emim][BF$_4$] with 2-methoxyethanol using thermo acoustic, volumetric and optical properties. *Thermochimica Acta*, 630: 37-49.

Reddy, M.S., Raju, K.T.S.S. and Rao, S.G., 2016. The study of solute–solvent interactions in 1-ethyl-3-methylimidazolium ethylsulfate+ 2-ethoxyethanol from density, speed of sound and refractive index measurements. *Journal of Molecular Liquids*, 218: 83-94.

Redhi G.G., 2003, *PhD thesis, UKZN, Durban*.

Redlich, O. and Kister, A.T., 1948. Algebraic representation of thermodynamic properties and the classification of solutions. *Industrial & Engineering Chemistry*, 40(2): 345-348.

Ribeiro, A.P.C., Vieira, S.I.C., França, J.M., Queirós, C.S., Langa, E., Lourenço, M.J.V., Murshed, S.M.S. and de Castro, C.N., 2011. Thermal properties of ionic liquids and ionanofluids. In *Ionic Liquids: Theory, Properties, New Approaches*. InTech.

Rogers, R.D., Seddon, K.R. and Volkov, S., 2003. Green Industrial Applications of Ionic Liquids Kluwer Academic.

Sattarib, M., Gharagheizi, F., Ilani-Kashkouli, P., Mohammadi, A.H. and Ramjugernath, D., 2014. Determination of the speed of sound in ionic liquids using a least squares support vector machine group contribution method. *Fluid Phase Equilibria*, 367: 188-193.

Shah, M.R., Anantharaj, R., Banerjee, T. and Yadav, G.D., 2013. Quaternary (liquid+ liquid) equilibria for systems of imidazolium based ionic liquid+ thiophene+ pyridine+ cyclohexane at 298.15 K: Experiments and quantum chemical predictions. *Journal of Chemical Thermodynamics*, 62: 142-150.

Shamsuri, A.A., 2011. Ionic liquids: preparations and limitations. *Makara Journal of Science*, 14: 101-106.

Shao, D., Lu, X., Fang, W., Guo, Y. and Xu, L., 2012. Densities and viscosities for binary mixtures of the ionic liquid N-ethyl piperazinium propionate with n-alcohols at several temperatures. *Journal of Chemical & Engineering Data*, 57(3): 937-942.

Sibiya P.N. 2008. Excess molar volumes, Partial molar volumes and isentropic compressibilities of binary systems (ionic liquid + alkanol), *M.Tech thesis, DUT, Durban*.

Sibiya, P.N. and Deenadayalu, N., 2008. Excess molar volumes and isentropic compressibility of binary systems {trioctylmethylammonium bis (trifluoromethysulfonyl) imide + methanol or ethanol or 1-propanol} at different temperatures. *Journal of Chemical Thermodynamics*, 40(7): 1041-1045.

Sibiya, P.N. and Deenadayalu, N., 2009. Excess molar volumes and partial molar volumes of binary systems (ionic liquid+ methanol or ethanol or 1-propanol) at T = (298.15, 303.15 and 313.15) K. *South African Journal of Chemistry*, 62(1): 20-25.

Singh S., 2013, *M.Tech thesis, Durban University of Technology*, Durban. 87-89.

Singh, S., Aznar, M. and Deenadayalu, N., 2013. Densities, speeds of sound, and refractive indices for binary mixtures of 1-butyl-3-methylimidazolium methyl sulphate ionic liquid with alcohols at T=(298.15, 303.15, 308.15, and 313.15) K. *Journal of Chemical Thermodynamics*, 57: 238-247.

Singh, S., Bahadur, I., Redhi, G.G., Ebenso, E.E. and Ramjugernath, D., 2014. Density and speed of sound of 1-ethyl-3-methylimidazolium ethyl sulphate with acetic or propionic acid at different temperatures. *Journal of Molecular Liquids*, 199: 518-523.

Singh, V.V., Boopathi, M., Ganesan, K., Singh, B. and Vijayaraghavan, R., 2010. Ionic liquid as an alternative greener sensing medium for the chemical warfare agent. *Electroanalysis*, 22(12): 1357-1363.

Stoimenovski, J., MacFarlane, D.R., Bica, K. and Rogers, R.D., 2010. Crystalline vs. ionic liquid salt forms of active pharmaceutical ingredients: a position paper. *Pharmaceutical research*, 27(4): 521-526.

Swapnil, D.A., 2012. Ionic liquids (a review): the green solvents for petroleum and hydrocarbon industries, *Research Journal of Chemical Sciences,* 2: 80-85.

Swatloski, R.P., Spear, S.K., Holbrey, J.D. and Rogers, R.D., 2002. Dissolution of cellulose with ionic liquids. *Journal of the American Chemical Society*, 124(18): 4974-4975.

Tokuda, H., Hayamizu, K., Ishii, K., Susan, M.A.B.H. and Watanabe, M., 2004. Physicochemical properties and structures of room temperature ionic liquids. 1. Variation of anionic species. *Journal of Physical Chemistry B*, 108(42): 16593-16600.

Tokuda, H., Hayamizu, K., Ishii, K., Susan, M.A.B.H. and Watanabe, M., 2005. Physicochemical properties and structures of room temperature ionic liquids. 2. Variation of alkyl chain length in imidazolium cation. *Journal of Physical Chemistry B*, 109(13): 6103-6110.

Vaid, Z.S., More, U.U., Oswal, S.B. and Malek, N.I., 2016. Experimental and theoretical excess molar properties of imidazolium based ionic liquids with isomers of butanol. *Thermochimica Acta*, 634: 38-47.

Vasantha Kumar, A., Redhi, G.G. and Gengan, R.M., 2016. Influence of Epoxy Group in 2-Pyrrolidonium Ionic Liquid Interactions and Thermo-Physical Properties with Ethanoic or Propanoic Acid at Various Temperatures. *ACS Sustainable Chemistry & Engineering*, 4(9): 4951-4964.

Vasanthakumar, A., Bahadur, I., Redhi, G. and Gengan, R.M., 2016. Synthesis and characterization of 2′, 3′-epoxy propyl-N-methyl-2-oxopyrrolidinium salicylate ionic liquid and study of its interaction with water or methanol. *RSC Advances*, 6(66): 61566-61575.

Vataščin, E. and Dohnal, V., 2015. Thermophysical properties of aqueous solutions of the 1-ethyl-3-methylimidazolium tricyanomethanide ionic liquid. *Journal of Chemical Thermodynamics*, 89: 169-176.

Vercher, E., Llopis, F.J., González-Alfaro, V., Miguel, P.J., Orchillés, V. and Martínez-Andreu, A., 2015. Volumetric properties, viscosities and refractive indices of binary liquid mixtures of tetrafluoroborate-based ionic liquids with methanol at several temperatures. *Journal of Chemical Thermodynamics*, 90: 174-184.

Walas, S.M., 1985. *Phase Equilibria in Chemical Engineering* Butterworth. Stoneham, MA.

Walden, P., 1914. Molecular weights and electrical conductivity of several fused salts. *Bull. Academic Imperial Science. (St. Petersburg)*, 8: 405-422.

Wang, X., Wang, X. and Song, B., 2015. Densities and viscosities of binary mixtures of 2, 2, 4-trimethylpentane+ 1-propanol,+ 1-pentanol,+ 1-hexanol, and+ 1-heptanol from (298.15 to 323.15) K. *Journal of Chemical & Engineering Data*, 60(6): 1664-1673.

Wasserscheid, P. and Welton, T. eds., 2008. *Ionic liquids in synthesis* (Vol. 1). Weinheim: Wiley-Vch.

Wilkes, J.S. and Zaworotko, M.J., 1992. Air and water stable 1-ethyl-3-methylimidazolium based ionic liquids. *Journal of the Chemical Society, Chemical Communications*, 13: 965-967.

Wilkes, J.S., Levisky, J.A., Wilson, R.A. and Hussey, C.L., 1982. Dialkylimidazolium chloroaluminate melts: a new class of room-temperature ionic liquids for electrochemistry, spectroscopy and synthesis. *Inorganic Chemistry*, 21(3): 1263-1264.

Wong, N.C. and Knobler, C.M., 1991. Light-scattering studies of phase separation in isobutyric acid+ water mixtures: Hydrodynamic effects. *Physical Review A*, *24*(6): 3205.

Wu, B., Reddy, R. and Rogers, R., 2001. Novel ionic liquid thermal storage for solar thermal electric power systems. *Solar Engineering*, 445-452.

Yang, C., Xu, W. and Ma, P., 2004. Thermodynamic properties of binary mixtures of p-xylene with cyclohexane, heptane, octane, and N-methyl-2-pyrrolidone at several temperatures. *Journal of Chemical & Engineering Data*, 49(6): 1794-1801.

Zafarani-Moattar, M.T. and Shekaari, H., 2005. Volumetric and speed of sound of ionic liquid, 1-butyl-3-methylimidazolium hexafluorophosphate with acetonitrile and methanol at T = (298.15 to 318.15) K. *Journal of Chemical & Engineering Data*, 50(5): 1694-1699.

Zhang, S., Li, X., Chen, H., Wang, J., Zhang, J. and Zhang, M., 2004. Determination of physical properties for the binary system of 1-ethyl-3-methylimidazolium tetrafluoroborate+ H_2O. *Journal of Chemical & Engineering Data*, 49(4): 760-764.

Zhong, Y., Wang, H. and Diao, K., 2007. Densities and excess volumes of binary mixtures of the ionic liquid 1-butyl-3-methylimidazolium hexafluorophosphate with aromatic compound at T = (298.15 to 313.15) K. *Journal of Chemical Thermodynamics*, 39(2): 291-296.